Volume XXXVII

GEMS & GEMOLOGY

Spring 2001

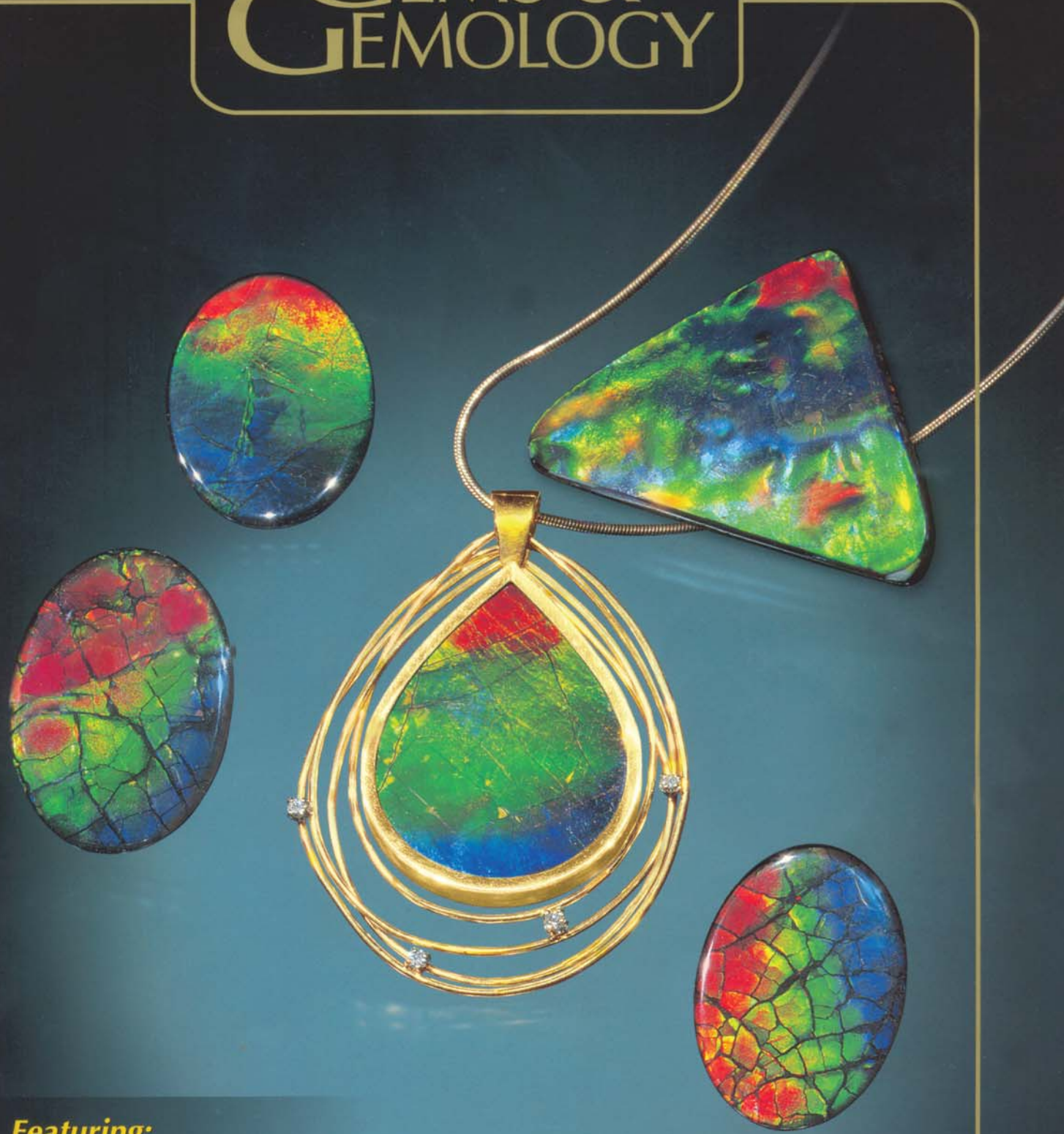

Featuring:

Ammolite . . . Argyle Diamond Deposit
Synthetic Red Beryl . . . Tucson Report

THE QUARTERLY JOURNAL OF THE GEMOLOGICAL INSTITUTE OF AMERICA

GEMS & GEMOLOGY

SPRING 2001 VOLUME 37, NO. 1

pg. 5

pg. 27

pg. 43

EDITORIAL

FEATURE ARTICLES

REGULAR FEATURES

pg. 74

The Dr. Edward J. Gübelin Most Valuable Article Award

The ballots are in, and we are pleased to announce the winners of this year's Dr. Edward J. Gübelin Most Valuable Article Award. We extend our sincerest thanks to all the subscribers who participated in the voting.

The first-place article, "Gemstone Enhancement and Detection in the 1990s" (Winter 2000), examined the prominent gem treatments of the last decade and discussed methods for their detection. Finishing in a close second place was "GE POL Diamonds: Before and After" (Fall 2000), which provided important clues to the identification of type IIa diamonds that had undergone high pressure/high temperature (HPHT) processing by General Electric. Third place was awarded to "Gem Localities of the 1990s" (Winter 2000), a review of the decade's new gemstone sources and its most important producing localities.

The authors of these three articles will share cash prizes of $1,000, $500, and $300, respectively. Following are photographs and brief biographies of the winning authors.

Congratulations also to Ron Suddendorf of Darnestown, Maryland, whose ballot was drawn from the many entries to win a leather portfolio and a five-year subscription to *Gems & Gemology*.

See some changes in this issue? With the new decade-century-millennium, we've been updating the design of *Gems & Gemology* and have expanded the Gem News section to Gem News International. Please be assured that there has been no change in the quality of the information provided throughout. Just a more contemporary look for a publication—now 67 years young—that will continue to keep you on the leading edge of gemology as we enter this new era.

Alice S. Keller, Editor
akeller@gia.edu

First Place

Gemstone Enhancement and Detection in the 1990s
Shane F. McClure and Christopher P. Smith

Shane McClure, G.G., is director of West Coast Identification Services at the GIA Gem Trade Laboratory in Carlsbad. With over 20 years of laboratory experience, Mr. McClure is well known for his articles and lectures on gem identification. He is also an editor of the Gem Trade Lab Notes section. Chicago native **Christopher Smith**, G.G., is director of the Gübelin Gem Lab in Lucerne, Switzerland. A prolific author, Mr. Smith is a member of the *Gems & Gemology* Editorial Review Board.

Shane McClure

Christopher Smith

George Bosshart

Johann Ponahlo

Vera Hammer

Helmut Klapper

Karl Schmetzer

James Shigley

Dona Dirlam

Brendan Laurs

Edward Boehm

William Larson

Second Place

GE POL Diamonds: Before and After

Christopher P. Smith, George Bosshart, Johann Ponahlo, Vera M. F. Hammer, Helmut Klapper, and Karl Schmetzer

Christopher Smith is profiled in the first-place entry. **George Bosshart**, who holds a degree in mineralogy from the Swiss Federal Institute of Technology in Zürich, is chief gemologist at the Gübelin Gem Lab. He currently is involved in research on HPHT-enhanced diamonds. **Johann Ponahlo** has been an independent research associate at the Museum of Natural History in Vienna since 1990. A physicochemist with a degree from the Technical University of Vienna, Dr. Ponahlo specializes in the study of cathodoluminescence in gems, particularly diamonds and jade. **Vera M. F. Hammer** has been the curatorial assistant for the mineral and gem collection of the Federal Gem Institute at the Museum of Natural History in Vienna since 1992. Dr. Hammer studied mineralogy and crystallography at the University of Vienna. Her research specialties are X-ray diffraction analysis, the gemology of colored diamonds, and UV-Vis-IR-spectroscopy of colored gemstones. **Helmut Klapper** received his doctorate in crystallography from the University of Cologne. Since 1990, he has been professor of mineralogy and crystallography and head of the crystal growth laboratory of the University of Bonn. Dr. Klapper's main research fields are crystal physics, crystal growth, and the characterization of crystal defects by X-ray diffraction topography. **Karl Schmetzer**, who obtained his doctorate in mineralogy and crystallography from Heidelberg University, is a research scientist residing in Petershausen, near Munich, Germany. Dr. Schmetzer has written numerous articles on natural and synthetic gems, and is also a member of the *G&G* Editorial Review Board.

Third Place

Gem Localities of the 1990s

James E. Shigley, Dona M. Dirlam, Brendan M. Laurs, Edward W. Boehm, George Bosshart, and William F. Larson

James Shigley is director of GIA Research in Carlsbad. Dr. Shigley, who received his Ph.D. in geology from Stanford University, has published a number of articles on natural, treated, and synthetic gems. He is also a member of the *G&G* Editorial Review Board. **Dona Dirlam**, G.G., is director of the Richard T. Liddicoat Library and Information Center at GIA in Carlsbad. She has a B.Sc. from the University of Minnesota and an M.Sc. in geology and geophysics from the University of Wisconsin, Madison. **Brendan Laurs**, G.G., is senior editor of *Gems & Gemology*. He obtained a B.Sc. in geology from the University of California at Santa Barbara and an M.Sc. in geology from Oregon State University. Prior to joining GIA, Mr. Laurs gained experience as an exploration geologist specializing in colored gems. **Edward Boehm**, G.G., is a gem dealer and gemological consultant. President of JOEB Enterprises in Solana Beach, California, Mr. Boehm has a degree in geology and German from the University of North Carolina in Chapel Hill. **George Bosshart** is profiled in the second-place entry. **William Larson** is president of Pala International (Fallbrook, California), a company that has been involved with gem-mining projects worldwide. Mr. Larson holds a degree in geological engineering from the Colorado School of Mines. He has traveled extensively to gem deposits, including 135 trips into the Far East and more than 40 visits to Africa.

AMMOLITE: IRIDESCENT FOSSILIZED AMMONITE FROM SOUTHERN ALBERTA, CANADA

By Keith A. Mychaluk, Alfred A. Levinson, and Russell L. Hall

A relative newcomer to the world gem market (since the 1960s), Ammolite is a form of aragonite that is obtained from vivid iridescent fossilized ammonite shells mined in Alberta, Canada. The gem material, from the extinct species Placenticeras meeki *and* P. intercalare*, is found only in certain horizons of the Bearpaw Formation of Late Cretaceous age (about 70–75 million years old). Because the iridescent layer is generally thin and fragile, most Ammolite is fashioned into assembled stones. This article describes the history of Ammolite as a gem material and the geologic setting of the main producing mines; offers an explanation for the formation of Ammolite and the origin of its color (i.e., iridescence caused by an interference phenomenon); presents production data, gemological properties, and a grading classification; and describes the manufacturing process.*

Ammolite is one of the few new natural gem materials to enter the marketplace in the last 50 years (figure 1). Like tanzanite and sugilite—which were introduced to the trade in 1967 and 1980, respectively—Ammolite occurs in sufficient quantities to be economically significant. Ammo*l*ite is a trade name for the iridescent, nacreous layer of the shell of specific fossil ammonites (figure 2) found in the Bearpaw Formation of Late Cretaceous age (figure 3). Commercial quantities of gem-quality Ammolite have been reported only from southern Alberta and only from the two ammonite species *Placenticeras meeki* and *P. intercalare*. Ammo*n*ite is a paleontologic term applied to a group of extinct marine cephalopods (squid-like organisms with disk-shaped coiled shells that are divided internally into chambers) that were particularly abundant during the Jurassic and Cretaceous periods (about 200–65 million years ago).

Ammolite has similarities to some modern shells such as abalone and paua, but the only fossil shell that resembles Ammolite with respect to play of color is lumachelle (Sinkankas, 1997), the iridescent fossiliferous marble that is best known from the lead mines at Bleiberg, Austria (Niedermayr, 1994). However, any similarities between Ammolite and other iridescent shell materials are superficial. Although the iridescence of lumachelle is associated with an ammonite, specifically *Carnites floridus*, this species is significantly older (Late Triassic in age) than those that give rise to Ammolite, and the two materials have different geologic occurrences. Further, lumachelle differs from Ammolite in appearance (e.g., most Ammolite has a characteristic fracture pattern). The former has been used primarily for nonjewelry purposes (i.e., as an ornamental stone) and, according to some who have seen the two materials (e.g., Sinkankas, 1976; Pough, 1986), Ammolite has superior iridescence.

Ammolite layers are typically thin (0.5–8 mm before polishing and 0.1–3 mm after polishing). They are composed predominantly of soft aragonite (3½–4 on the Mohs scale), yet they are sufficiently thick and

See end of article for About the Authors information and acknowledgments.
GEMS & GEMOLOGY, Vol. 37, No. 1, pp. 4–25

Figure 1. These Ammolites are from the St. Mary River area, Alberta, Canada. The rough specimen (3 × 4 cm) is typical of the high-quality Ammolite seen on the market today. Note the numerous iridescent color panes (i.e., flat areas of uniform color) that are separated by thin "healed" fractures. The two loose stones are Ammolite triplets (each 1.5 × 2.0 cm); the one on the left is made with type 2 sheet *Ammolite, and the other with the more common type 1* fractured *Ammolite. The brooch, by Llyn Strelau of Jewels By Design (Calgary), contains a 17.85 ct one-sided solid Ammolite set in 18K gold with ruby, fire opal, yellow sapphire, chrome tourmaline, blue sapphire, amethyst, and diamond. Courtesy of Korite International; photo © Harold & Erica Van Pelt.*

durable (including the ability to take a polish) to be manufactured into jewelry. In fact, freeform pieces of solid Ammolite over 100 ct have been reported (Wight, 1995). Iridescence produces the vivid colors in this material. The fact that Ammolite can be manufactured into jewelry distinguishes it from other iridescent materials obtained from various fossils (including other ammonites) that are frequently filmlike, have dull colors, or are otherwise unsuited for gem purposes. Nevertheless, because Ammolite usually occurs as thin, soft plates, it is found in jewelry primarily as assembled stones, such as triplets—a thin layer of Ammolite attached to a shale backing and covered with a synthetic spinel or quartz cap. Since 1980, both solid Ammolite and assembled Ammolite gemstones have become increasingly available. It is estimated that a total of about 600,000 pieces of Ammolite jewelry have been produced since significant commercial production began 20 years ago (P. Paré, pers. comm., 2001).

The purpose of this article is to update gemologists and jewelers on this unique gem material. For this study, we focused almost exclusively on material from the mining and manufacturing operations of Korite International Ltd. (henceforth Korite), Calgary, Alberta, because: (1) about 90% of the commercially available material historically has, and still does, come from Korite's mines; (2) almost all published information on Ammolite is based on specimens obtained from this company; (3) several other smaller Ammolite miners and manufacturers were offered the opportunity to participate in this study, but only one (S. Carbone) agreed to do so; and (4) Korite allowed us unrestricted visitation to their mining and manufacturing operations, and supplied us with production data as well as specimens for research. In addition

Figure 2. Ammonites are extinct mollusks of the class Cephalopoda, order Ammonoidea. This brightly colored ammonite (47.3 cm in diameter) of the species Placenticeras intercalare, *obtained from the Bearpaw Formation, near Lethbridge, Alberta, lived about 70 million years ago. The outer iridescent layer is the material from which gem Ammolite may be obtained, although more commonly it comes from naturally compacted and crushed specimens; complete specimens, such as the one pictured here, are typically more valuable left intact. Photo courtesy of Canada Fossils Ltd.*

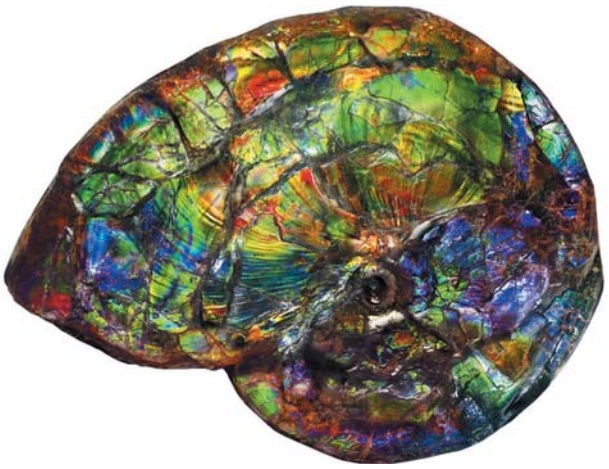

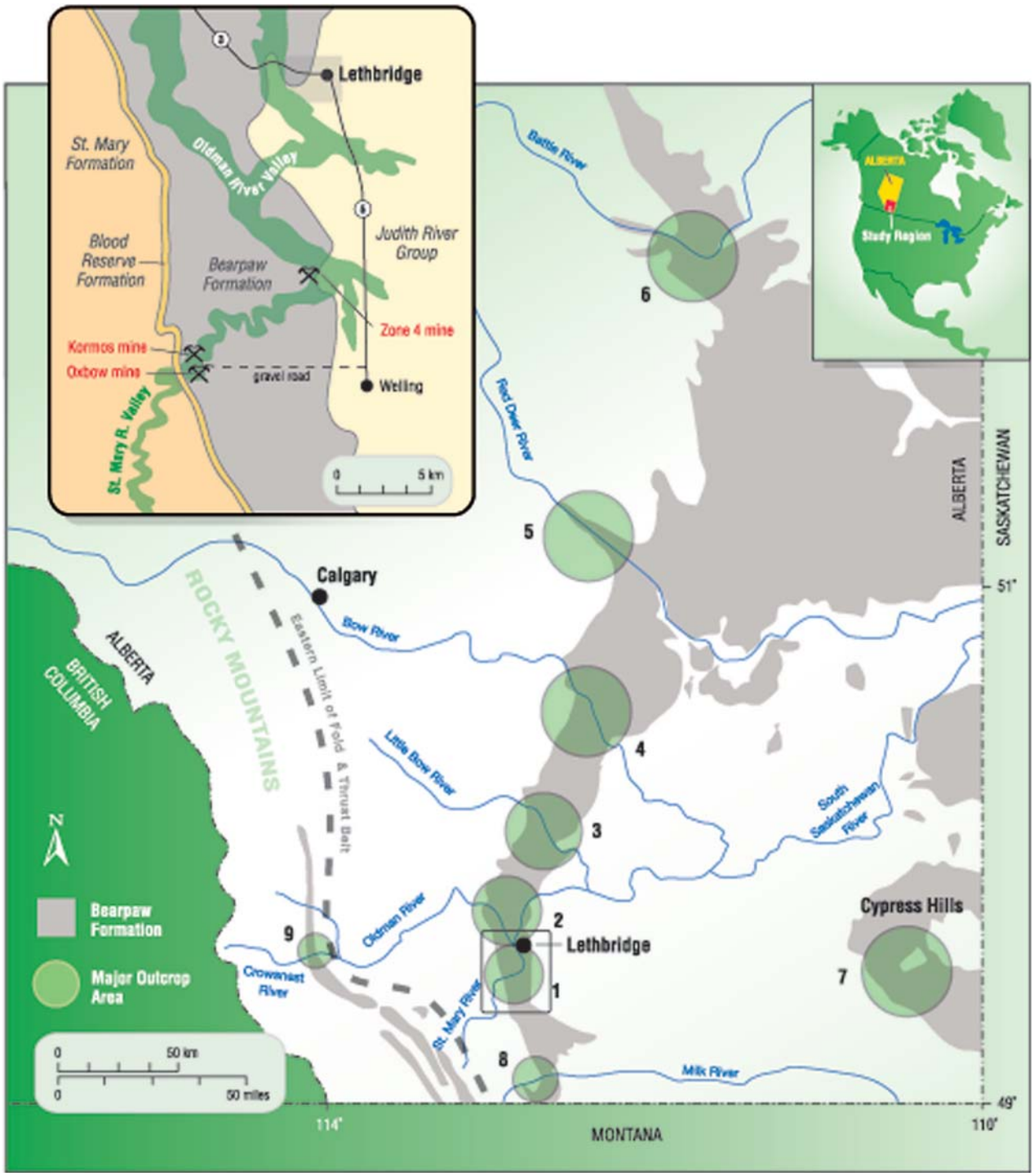

Figure 3. This map of the Bearpaw Formation of southern Alberta, Canada, shows both the bedrock geology and the location of the main Ammolite mining and collecting areas discussed in the text. Open circles represent areas of significant Bearpaw Formation outcrop, which is usually exposed in river valleys, where: 1 = St. Mary River, 2 = Oldman River, 3 = Little Bow River, 4 = Bow River, 5 = Red Deer River, 6 = Battle River, 7 = Cypress Hills, 8 = Milk River, and 9 = Crowsnest River. Ammonites can be collected at all locations, but Ammolite has only been reported from areas 1 through 5, with 1 being the best. Outcrops at 9 are located in the foothills of the Rocky Mountain fold and thrust belt. (Map modified from Tsujita and Westermann, 1998.) Inset*: This "close-up" map shows the location of the three main mine sites discussed in this article: Kormos, Oxbow, and Zone 4. All are along the St. Mary River (location 1; map modified from Ward et al., 1982).*

to the gemological research described below, we studied outcrops and collected specimens from the St. Mary, Bow, Red Deer, and South Saskatchewan rivers, as well as the Cypress Hills area.

HISTORY OF AMMOLITE AS A GEM MATERIAL

Dowling (1917) provided the first description of the southern Alberta ammonites that yield Ammolite from samples recognized in 1908. However, the first recorded use of ammonite shell as a gem material was not until 1962, by amateur lapidaries who displayed their creations at a local gem show in Nanton, Alberta (Stafford, 1973a,b). Marcel Charbonneau, owner of a Calgary jewelry store, introduced the name *Ammolite* (the first trade name for this material) in 1967. He and Mike Berisoff, a geologist from Calgary (with whom he formed Ammolite Minerals Ltd.), were the first to collect Ammolite and create doublets for commercial purposes (Hadley, 1981a,b; Barnson, 2000). Ammolite Minerals Ltd. (1967–1970) collected rough Ammolite from the Kormos family ranch along the St. Mary River, near Lethbridge; this valley remains the source for most commercial Ammolite (see Mining Operations below). However, these early assembled Ammolites developed flaws (layers would separate), so they contacted Santo Carbone, a geologic technician with the Geological Survey of Canada, to improve the cutting and manufacturing techniques. Subsequently, Mr. Carbone was the first to discover fractured (type 1) Ammolite (see below; Hadley, 1981a,b; Kraus, 1982; Brown, 1984) on the Kormos ranch, in an area that would later be labeled the K Zone. The first published description of Ammolite in a major trade magazine appeared in 1969 (Leiper, 1969).

In the 1970s, Mr. Carbone formed a new commercial venture with Dr. Wayne Bamber and Thomas McArthur, both of Calgary. They introduced a second trade name, *Calcentine*, in 1975 (Crowningshield, 1977; Zeitner, 1978; Barnson, 2000). Coined in honor of the city of *Cal*gary *cen*tennial (in 1975), the name was seldom used after 1981. In 1977, Mr. Carbone joined with Roy, Albert, and Sylvia Kormos to form Canadian Korite Gems (now Korite International). In 1979, Rene Vandervelde of Calgary (currently the chairman of Korite) purchased the Kormos family interests in Korite and brought modern business practices to the fledgling industry (Barnson, 2000). Mr. Carbone left Korite in 1980 and is currently manufacturing assembled Ammolite (see Manufacturing below). In 1981, Korite introduced a third trade name, *Korite* (Wight, 1981; Kraus, 1982; Brown, 1984). By the end of 1983, however, *Ammolite* had reappeared (Boyd and Wight, 1983; Pough, 1986). It was trademarked by Korite, who placed it in the public domain in 1997, so that *Ammolite* is now the standard designation for this material (Sinkankas, 1997).

Ammolite has also been referred to as "ammonite shell" (Stafford, 1973a,b,c) and simply as "gem aragonite" or "gem ammonite" (Barnson, 2000). *Aapaok* (*Gem Reference Guide*, 1995) was a trade name given to this material by certain members of the Blood Indian band during their brief (1980–1981) manufacture of Ammolite triplets from material obtained on their land (P. Paré, pers. comm., 2000). The first commercial appearance of Ammolite in the United States was in 1968, at gem shows in Seattle and Anaheim (Barnson, 2000). Ammolite was introduced in Germany, at Idar-Oberstein, in 1979 (Gübelin, 1980).

In the 1980s, Ammolite expanded its presence in the world market, the result not only of increased jewelry-grade supplies and improved methods of processing raw material into gemstones, but also of articles by a number of respected gemologists (Gübelin, 1980; Wight, 1981; Pough, 1986). In 1981, the CIBJO Colored Stones Commission recognized Ammolite as a gemstone, more specifically, as a "Permitted Name" in the "Variety and Commercial" columns against aragonite in their glossary (letter dated March 31, 1982 from E. A. Thomson to R. Vandervelde; Boyd and Wight, 1983; Dick, 1991). As a consequence of heavy Japanese tourism to the Canadian Rockies (in particular, Banff, Alberta) during the 1980s, which accounted for about 50% of sales of Ammolite and Ammolite triplets in 1985, this gem material became widely known in Japan ("Organic Alberta gemstone posed …", 1985; Pough, 1986). Since 1983, when mining started at the open-pit Kormos mine, high-quality material has been offered regularly at the Tucson gem shows.

By 1998, the Canadian mining industry had also recognized the economic potential of Ammolite. At that time, the government of Alberta approved 119 leasing agreements for Ammolite mining, which covered 13,350 hectares in the names of 42 individuals and companies. Nevertheless, Korite is currently the only major producer. Today, work at the Kormos mine is temporarily suspended, and production comes from Korite's nearby (0.5 km) Oxbow

Figure 4. The open-pit Oxbow mine, located on the Blood Indian Reserve, currently is the main source of Ammolite. An orange-colored backhoe, sitting directly on the K Zone (see text), is barely visible in the center of the photograph. The St. Mary River (not visible) runs along the base of the cliff in the distance. Note on the left side of the pit that the lighter soil represents alluvial deposits, whereas the underlying gray stratum is the Bearpaw Formation. The cliff on the right caps the gray Bearpaw Formation with tan-colored glacial sediments. Photo taken looking north; courtesy of Korite International.

(figure 4) and (12 km) Zone 4 mines (the latter two were activated only after arrangements were made with the Blood Indian band, which owns the mineral rights at these locations). Korite manufactures all its production into gems; it does not sell Ammolite rough (P. Paré, pers. comm., 2000). Presently, 70% of Korite's production is sold in Canada, half of which is purchased by overseas visitors ("Gemstone unique to Canada…," 1999). Elsewhere on the Blood Indian Reserve, various tribe members and groups (such as Black Horse Mines) collect Ammolite and either sell rough (to other manufacturers, such as Korite) or finished triplets (Barnson, 2000).

In 1998 Ammolite was declared to be a mineral rather than a fossil under Alberta law (Hembroff, 1998). If Ammolite had been declared a fossil, mining could have been greatly restricted or even denied on the basis of certain legislation (A. Ingelson, pers. comm., 2000).

LOCATION AND ACCESS

Southern Alberta is primarily prairie with gently rolling hills (again, see figure 4). Natural vegetation includes a variety of grasses and low-growing bushes; trees are limited to stands of cottonwood in the river valleys. The region is dry, with the principal land use being farming and ranching. Several valleys, including that of the St. Mary River, cut across the prairie landscape, exposing rocks deposited during the latter part of the Cretaceous period.

The Oxbow and Kormos mines are easily accessed by driving 15 km (9 miles) south from Lethbridge, Alberta, on Highway 5 (again, see figure 3). One kilometer north of the town of Welling, an unmarked gravel road leads to the mines approximately 10 km (6 miles) to the west, on the east bank of the St. Mary River. Prior permission to visit the site must be obtained from Korite International.

GEOLOGY AND OCCURRENCE

The living ammonite closely resembled a modern squid, and both are members of the class Cephalopoda. Ammonites populated the Jurassic and Cretaceous seas worldwide in large numbers; they were apparently victims of the same extinction event that wiped out the dinosaurs at the end of the Cretaceous period (65 million years ago). The ammonite has been compared to *Nautilus*, a distantly related cephalopod that survives today in the southwest Pacific, around places such as the Philippines, Fiji, Indonesia, and northern Australia.

Fossil ammonoids occur throughout the Bearpaw Formation in southern Alberta. The most common are *Placenticeras meeki* and *P. intercalare*, which show no particular geographic distribution patterns. Because their shells (typically 70 cm in diameter at maturity) are equally abundant in sediments originally deposited in both offshore and near-shore marine environments, they are thought to have inhabited the upper 10–30 m of the water column (Tsujita and Westermann, 1998).

To date, marketable Ammolite has been found in, and commercially exploited from, only the Bearpaw Formation of southern Alberta, which consists primarily of dark-colored marine shales that are interbedded with several sandstone units. These sediments were deposited 70–75 million years ago (during Late Cretaceous time), when the interior of North America was inundated by the Bearpaw Sea (also known as the Western Interior Seaway or the Pierre Sea), which extended from the present-day Gulf of Mexico to the Arctic Ocean (Tsujita and Westermann, 1998). Dominating the marine faunas within this seaway were vast numbers of ammonites,

whose shells are now the source of Ammolite.

Outcrops of the Bearpaw Formation are recognized in the Canadian provinces of Alberta and Saskatchewan, and in the U.S. state of Montana, where the type locality was first described and named after the Bearpaw Mountains (Hatcher and Stanton, 1903); the formation is known by a variety of other names in other states and provinces. However, there are no commercial occurrences of Ammolite outside of Alberta, although several attempts have been made to find such deposits (P. Paré, P. Evanson, and A. Ingelson, pers. comms., 2000).

At the Korite mine sites along the St. Mary River, the Bearpaw Formation is 232 m (761 ft) thick. It contains numerous bentonite (volcanic ash) layers and, in its upper two-thirds, three sandstone members: the Magrath, Kipp, and Rye Grass (figure 5). Since Ammolite is found in distinct horizons within the Bearpaw Formation, knowledge of this stratigraphy helps geologists pinpoint gem deposits.

Figure 6. A Korite employee inspects a recently uncovered ironstone concretion from the K Zone (see text) of the Kormos mine. The disk shape of this concretion is an indication that an ammonite—and therefore Ammolite—may be found within. Photo by Art Barnson, Barnson Photography.

Figure 5. This stratigraphic section of the Bearpaw Formation shows the location of important sandstone members, the double-ash (bentonite) layer, and the two known economic Ammolite-bearing horizons (K Zone and Zone 4; see text) in the St. Mary River area of southern Alberta; the lateral extent of these units is limited. Modified from Link and Childerhose (1931).

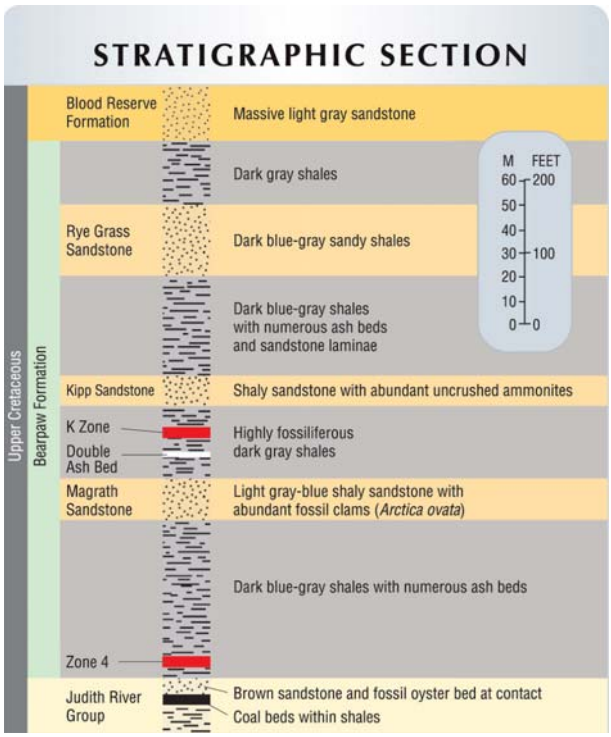

Extensive glaciation in southern Alberta during the last southerly advance (22,000–36,000 years ago) of ice as part of the Pleistocene "ice age" resulted in the deposition of glacial overburden. At the Korite mine sites, these glacial deposits are about 15–30 m thick. Fortunately, the St. Mary River has cut into both the glacial deposits and the Bearpaw Formation, exposing ammolite-bearing horizons in certain places. However, even here the Bearpaw Formation is buried under a veneer of alluvial gravels and sediments, generally 2–5 m thick. Since the formation dips 3° to 6° to the west at all Korite

The Bearpaw Formation contains numerous layers with hard siderite ($FeCO_3$) concretions. These concretions form by precipitation from an aqueous solution around a nucleus (Jackson, 1997) that is commonly a fossil, such as an ammonite. It is within such ironstone concretions that gem-quality Ammolite is typically (but not exclusively) found. The concretion's overall shape will commonly mimic the shape of its nucleus, thus giving an indication of its economic potential. For example, ammonite-bearing concretions are typically disk shaped (generally 20–60 cm, but as large as 1 m; see, e.g., figure 6), whereas round or spherical concretions rarely contain ammonites. Small- to medium-size concretions, 15–60 cm in diameter, found in the K Zone (see below) yield the best Ammolite for Korite (P. Paré, pers. comm., 2000).

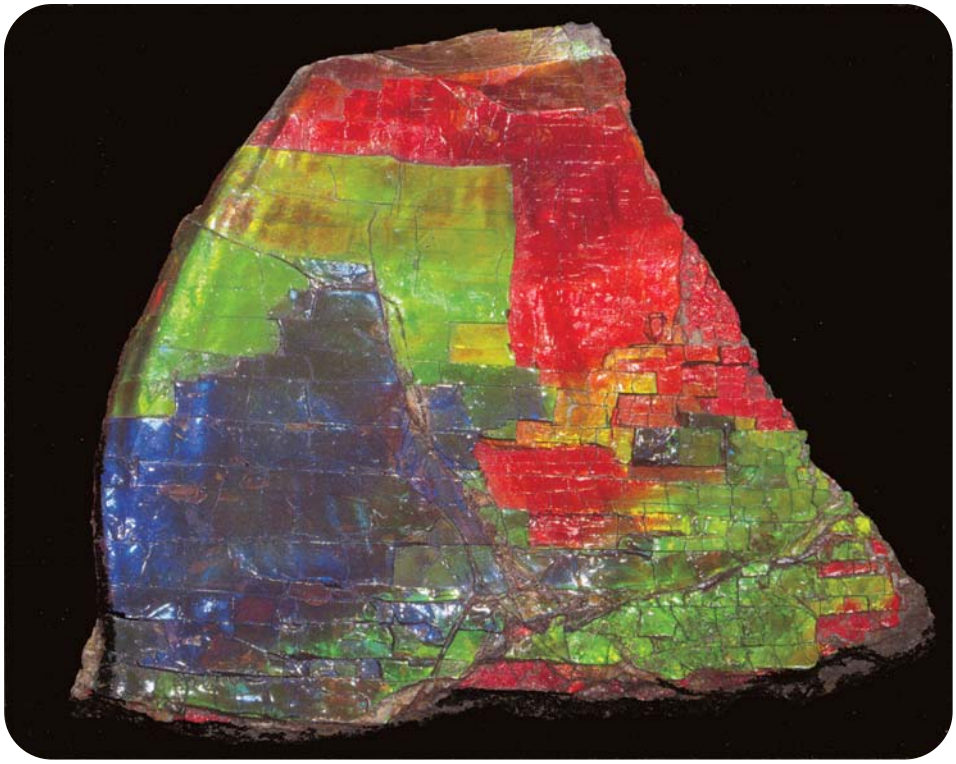

Figure 7. This exceptional specimen of Zone 4 Ammolite shows (almost) the complete color spectrum. Such material, which is of non-concretionary origin, occurs as sheets (referred to as type 2; see text) and has not been fractured by geologic processes. Note the large color panes (flat areas of uniform color), typical of type 2 Ammolite, as compared to the smaller color panes of type 1 material (again, see figure 1). The specimen is 11 cm along the longest (bottom) edge. Courtesy of Korite International; photo © Harold & Erica Van Pelt.

mine sites (P. Paré, pers. comm., 2000), the K Zone is too deeply buried under much of the neighboring territory to exploit at this time. A short distance to the east, it has been eroded away. Due to the effects of groundwater and various other natural processes (e.g., extreme temperatures, frost), the aragonite in most ammonite shells in the oxidized zone—the upper 3 m of the Bearpaw Formation, where it contacts glacial or alluvial deposits—has been converted to white calcite ("calcified ammonite"), which has no gem value.

DISTRIBUTION AND CHARACTERISTICS OF AMMONITES AND AMMOLITE IN THE BEARPAW FORMATION

General. Although fossil ammo*n*ites are found throughout the Bearpaw Formation in southern Alberta, Ammo*l*ite distribution varies widely with respect to both quantity and quality. Almost all the ammonites that produce marketable Ammolite have been mined or collected in the western part of southern Alberta. Ammolite from other parts of the Bearpaw Formation may be too thin or flaky to withstand polishing, although some can be stabilized with an epoxy resin or similar material for manufacture into gemstones (see below). Moreover, some Ammolite-bearing horizons within the Bearpaw Formation are too deeply buried to allow for commercial extraction (Korite's current open-pit mining methods are only economic to depths of 20 m; P. Paré, pers. comm., 2000). There have been many commercial failures as a result of these factors.

There is no known exploration technique (e.g., geophysical, remote-sensing) to locate or evaluate buried ammonites (although ground-penetrating radar may have potential in this regard). Only expensive test mining has proved helpful. Korite alone has excavated 20 trenches (6 m deep × 15 m wide × 5–30 m long) and 30 test pits (9 m deep × 5 m diameter) throughout southern Alberta since 1977 (P. Paré, pers. comm., 2000).

In the course of exploration and mining, Korite has identified two horizons or "zones" within the Bearpaw Formation—the K Zone and Zone 4—that contain commercial quantities of Ammolite. The company also has recognized two distinct types of Ammolite that are associated with these two zones. Type 1 is *fractured Ammolite* (same as Barnson's [2000] "compacted Ammolite"), that is, Ammolite that has undergone compaction and fracturing, with the fractures subsequently "healed" naturally with carbonate and/or clay matrix material. This type does not require stabilization for manufacture into jewelry (again, see figure 1). Ammolite from the K Zone is typically found in concretions that yield

TABLE 1. Characteristics of K Zone and Zone 4 ammonites and Ammolite.

Attribute	K Zone	Zone 4 Concretionary	Zone 4 Non-concretionary
1. Fossil specimen potential and quality of Ammolite	Poor-quality fossil specimens (due to compaction and presence within concretions); high-quality Ammolite	Poor-quality fossil specimens and lower-quality Ammolite than K Zone (constitutes 50% of Zone 4 material)	Few complete fossils; most ammonites are compacted but not fractured; high-quality Ammolite
2. Type and thickness of Ammolite layer	Type 1 (fractured); film-like to 8 mm thick in rough	Same as K Zone	Type 2 (sheet); thickness same as K Zone
3. Durability of Ammolite	Stable, does not deteriorate, resists wear with normal jewelry usage	Same as K Zone	Sheet-like material may delaminate
4. Stabilization of Ammolite	Rarely required	Rarely required	Commonly, but not always, required
5. Size of Ammolite panes (i.e., flat areas of uniform color); and thickness of healed fractures between panes	Small panes (average 2–5 mm, maximum 1 cm); fracture fillings between panes average 1 mm; in general, smaller panes with thin healed fractures result in the most durable Ammolite	Larger panes than in K Zone (average 5–7 mm, maximum 1 cm); healed fractures between panes are thicker (2–3 mm) than in K Zone Ammolite, which detracts from beauty	Relatively large panes (typically 2–3 cm, maximum 10 cm); no fractures
6. Color display of Ammolite	Red, orange, yellow, green, and blue are characteristic. "Full color spectrum" is common except for violet, which is rare	Orange, yellow, and green are most common, with no red and little blue	Same colors as K Zone (except blue is more common), but usually only two predominate

type 1 material. Type 2 is *sheet Ammolite* (same as Barnson's [2000] "noncompacted Ammolite"), that is, Ammolite that has undergone compaction but not the fracturing and subsequent healing stages (figure 7). For manufacture into jewelry, some type 2 Ammolite must first be stabilized, as it may have a tendency to delaminate. Ammolite from Zone 4 that does not originate from concretions is commonly type 2 material. Table 1 lists the characteristics of each type of Ammolite and the zone in which it is typically found.

K Zone. The vast majority of commercially available Ammolite has been derived from concretions in the K (for Korite) Zone. About 3.6 m thick, it is located approximately 120 m (400 ft) below the top of the Bearpaw Formation, between the Kipp and Magrath sandstone members (again, see figure 5) and 9–12 m (30–40 ft) above the double-ash (bentonite) layer identified by Link and Childerhose (1931), as seen in figure 8. Complete, museum-quality ammonites (such as the one pictured in figure 2) from the K Zone are very rare; most have been crushed (P. Paré, pers. comm., 2000). Both the Oxbow and Kormos open-pit

Figure 8. This view shows a cliff face in the Bearpaw Formation (the gray stratum right above the green valley floor) on the St. Mary River, 0.5 km northeast of the Kormos mine. The thin, white double-ash layer (see arrows) helps geologists locate the most important Ammolite-bearing horizon (the K Zone), which is typically 9–12 m (30–40 ft) above this marker. Also visible on the surface (tan color at the right forefront) are the glacial sediments that blanket this area. Photo taken looking north; courtesy of Korite International.

mines are positioned to take advantage of the outcropping of the K Zone.

Zone 4. This approximately 2-m-thick horizon (also known as the Blue Zone) is about 4.5 m (15 ft) above the base of the Bearpaw Formation (again, see figure 5). About half of the ammonites derived from this unit were never encased within concretions ("non-concretionary"), and these typically yield type 2 sheet Ammolite. The concretionary ammonites from Zone 4, similar to those in the K Zone, have been compacted, fractured, and healed (type 1 Ammolite) and do not need to be stabilized. However, this Zone 4 fractured material has certain features (e.g., it displays none of the red and little of the blue colors) that are less desirable than K Zone fractured Ammolite; consequently, Korite does not currently manufacture it into gemstones. The two varieties of Ammolite are also found in distinct layers within Zone 4.

THE ORIGIN OF AMMOLITE

While Jurassic and Cretaceous rocks all over the world contain abundant fossil ammonites, so far Ammolite has been obtained from only a few localities in southern Alberta and only within the Bearpaw Formation. To date, just two species of ammonite, *Placenticeras meeki* and *P. intercalare*, have yielded marketable Ammolite; other fossil ammonoids found in the same formation, such as *Baculites compressus*, have not yielded iridescent material of sufficient thickness and durability for use in jewelry (P. Paré, S. Carbone, and P. Evanson, pers. comms., 2000). These facts suggest that some unusual circumstances are responsible for the formation of Ammolite.

The Depth-of-Burial Factor. As part of our fieldwork, we collected Ammolite from various parts of Alberta and met with several individuals involved in Ammolite exploration. Our findings indicate that the quality of Ammolite improves westward in southern Alberta. For example, the colors exhibited by fossil ammonites from the Cypress Hills area (white with faint iridescence) and the Bow River area (typically red-brown)—in southeast and south-central Alberta, respectively (again, see figure 3)—are significantly less vivid than those found in ammonites along the St. Mary River valley in the southwest. As shown in Mossop and Shetsen (1994), rocks in the western part of southern Alberta (e.g., the St. Mary River area) underwent significantly more burial than those in the eastern part (e.g., the Cypress Hills area). On the basis of thermal maturation studies of organic material of the Judith River Group, which immediately underlies the Bearpaw Formation (England and Bustin, 1986), we estimate that the Bearpaw Formation was buried to a depth of about 4 km in the St. Mary River area (and has since been uplifted and exposed at the surface). The Bearpaw Formation in southeast and south-central Alberta, on the other hand, was not buried as deep.

We propose that the *increased* depth of burial resulted in a form of diagenesis (i.e., alterations undergone by sediment subsequent to deposition), as yet unidentified, on ammonite shells within the Bearpaw Formation of southwestern Alberta, specifically in the St. Mary River area. The diagenesis intensified the colors on some ammonite shells. During this process, however, the aragonite did not convert to calcite, the more stable form of $CaCO_3$, as would be expected in 70-million-year-old material. If such conversion had occurred, Ammolite would not have formed. Niedermayr and Oehner (1995) and Niedermayr (1999) suggested that high amounts of Fe and/or Mg in the Bearpaw Formation (including the concretions) might be a factor in inhibiting the conversion.

Pough (1986) was the first to suggest that alteration by burial (accompanied by compression and alteration of the organic matter within the nacre) might be a factor in the formation of Ammolite, but he did not discuss the effects of the *relative differences* in the depth of burial of ammonite shells in the Bearpaw Formation between eastern (little or no iridescence) and western (vivid iridescence) Alberta. However, P. Paré (pers. comm., 2000) has noted that only rarely can shell from *Placenticeras* ammonites obtained from the Kipp sandstone member (sandy shale; again, see figure 5) of the Bearpaw Formation, in the St. Mary River valley, be used as a source of Ammolite. This suggests that the high sand content of the Kipp member may have prevented or impeded Ammolite formation. Clues to the origin of Ammolite may also be found in the original architecture or chemical constituents (e.g., the organic component, trace elements) of the shell, since only certain ammonite species are predisposed to forming Ammolite. Additional research is needed to explain fully the process that has occurred.

Fractured (Type 1) *versus* Sheet (Type 2) Ammolite. An explanation for the origin of the two types of

Ammolite, fractured (type 1) and sheet (type 2), can be found in the rate and extent of sediment infill into ammonite shells following the death of the animal. After *Placenticeras* ammonites died, their shells sank to the bottom of the Bearpaw Sea. Some of these shells were quickly buried, with little or no sediment filling the empty shell chambers. Their internally unsupported shells were subsequently compacted and fractured (and later healed), which resulted in type 1 Ammolite (K Zone material; again, see figure 1). However, it is likely that the chambers in those shells that were not buried rapidly would have filled with sediment, so that the ammonite shell was internally supported. Such shells would resist fracturing during compaction, thus giving rise to type 2 Ammolite (sheet material characteristic of Zone 4; again, see figure 7). Ward et al. (1982) were the first to note that the lack of sediment infill into the empty chambers of *Placenticeras* shells following burial resulted in a high ratio of compacted shells in several zones; however, they did not extend this observation to the origin of fractured type 1 Ammolite within the Bearpaw Formation. Type 1 Ammolite is usually (but not always) found within ironstone concretions, whereas type 2 Ammolite is not (again, see table 1), which suggests that concretions play a role in developing the type 1 material.

MINING OPERATIONS

Surface Collecting. Since the early 1960s, Ammolite has been collected by amateurs and small commercial lapidaries from the vicinity of the St. Mary River (e.g., Stafford, 1973a). These finds occur in the riverbed and along the valley walls, where ammonites are exposed by erosion. Subsequently, Ammolite was discovered in the gravel bars of numerous other rivers throughout southern Alberta where the Bearpaw Formation is exposed (again, see figure 3); mining claims currently are held on the Bow, Little Bow, Oldman, and Red Deer rivers. We estimate that 5%–7% of current Ammolite production is derived from surface-collected material, all by small producers. An additional 2% of the total is obtained by small producers from small test pits in the Bearpaw Formation. Similarly, about 1% of Korite's production is from concretions collected on the surface in the St. Mary River valley (P. Paré, pers. comm., 2000).

Open-pit Mines. Only two mines—Kormos and Oxbow—have produced gem-quality Ammolite in significant quantities. Both are open-pit operations on the banks of the St. Mary River (again, see figures 3 and 4). Essentially all (99%) of Korite's production has come from open-pit mines, with the remainder from the surface source mentioned above (P. Paré, pers. comm., 2000). The Kormos mine was active from 1983 to 1994; since then, operations have been suspended, although long-range plans are to reactivate the mine. Production at the Oxbow mine started in 1994 and has continued to the present.

In recent years, Korite has mined between 2 and 5 acres annually to achieve a production of about 57,000 finished pieces of Ammolite and assembled Ammolite gems per year (P. Paré, pers. comm., 2001). Between 1983 and 1999, Korite excavated 40 acres of land, of which 35 acres have been restored to their natural state.

Mining Methods. Initially, the topsoil, sand, and gravel layers are stripped and stockpiled for later site reclamation. The underlying Bearpaw Formation is then excavated with a large backhoe (again, see figure 4). Blasting is not required because the shales are so easily worked. Mining is conducted from March through November, as winter operations of this type are difficult in Canada.

Most Ammolite is protected in concretions that are more durable than the surrounding shale. This has led to the development of a rather simple, but effective and economical, mining process. Korite's mining team consists of four individuals: a backhoe operator, a dump truck operator, and two sorters or "spotters." The backhoe operator excavates the shale and then "sifts out" the soft, uneconomic material with a side-to-side motion of the machine, leaving the hard concretions in the shovel. The spotter carefully observes material in the bucket of the backhoe, looking for disk-shaped concretions (figure 9), which represent only about 10% of the concretions found in the K Zone (P. Paré, pers. comm., 2000). Waste shale is removed by dump truck and also stockpiled for reclamation.

After the spotter has closely inspected the disk-shaped concretions, he uses a sledgehammer to break open those he feels have the potential for Ammolite (figure 10). The Ammolite attached to ironstone matrix is placed in "tubs," each of which holds about 45 liters of material. The Oxbow mine produces about five tubs of raw material daily (P. Paré, pers. comm., 2000). After the concretions are trimmed with hammers and a rock saw at the mine, daily production is reduced to about one tub of

Figure 9. As the backhoe removes the Bearpaw shale at the Oxbow mine, a "spotter" searches the bucket for disk-shaped concretions. Note how friable the shale is. Photo courtesy of Korite International.

Figure 10. This close-up shows a "spotter" after he has broken open a promising concretion (note the colors on the broken layer). Only disk-shaped concretions, which represent about 10% of the concretions in the K Zone, will contain Ammolite. Photo by Art Barnson, Barnson Photography.

Ammolite on matrix, which eventually is shipped to the main manufacturing facility in Calgary. The authors did observe much colorful material being rejected at the mine site and thrown back into the pit. It was explained that this material was too thin, patchy, or irregular to use in jewelry.

The mining method described above is only effective for Ammolite encased in concretions and undoubtedly would destroy less durable material. For example, Zone 4 non-concretionary (type 2 sheet) material is mined by Korite in a slightly different manner. After the overburden has been removed, excavators dig into the zone until any sign of Ammolite colors appear. Material is then collected by hand, which makes this a much slower operation. The economic potential of Zone 4 was first recognized in 1996, and mining at the Zone 4 pit began in August 1999.

Exploitation of the K Zone and Zone 4 in other areas of southern Alberta is constrained by the amount of overburden that must be removed for open-pit mining (again, see figure 8). Underground mining is not feasible in the soft, friable shales of the Bearpaw Formation.

AMMOLITE PRODUCTION

Korite has the only ongoing mechanized mining operation; all other Ammolite mining activities are artisanal, that is, small workings for which accurate records are seldom available. Thus, we are aware of no reliable production statistics for Ammolite other than those from Korite. Production of finished Ammolite by Korite consists predominantly of triplets, but there are also "solids" and doublets (P. Paré, pers. comm., 2001). Triplets (sold by size) consist of a colorless cap and a dark backing that are attached to a thin Ammolite layer (again, see figure 1), whereas doublets (sold by carat weight) are an Ammolite layer attached to a backing (without a cap). Two types of solids are produced: two-sided (Ammolite on both sides; figure 11), and one-sided (a natural assemblage of Ammolite attached to its shale backing); each is sold by the carat (see Visual Appearance below for average weights and dimensions in each category). At Korite, stabilization with an epoxy resin is applied to some, but not all, solids and doublets, but never to the Ammolite used in triplets; material derived from the K Zone is rarely stabilized (P. Paré, pers. comm., 2001). Other manufacturers have recently introduced other types of assembled stones (see Manufacturing below), but

their impact on overall Ammolite availability has not yet been felt.

Major production began in 1983, with the opening of the Kormos mine. That first year, 12,211 finished pieces were fashioned (12,004 Ammolite triplets, 183 one-sided solids, and 24 two-sided solids; none of this material was stabilized) from 20,500 tonnes of excavated shale (P. Paré, pers. comm., 2001). However, much of this early production included low-grade Ammolite that would not have been manufactured into gems in recent years (P. Paré, pers. comm., 2001). Some reports of early Korite production ("Ammolite. New gems from…", 1984; "Organic Alberta gemstone posed …", 1985; Vandervelde, 1993) suggested that less than 6,000 tonnes of shale was excavated in 1983, but this is not correct (P. Paré, pers. comm., 2001). Korite's production in 1999 (the most recent year for which Korite made data available to the authors), consisted of 55,000 Ammolite triplets, 1,500 Ammolite doublets (about 50% stabilized), 500 one-sided solids (about 50% stabilized), and only 25 two-sided solids (none stabilized); for a total of 57,025 finished stones (P. Paré, pers. comm., 2001). This production was derived primarily from the Oxbow mine, with the exception of small amounts from the Zone 4 mine and surface-collected material. At present, the Zone 4 mine contributes about 10% by volume, but only 5% by value, to Korite's overall production (P. Paré, pers. comm., 2001). The authors believe that the Korite operations represent about 90% of the production throughout Alberta. As such, we estimate that the total annual production of Ammolite (all categories) is currently more than 63,000 finished stones.

Huge amounts of rock are mined to obtain a relatively small amount of gem-quality Ammolite. In 1999, from 165,000 tonnes of excavated shale only 105,000 carats (21 kg) of Ammolite solids and assembled gemstones (including the backings but not the caps) were obtained (P. Paré, pers. comm., 2001). This is equivalent to a mere 0.64 ct per tonne of shale. Because the Ammolite layer in an average triplet is only 0.1 mm thick, the actual finished carat weight/tonne of Ammolite is, therefore, considerably less once the backing weight is subtracted.

STABILIZATION OF AMMOLITE

Stabilization—that is, impregnation of the material under pressure with an epoxy or other substance—is usually required to strengthen type 2 (sheet) Ammolite so that it can be manufactured into jewelry as solids or doublets. (As stated above, the

Figure 11. This rare two-sided solid Ammolite (3.1 × 4.2 cm) shows predominantly red and green on one side (left) and blue and green on the other. This piece was polished from unstabilized sheet material from Zone 4 and is 2 mm thick. Courtesy of Santo Carbone; photo © Harold & Erica Van Pelt.

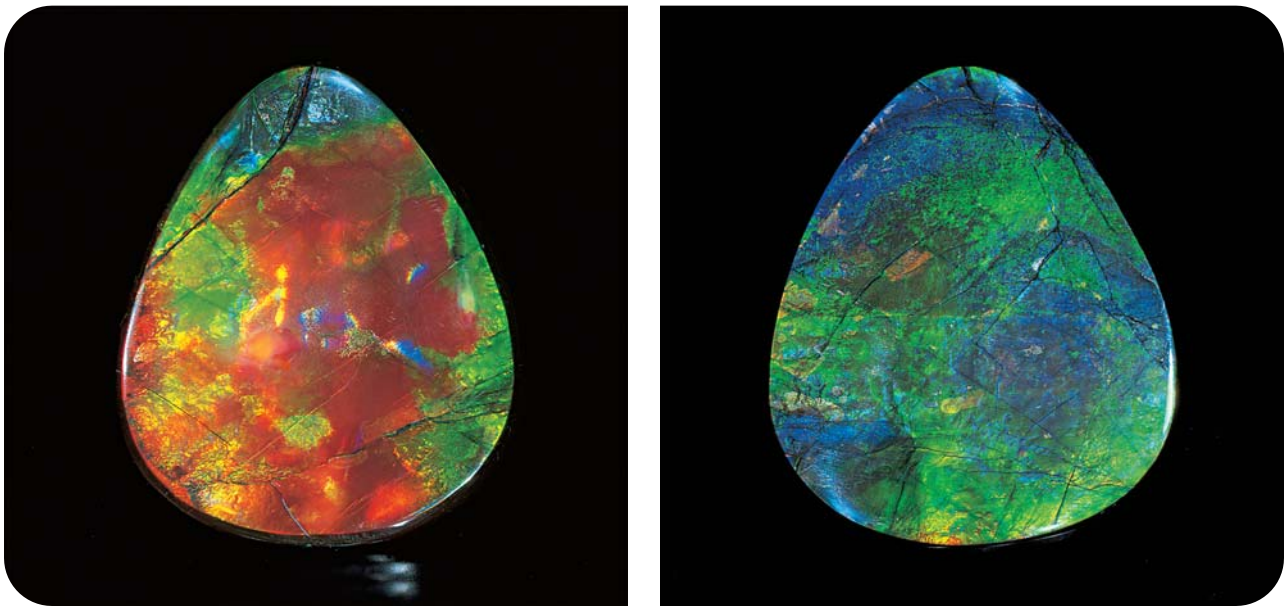

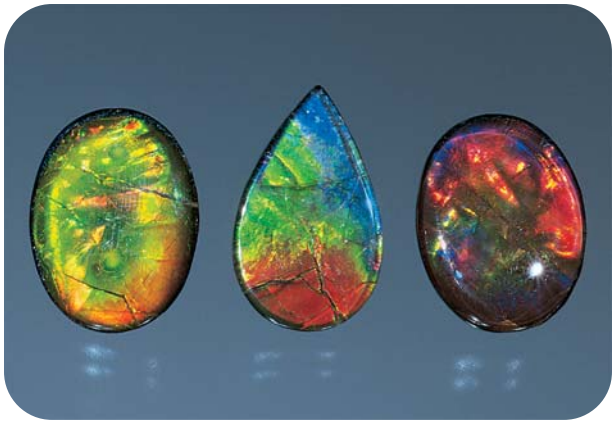

Figure 12. "Quadruplets"—here, the 1.9 × 1.5 cm oval on the left and the 2.0 × 1.5 cm oval on the right—are fashioned from two Ammolite layers with a shale backing and a synthetic spinel or quartz cap. The pear-shaped piece in the center is a triplet. Quadruplets courtesy of Santo Carbone; triplet courtesy of Korite International. Photo © Harold & Erica Van Pelt.

Ammolite incorporated into triplets is not stabilized.) Although it is likely that some Ammolite was stabilized and sold as early as the 1970s (see, e.g., Sinkankas, 1997), details of such treatments are lacking. Koivula and Kammerling (1991) were the first to document the stabilization of Ammolite, specifically a plastic impregnation that was used as early as 1989.

Figure 13. Auroralite is a patented assembled stone made by using fragments of Ammolite that are attached with epoxy to a carborundum backing and then capped with a transparent colorless material. The resulting mosaic exhibits a glitter effect. The larger of the two stones shown here measures 16 × 12 mm, and the smaller is 14 × 10 mm. Courtesy of Aurora Canadian Jewellery.

Korite began stabilizing some type 2 (sheet) Ammolite from Zone 4 in 1998. Before fashioning, Korite impregnates the rough material under pressure (1500 psi) by forcing a commercially available polymer (an epoxy resin) into the Ammolite layers with nitrogen gas (P. Paré, pers. comm., 2000). Other manufacturers may use different procedures and materials.

During the stabilization process, the entire sample is immersed in polymer. Subsequent polishing removes the epoxy on the surface, and the only remaining epoxy is between the layers. We studied six such specimens by viewing them microscopically (incident illumination) on their polished edges. It was possible to recognize the impregnation, though with difficulty, at magnifications greater than 30×. The impregnation appears as very thin seams of epoxy between the layers, and as small epoxy-filled voids.

Approximately 50% of the Ammolite solids and doublets that Korite placed on the market in 1999 were stabilized. Korite sells stabilized Ammolite for between one-third to one-half the price of untreated material of equivalent grade (P. Paré, pers. comm., 2000). The authors believe that perhaps one-third of the non-Korite production is also stabilized in some way, since it is mainly derived from surface-collected sheet material.

Some color enhancement of Ammolite triplets has been reported by Barnson (2000), where triplet backings (see Manufacturing below) are painted blue, green, or pink to enhance otherwise poorly colored Ammolite. We could not confirm use of this technique (P. Paré and S. Carbone, pers. comms., 2001). Other enhancement techniques that are effective with some gemstones, such as heat treatment and irradiation, are not applied to Ammolite as they would damage the material.

MANUFACTURING

Early descriptions of Ammolite manufacturing procedures, which were based on surface-collected materials (Stafford, 1973b,c; Jarand, 1982), are of historical interest only; for example, freeforms are no longer tumbled in sawdust. Further, early Ammolite triplets were made with surface-collected type 2 (sheet) Ammolite; many of these early gems tended to separate along the glued layers. Santo Carbone was the

first to correct these problems and perfect the manufacturing techniques that are now used to produce high-quality assembled gems. Today, the modern manufacturing facilities of Korite in Calgary, which employs about 20 full-time cutters (about 50 staff members total), dominate the production of Ammolite for the world market, although there are several smaller operations throughout Alberta.

Rough Ammolite that is sufficiently thick and durable for manufacture into solids goes through the following steps: slabbing; trimming; stabilizing, if necessary; grinding to optimum colors; polishing; and shaping. Note that the cutter will constantly grind a piece of Ammolite until it shows the most attractive color display; this delicate technique takes years of experience to perfect—too much grinding could destroy a good color suite and pattern. Material that is made into triplets (again, see figure 1) goes through a similar set of early steps, but after a first grinding to reach optimal colors (the Ammolite will still be relatively thick), a spinel or quartz cap is attached with epoxy to the Ammolite, the back of the gem material is ground again to reduce thickness, and a piece of shale (typically from the Bearpaw Formation) that has been coated with lampblack is attached with epoxy to form a backing. A final trimming provides calibrated sizes. Using much the same process, Korite will attach a natural shale backing to polished pieces of Ammolite that are too thin and fragile for use as solids to create doublets. For some of his assembled stones, Mr. Carbone uses two individual Ammolite layers together with the backing and the cap (forming an Ammolite "quadruplet"), which increases the quantity and intensity of colors in the finished piece (see figure 12). Barnson (2000) provides step-by-step details of the manufacturing process.

Mr. Carbone also creates a unique mosaic-like Ammolite "triplet" that has been marketed exclusively since 1997 by Aurora Canadian Jewellery as Auroralite (figure 13). These triplets have a glitter effect produced by a patented process (Carbone, 1991) in which multi-colored fragments of Ammolite (0.5–3 mm wide) are attached with epoxy to a synthetic spinel or quartz cap. Air trapped in the epoxy is removed in a vacuum unit and then the cap is placed in a preheated oven to harden the epoxy to a gel-like state. At this point, grains of carborundum are sprinkled on the epoxy to form the base. Recently, Johnson et al. (2000) described these triplets, which Korite had provided for examination and were erroneously attributed to their mining operation.

In recent years, other innovative uses have been found for material that is not suited for manufacture into solids or assembled stones. For example, mosaics of small Ammolite fragments have been cemented into watch faces and other forms of jewelry.

TABLE 2. Grading categories of Ammolite.

Grade	Description
Extra fine	Stone exhibits three or more sharp and brilliant colors (usually red, yellow, green, and/or blue). Colors are naturally bright with no obvious dark areas. Show of color does not depend on orientation. Fractures are in aesthetically pleasing patterns and, more importantly, are narrow. Stones with rare colors, specifically blue and purple, are most desirable.
Fine	Stone exhibits at least two distinct colors. Colors are not as bright as those in "Extra Fine" grade, and the stone may have some dark areas. Show of color does not depend on orientation. Fractures may distract somewhat from the beauty of the stone.
Good	Stone exhibits at least one distinct color or play of color. Dark areas are more apparent than in "Fine" grade material. The color may be directional. Fracture patterns may be distracting.
Fair	Colors and color changes are less distinct than "Good" grade. Colors commonly are from the middle of the spectrum, i.e., yellow and green. Directional color display is more apparent than in "Good" grade stones. Fracture patterns may be distracting. This category represents most of the current production (38%).
Poor	Faint colors or play of color, sometimes with a brown overtone; Noticeably poor brilliance.
Commercial	Dark brown or gray body color with faint color patches. May have unappealing fracture patterns. Lowest quality; currently not offered or commercially available from Korite although it is being kept in inventory.

QUALITY GRADING OF AMMOLITE

Although an internationally accepted grading system for Ammolite does not exist, Korite has developed its own in-house grading system. A number of abbreviated versions of this same system have been published (Barnson, 1996; "Gemstone unique to Canada …," 1999; Barnson, 2000).

There are six recognized grades of Ammolite as described in table 2: Extra Fine, Fine, Good, Fair, Poor, and Commercial (which correspond to Korite's AA, A+, A, A-, B, and C). The three factors in determining the grade of a polished (unmounted)

Figure 14. These three pieces of jewelry illustrate some of the many patterns seen in Ammolite, including the broad panes of individual colors in sheet material (the earrings) and the narrow fractures (pendant at upper right, 40 × 25 mm) and broader fractures (clasp at lower left, 25 × 20 mm) associated with fractured material. Earrings courtesy of Carolyn Tyler; pendant and clasp courtesy of Korite International.

Ammolite solid or assembled stone are: color range and display, intensity of iridescence, and pattern. The grade distribution, as a percent of Korite's total sales for 2000 (P. Paré, pers. comm., 2001), was: Extra Fine—6%, Fine—5%, Good—21%, Fair—38%, and Poor—30% ("Commercial" grade material was not sold).

Figure 15. Among the rarest of the patterns seen in Ammolite is this suture pattern, which mimics the internal structure of the original shell. These Ammolites (both one-sided solids) measure 4.1 × 3.1 cm and 3.2 × 2.6 cm. Courtesy of Santo Carbone; photo © Harold & Erica Van Pelt.

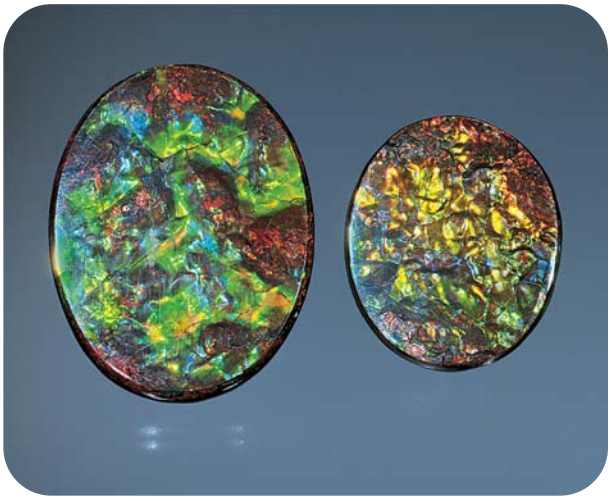

Color Range and Display. In general, the more colors displayed, the higher the grade. Thus, stones that exhibit the full color spectrum, and especially blue and violet or purple (the latter is particularly rare), are most desirable. Stones that exhibit only one color, especially entirely red or brown (which, after white, are the most common colors found on Bearpaw Formation ammonite), are less desirable.

Intensity of Iridescence. The ideal Ammolite shows sharp color sections and bright hues. Although some stones exhibit a full color spectrum, the colors may appear dark when illuminated from different directions. Such a directional display of color detracts from the beauty, and hence the value, of a stone and can generate a grade no higher than Fine.

Pattern. Pattern is the composite appearance of the color panes in relation to the dark, non-iridescent fracture system that permeates the specimen and frames them (commonly referred to as "stained glass window" effect; see figure 14 and other Ammolite photos in this article). Quality grading for pattern is usually more applicable to type 1 Ammolite. Stones with wide fractures on the surface are graded lower than stones with few or very narrow fractures. Some stones may also exhibit a "suture" pattern derived from the original shell structure (see figure 15). Although common to many types of fossil ammonites, suture patterns in finished Ammolite gems are rare.

CHARACTERIZATION OF AMMOLITE

Materials and Methods. Korite provided samples of both rough and polished Ammolite from the Oxbow and Zone 4 mines. Every variety of Ammolite was represented: fractured (type 1) and sheet (type 2); all colors, but particularly red, green, and blue; two-sided solids, one-sided solids, doublets, and triplets in various stages of production; and stabilized and unstabilized material. In addition, we studied two concretions. In total, 93 samples were subjected to some type of analysis from among many hundreds of specimens placed at our disposal by Korite. We performed visual and microscopic observation on approximately 50 additional samples.

Samples were examined with magnification ranging from 10× to 45×, usually with a GIA Gem Instruments Mark VI Gemolite microscope. Refractive indices (10 samples) were measured on a GIA Gem Instruments Duplex II refractometer with a monochromatic sodium-equivalent light source. Specific gravity (7 samples) was measured by the hydrostatic method with a Mettler H31 balance. Fluorescence (8 samples) was determined with a GIA Gem Instruments ultraviolet lamp. Thin sections—four of type 1 (fractured) and three of type 2 (sheet) material—were studied and photographed with a Zeiss Axioplan binocular polarizing microscope. Hardness (4 samples) was estimated by scratching Ammolite with calcite and fluorite.

X-ray diffraction patterns (10 samples) were obtained on a Scintag Model XDS 2000 instrument, and the data were interpreted using the Material Data Inc. "Jade XRD Processing" software package. We conducted scanning electron microscope studies with a Cambridge Stereoscan 250 instrument to determine the microstructural characteristics of Ammolite layers and their correlation with color (if any). We had 41 samples (all rough; consisting of both type 1 and type 2 Ammolite) mounted and prepared (e.g., coated with gold) "on edge" so that the horizontal layers were perpendicular to the electron beam. Only red, green, or violet/purple material was used, as these colors represent the long, intermediate, and short wavelengths of visible light as well as the range of colors found in Ammolite. An attached Kevex Micro-X 7000 Analytical Spectrometer was used for energy-dispersive elemental analysis (SEM-EDX) on 6 rough samples (three of type 1 and three of type 2), which were analyzed parallel to the upper surface. Prof. G. R. Rossman obtained visible/near-infrared spectra (2 samples) with a custom-made reflectance spectrometer.

Results. The results of our research are given in table 3 and discussed below.

Composition. The X-ray diffraction (XRD) studies confirmed that the composition of Ammolite is essentially pure aragonite; organic matter, which is undoubtedly present (see below, Mineralogy of Ammolite) is not detected by this technique. Only calcium was detected (by SEM-EDX) on the iridescent Ammolite surfaces, except for trace amounts of strontium and iron.

The material that comprises the non-iridescent

TABLE 3. Properties of Ammolite.

Property	Description
Mineral name	Aragonite
Composition	$CaCO_3$
Crystal system	Orthorhombic
Morphology (of rough)	Type 1 (fractured): Flat iridescent layers are fractured and the fractures are healed with non-iridescent material, resulting in a mosaic texture Type 2 (sheet): Flat areas have no fractures and no special features (except rare suture patterns) Thickness of layers rarely exceeds 8 mm
Iridescent color	All colors, with red and green most abundant; blue is rare and purple extremely rare
Clarity	Normally opaque; transparent or translucent in very thin sheets
Luster	Vitreous to resinous
Hardness	3.5
Toughness	Red Ammolite is relatively tough, but blue and purple are brittle
Refractive indices	Low values: 1.525–1.530 High values: 1.665–1.670
Birefringence	0.135–0.145
Specific gravity	2.76–2.84
UV fluorescence	Iridescent material inert to both long- and short-wave UV; non-iridescent healed fracture material has weak yellow fluorescence, stronger to long-wave UV
Parting	Parting along flat layers most common in rough type 2 Ammolite
Inclusions	Pyrite, organic matter; these only occur between Ammolite layers and cannot be seen from the surface of polished stones
Durability	Solids should be handled carefully because of softness and susceptibility to chemicals, household products, and excessive heat; triplets (with quartz or synthetic spinel caps) are stable under normal conditions
May be confused with	Opal, fire agate, labradorite, and various modern (e.g., abalone) or other fossilized (e.g., lumachelle) shell materials

healed fractures is also predominantly aragonite (as reported by Wight, 1981), but calcite was the main filler in some of the fractures. In addition, S. Carbone (pers. comm., 2000) has identified clay minerals (species unidentified) in some fractures, and this is consistent with our detection by SEM-EDX of Al and Si (the main chemical components of clays) during qualitative analysis of several fracture fillings.

XRD analysis of the host concretions showed that they contain siderite ($FeCO_3$), which is in agreement with Niedermayr (1999).

Visual Appearance. In the rough, type 1 (fractured) Ammolite ideally appears as a collage of vivid iridescent colors (all colors of the spectrum, with red and green the most abundant), separated by healed fractures. However, the number and quality of the colors can vary over short distances (e.g., a few millimeters). Type 2 (sheet) Ammolite, on the other hand, usually has two predominant spectral colors, which vary by the piece (color panes up to several centimeters are common). Although the iridescent areas in both types are generally less than 20 cm (~8 inches) in maximum dimension, only much smaller areas, particularly in the type 1 variety, will have uniform color, quality, or thickness. The Ammolite layers, which are supported on shale or concretionary material, may vary in thickness from about 8 mm to film-like in the same sample.

Data supplied by Korite, and verified by the authors, for fashioned material indicate that an average Ammolite triplet will consist of a 0.1-mm-thick Ammolite layer with a 1-mm-thick shale backing and a 1.5-mm-thick synthetic spinel cap, weigh a total of 2.5 ct, and measure 11 × 9 mm (oval). Average doublets have a 1-mm-thick Ammolite layer with a 2.5-mm-thick shale backing, weigh 18 ct, and measure 29.5 × 28.5 mm. An average one-sided solid also consists of a 1-mm-thick Ammolite layer, which is naturally attached to a 2.5-mm-thick shale matrix; it weighs 17 ct and measures 29 × 28 mm. Average two-sided Ammolite solids are typically 3 mm thick, weigh 15 ct, and measure 28 × 24 mm. In general, stabilized Ammolite solids and doublets are larger than their unstabilized counterparts and can range up to 50 mm (and, rarely, as large as 100 mm) in longest dimension.

Diaphaneity and Luster. Ammolite is transparent or translucent to transmitted light only in extremely thin sheets, such as those used for assembled stones. Because these always have a dark backing, however, the material seen in jewelry (including one- and two-sided solids) is opaque. Luster ranges from vitreous to resinous, and the intensity may vary considerably between samples, from very dull to intense.

Hardness. The Mohs hardness of Ammolite is 3.5; it can be scratched by fluorite (H=4) but not by calcite (H=3).

Refractive Indices and Birefringence. We recorded R.I. values for 10 polished stones, five each of type 1 (fractured) and type 2 (sheet). Five were red, four were green, and one was blue. The low values ranged from 1.525 to 1.530, and the high values measured were 1.665–1.670. We found no relationship between color and R.I. Birefringence was 0.140–0.145 in eight of the 10 samples; for two green samples—one of each type—the birefringence was 0.135, but we are unable to attach any significance to this difference. These data are very similar to those reported by Wight (1981).

Specific Gravity. The seven samples selected for S.G. determinations were all double-sided solids and predominantly red (purposely chosen to minimize any possible variance related to color). The S.G. of the four type 1 (fractured) Ammolites ranged from 2.81 to 2.84. The values obtained for the three type 2 (sheet) Ammolites averaged 2.76, 2.76, and 2.84. Wight (1981) determined the S.G. for Ammolite (type 1 from the now-closed Kormos mine; number of samples studied not stated) to be 2.80 ± 0.01. The S.G. of pure aragonite is 2.94 (*Gem Reference Guide*, 1995). The lower values presented here for type 1 Ammolite can be explained by the presence within Ammolite of small amounts of organic matter and calcite, which have lower S.G.'s; in type 2 Ammolite, voids between the layers also contribute to a lower S.G. Inclusions of pyrite (S.G. about 5), discussed below, will increase the overall S.G. of the Ammolite.

Fluorescence. Yellow ultraviolet fluorescence (long-wave stronger than short-wave) was observed only in the material healing the non-iridescent fractures of type 1 Ammolite. Whereas Wight (1981) describes this fluorescence as bright or intense, we classify it as weak.

Parting. All Ammolite may part into sheet-like layers, although type 2 Ammolite is more susceptible. Cleavage was not observed.

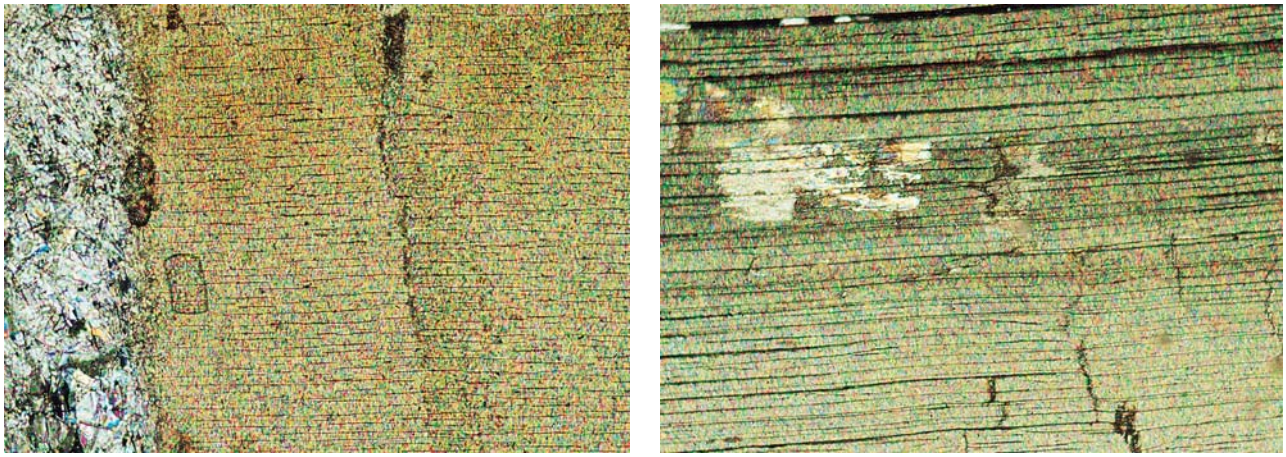

Figure 16. These two thin sections of ammolite (type 1 from the K Zone on the left and type 2 from Zone 4 on the right) were photographed in polarized light perpendicular to the flat surface (parallel to the edge) of each stone. Thin, prismatic crystals of aragonite are seen in both types of Ammolite. In the type 1 material, however, they are in laminae (layers) of limited extent arranged with a shingle effect; fractures are abundant (one is seen here on the left side of the photo cutting across the laminae at right angles) and are filled with coarse secondary aragonite and sometimes calcite and clays. The aragonite layers in type 2 Ammolite are essentially continuous; they are not interrupted by fractures. The relatively thick dark layer at the top of this photo contains organic matter (black) as well as minute disseminated pyrite grains (not visible). The shell layer in both samples is 2–3 mm thick. The width of each photomicrograph represents 2.3 mm.

Inclusions. Zeitner (1978), Koivula (1987), and Wight (1993) have reported pyrite blebs in finished Ammolite. We also identified pyrite, by XRD analysis. This was seen in small amounts in thin sections as an opaque, highly reflective, yellowish mineral that occurred as blebs or comprised very thin layers within the Ammolite. Both pyrite and organic matter (see Mineralogy of Ammolite below) occur between Ammolite layers and cannot be seen from the surface of polished stones. Stafford (1973b) and Sinkankas (1976) reported the occurrence of hydrocarbons in finished Ammolite; however this "inclusion" was artificial, in that it had been introduced by the oil-lubricated saws used to cut the earliest Ammolites.

Other Microscopic Studies. Thin sections (microscopic studies) of the nacreous layers from type 1 (from the K Zone) and type 2 (from Zone 4) Ammolites are shown in figure 16. In both cases, the microstructure shows fine laminae (layers) of prismatic aragonite crystals. In the type 1 specimen, however, these laminae are of limited lateral extent and exhibit a "shingle" structure; in addition, a natural fracture-healing material (aragonite, calcite and/or clay minerals) is evident. In the type 2 specimen illustrated, the laminae are much more continuous and are not cross-cut with fracture fillings. We believe that the material that fills fractures, and the shingle structure in the type 1 material, jointly act as a "structural support" for the aragonite laminae, so that this material can be used in jewelry without stabilization. As noted above, type 2 material lacks this structural support and may have to be polymer-impregnated before it can be manufactured into jewelry.

Scanning electron microscopy revealed additional details of the nacreous layer. As figure 17 illustrates, red Ammolite is composed of stacked columns of aragonite tablets. The aragonite tablets in green Ammolite are thinner and occur in a less organized vertical arrangement. Purple Ammolite has even thinner tablets, which show no stacking arrangement.

Discussion. *Mineralogy of Ammolite.* Shell microstructure studies of the modern *Nautilus*, fossil ammonites, and specimens from many other Mollusca (Wise, 1970; Grégoire, 1987; Dauphin and Denis, 1999) have shown that they are all composed of layers of aragonite crystals with small amounts of organic material (usually between 0.01 and 5 wt.%; Lowenstam and Weiner, 1989). This combination of thin tablets of aragonite interleaved with much thinner sheets of organic matter, frequently with a mother-of-pearl luster, is known as nacre (Jackson, 1997). Using SEM imaging, Dauphin and Denis (1999) established that the shells of living *Nautili* have three layers, each of which is characterized by

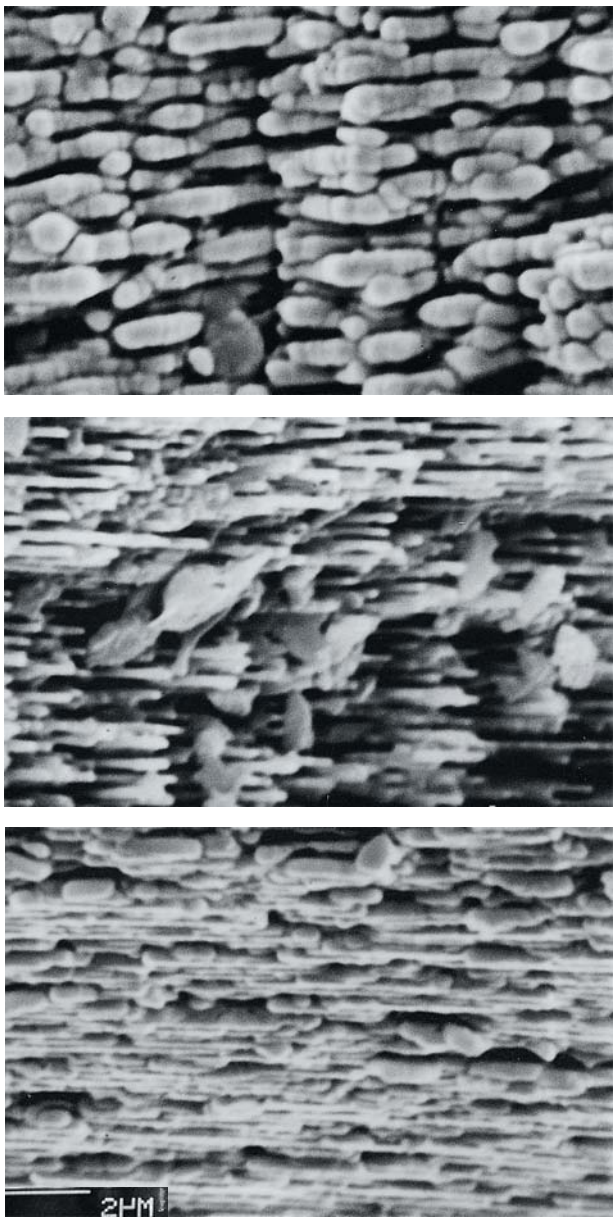

Figure 17. Distinct differences in the arrangements, sizes, and shapes of the aragonite crystals in Ammolite can be seen in the scanning electron micrographs of these representative red (top), green (center), and purple (bottom) samples. Scale bar is 2 microns.

different shapes and arrangements of crystals: (1) an outer spherulitic-prismatic layer; (2) a middle, thicker, nacreous layer; and (3) an inner, thin prismatic layer. Fossilized ammonite shells usually have only the nacreous layer preserved.

That ammonite shells were originally composed of aragonite has been known since the late 1800s (reviewed by Grégoire, 1987; Lowenstam and Weiner, 1989). We have confirmed that Ammolite is also composed of aragonite, in agreement with Wight (1981). Lowenstam and Weiner (1989) noted that the oldest known sedimentary deposit with abundant aragonite fossils dates from the Carboniferous Period (about 340 million years ago); the ammonites from which Ammolite is derived lived between 75 and 70 million years ago (see Geology and Occurrence section above).

The Microstructure of Ammolite and Its Correlation with Color. In addition to the differences in thickness and organization of the aragonite tablets noted with SEM for the different colors of Ammolite, we have also observed that Ammolites of different colors have different physical attributes, which we suggest are related to their unique microstructures. Red Ammolite is stronger (tougher, easier to manufacture into gemstones) than green Ammolite, while purple Ammolite is the weakest of all. Further, cutters (e.g., S. Carbone, pers. comm., 2000) have observed (qualitatively) that the hardness of Ammolite, at least in polishing, varies with color and decreases in the order red-green-purple. We suggest that this is another manifestation of the microstructure differences of the various colored Ammolites illustrated in figure 17. If this is the case, a corollary might be that the rarity of purple and blue Ammolite can be explained by the fact that the microstructures responsible for these colors are less likely to have survived in the natural environment due to their relative weakness.

Cause of Color in Ammolite. Several explanations have been proposed for the cause of the iridescent color of Ammolite. All the explanations fall into two basic categories: *interference* (Pough, 1986; Fritsch and Rossman, 1988; Vandervelde, 1993; Niedermayr and Oehner, 1995; Niedermayr, 1999), or *diffraction* (Leiper, 1969; Wight, 1981; Brown, 1984; Vandervelde, 1991). However, none of the above references offered experimental work to confirm either explanation. Although both interference and diffraction can produce color in minerals when white light interacts in certain ways within a specimen, the mechanism of the reaction, and its result, will be specific for each phenomenon (for more on these mechanisms, see Fritsch and Rossman, 1988, pp. 86–89).

The visible/near-infrared reflectance spectrum obtained from a piece of type 2 (sheet) Ammolite

from Zone 4 (illuminated with white light) indicates that light reflected from the yellow-green portion of the shell is more intense in a band that is centered at about 568 nm. This spectrum is consistent with what would be expected for an interference phenomenon, as light passes through and reflects back from multiple layers of aragonite of uniform thickness (G. R. Rossman, pers. comm., 2000). This model is confirmed by the observation of uniform layers in the electron micrograph of a section of Ammolite (again, see figure 17). The lack of an array of uniform grooves or ridges, such as is found in diffraction gratings, and the comparatively large width of the band in the reflectance spectrum (lack of a pure spectral color), argue against diffraction to explain the color in Ammolite (G. R. Rossman, pers. comm., 2000).

Tilting has the effect of changing the relative position of interfering light waves, thus producing a different color in most Ammolites (this is the same as directional color mentioned in the Quality Grading section). When a piece of predominantly red Ammolite is tilted, the colors change in the sequence orange, yellow, and green. When a piece of predominantly green Ammolite is tilted, blue may be obtained. There is almost no change of color when a piece of purple or blue Ammolite is tilted.

In addition, as noted above, the color of Ammolite can be shown to depend, at least to some extent, on the amount of polishing, which affects the final thickness of the nacre. Thus, if the original color of a piece of Ammolite is blue, polishing exactly parallel to the surface will change the color in the following sequence: blue-green-yellow-orange-red (see figure 7; also, P. Paré and S. Carbone, pers. comms., 2000). This corresponds to the changes shown in figure 17, and the final color will be related to the structural characteristics (including both thickness and stacking arrangement) of the nacreous layer on the surface of the polished stone.

CARE AND DURABILITY

Ammolite is used in all forms of jewelry. Because it is soft and will scratch easily, solid Ammolite is best suited for brooches, pendants, or earrings rather than rings. Since Ammolite, like pearls, is delicate and consists of aragonite, many of the care and cleaning recommendations for pearls also apply to Ammolite. Ultrasonic and steam cleaners should never be used for solids; rather, a commercial pearl cleaner or a mild, warm soap solution is recommended (a maximum of 20 minutes in any fluid). Contact with heat, acids, perfumes, hairsprays, and many household commodities can cause loss of iridescence and other types of damage, particularly in solids.

Triplets with properly manufactured synthetic spinel or quartz caps may be cleaned, with caution, in ultrasonic cleaners. Warm soap and other mild solutions may also be used, again with caution. Although the cap will protect the Ammolite from scratches, care should be taken to avoid blows that could result in the separation of glued layers.

CONCLUSION

Ammolite is vivid iridescent fossilized ammonite shell (aragonite) that thus far has been obtained from only two ammonite species (*Placenticeras meeki* and *P. intercalare*), and only from those found in the Bearpaw Formation of southern Alberta, Canada. However, to be marketable as a gemstone, the Ammolite layers must not only show attractive color and pattern, but they must also be sufficiently thick and durable to withstand use in jewelry. Because of these durability concerns, most of the Ammolite currently in the marketplace is found as assembled stones (triplets consisting of a synthetic spinel or quartz cap, a layer of Ammolite, and a shale backing). Stabilization (with polymers) is also used on some Ammolite solids and doublets.

We believe the formation of Ammolite is directly related to depth of burial of the original ammonite. Hence, Ammolite exploration should be focused on areas where the Bearpaw Formation has been buried to optimum depth (4 km in the St. Mary River area) and re-exposed due to uplift and erosion. Delineation of commercial deposits of Ammolite, however, has proved difficult (in fact, the commercial operation described in Voynick [1993] no longer exists). To date, only two horizons within the Bearpaw Formation of southern Alberta support open-pit mining, and attempts to trace them out laterally within the formation have been unsuccessful. As such, assuming current economic conditions, Korite has estimated a 15-year mine life for both the Kormos (when reactivated) and Oxbow mines (P. Paré, pers. comm., 2000). However, Reiskind (1975) did establish that some concretionary layers within the Bearpaw Formation cover an enormous area; if this is the case, future discoveries may be sizable.

For the first two decades after its introduction in the early 1960s, Ammolite languished as a gem

material primarily because of the limited supply of durable rough, the lack of uniform marketing (e.g., a multitude of trade names), and the inconsistent quality of the assembled stones. In the past two decades, as a result of the development of new mines and improved manufacturing techniques for assembled stones and stabilizing material that delaminated, Ammolite has gained recognition worldwide. With a steady future supply, and wide versatility in today's jewelry designs, we are confident that Ammolite will continue to grow in popularity. ●

ABOUT THE AUTHORS

Mr. Mychaluk is a professional geologist in Calgary, Alberta, Canada. Dr. Levinson (levinson@geo.ucalgary.ca) and Dr. Hall are professor emeritus and associate professor, respectively, in the Department of Geology and Geophysics, University of Calgary.

Acknowledgments: The authors thank Pierre Paré, president of Korite International Ltd., Calgary, Alberta, for supplying research specimens, unpublished data, permission to visit the Korite manufacturing facilities in Calgary, and access to the Kormos and Oxbow Ammolite mines near Lethbridge. Santo Carbone of Calgary kindly reviewed this article and provided unpublished data and samples. Professor G. R. Rossman of the California Institute of Technology kindly supplied the reflectance spectrum and discussed with us the origin of color in Ammolite. D. Glatiotis and M. Glatiotis, Department of Geology and Geophysics, University of Calgary, are thanked for taking scanning electron micrographs and for X-ray diffraction patterns. Thanks also to Barnson Photography of Selkirk, Manitoba, and Aurora Canadian Jewellery of Calgary for providing photographs. Discussions with Allan Ingelson of Calgary and Paul Evanson of Edmonton were very informative.

REFERENCES

Ammolite. New gems from old fossils (1984) *Southern Jeweler*, Vol. 59, No. 9, pp. 25, 31.

Barnson D. (1996) *Ammolite*. Privately published by Donna L. Barnson, Selkirk, Manitoba, Canada, 24 pp.

Barnson D. (2000) *Ammolite 2. A Guide for Gemmologists, Jewellers and Lapidaries*. Privately published by Donna L. Barnson, Selkirk, Manitoba, Canada, 116 pp.

Boyd W.F., Wight W. (1983) Gemstones of Canada. *Journal of Gemmology*, Vol. 8, No. 6, pp. 544–562.

Brown G. (1984) Korite —A unique organic gem. *Australian Gemmologist*, Vol. 15, No. 6, pp. 206–208.

Carbone S. (1991) *Composite Gem Stone and Production Method*. Canadian Patent 1281871, issued March 26, 1991; U.S. Patent 5,015,499, issued May 14, 1991.

Crowningshield R. (1977) A new jewelry item. *Gems & Gemology*, Vol. 15, No. 10, p. 312.

Dauphin Y., Denis A. (1999) Diagenèse compareé des phases minérales et organiques solubles dans les tests aragonitiques de nautiles et d'ammonites. *Bulletin de la Société Géologique de France*, Vol. 170, No. 3, pp. 355–365.

Dick G. (1991) Short in supply, long in beauty. *American Jewelry Manufacturer*, Vol. 39, No. 7, pp. 34–35.

Dowling D.B. (1917) *The Southern Plains of Alberta*. Geological Survey of Canada, Memoir 93.

England T.D.J., Bustin R.M. (1986) Thermal maturation of the Western Canadian Sedimentary Basin south of the Red Deer River: I) Alberta Plains. *Bulletin of Canadian Petroleum Geology*, Vol. 34, No. 1, pp. 71–90.

Fritsch E., Rossman G.R. (1988) An update on color in gems, Part 3: Colors caused by band gaps and physical phenomena. *Gems & Gemology*, Vol. 24, No. 2, pp. 81–102.

Gem Reference Guide (1995) Gemological Institute of America, Santa Monica, CA, 270 pp.

Gemstone unique to Canada making waves (1999) *Jewellery News Asia*, No. 176, pp. 62, 64.

Grégoire C. (1987) Ultrastructure of the *Nautilus* shell. In W.B. Saunders and N.H. Landman, Eds., *Nautilus—The Biology and Paleobiology of a Living Fossil*. Plenum Press, New York, pp. 463–486.

Gübelin E. (1980) Ammolith. Ein neuer fossiler Schmuckstein. *Lapis*, Vol. 5, No. 4, pp. 19–24 (in German).

Hadley W.D. (1981a) "Korite"—Here are more details of this amazing "new" gemstone. *Rock & Gem*, Vol. 11, No. 4, pp. 60–61.

Hadley W.D. (1981b) "Korite"—A new gemstone that's 70 million years old. *Rock & Gem*, Vol. 11, No. 3, pp. 44–46.

Hatcher J.B., Stanton T.W. (1903) The stratigraphic position of the Judith River beds and their correlation with Belly River beds. *Science*, Vol. 18, No. 5, pp. 211–212.

Hembroff W.V. (1998) Action No. 9806-00404, Court of Queen's Bench of Alberta, Judicial District of Lethbridge/Macleod, July 16.

Jackson J.A. (1997) *Glossary of Geology*, 4th ed. American Geological Institute, Alexandria, VA, 769 pp.

Jarand W.H. (1982) Processing ammonite shell. *Lapidary Journal*, Vol. 36, No. 5, p. 948.

Johnson M.L., Koivula J.I., McClure S.F., DeGhionno D., Eds. (2000) Gem news: Mosaic ammonite. *Gems & Gemology*, Vol. 36, No. 3, pp. 261–262.

Koivula J.I. (1987) Pyrite in Canadian ammonite. *Australian Gemmologist*, Vol. 16, No. 8, pp. 304–307.

Koivula J.I., Kammerling R.C. (1991) Plastic-treated Ammolite. *Gems & Gemology*, Vol. 27, No. 1, p. 52.

Kraus P.D. (1982) Korite from Alberta, Canada. *Lapidary Journal*, Vol. 35, No. 10, pp. 1994, 1996.

Leiper H. (1969) A new fossil gem is found in Alberta, Canada. *Lapidary Journal*, Vol. 23, No. 7, pp. 932, 937. Reprinted in *Lapidary Journal*, Vol. 51, No. 4, 1997, p. 39.

Link T.A., Childerhose A.J. (1931) Bearpaw shale and contiguous formations in Lethbridge area, Alberta. *Bulletin of the American Association of Petroleum Geologists*, Vol. 15, Part 2, pp. 1227–1242.

Lowenstam H.A., Weiner S. (1989) *On Biomineralization*. Oxford University Press, Oxford, 324 pp.

Mossop G.D., Shetsen I., compilers (1994) *Geological Atlas of the Western Canada Sedimentary Basin*. Published jointly by the Canadian Society of Petroleum Geologists and Alberta

Research Council, Calgary, Alberta, 510 pp.
Niedermayr G. (1994) The Bleiberg box. *Lapidary Journal,* Vol. 48, No. 6, pp. 37–40, 42.
Niedermayr G. (1999) Der Schmuckstein aus der Schale. Ammolite. In R. Bode, J. Keilmann, W. Lieber, and G. Schairer, Eds., *Von Ammoniten und Zwillingen*, Mineralientage München Messethemenheft '99 Aussstellerverzeichnis, pp. 162–168.
Niedermayr G., Oehner K. (1995) Ammolite, ein organischer Schmuckstein aus Alberta, Kanada. *Mineralien-Welt*, Vol. 6, No. 6, pp. 41–46.
Organic Alberta gemstone posed numerous mining problems (1985) *Canadian Mining Journal*, Vol. 106, No. 4, p. 11.
Pough F.H. (1986) Ammolite—Grandmother-of-pearl. *Lapidary Journal*, Vol. 39, No. 10, pp. 35–41.
Reiskind J. (1975) Marine concretionary faunas of the uppermost Bearpaw Shale (Maestrichtian) in eastern Montana and southwestern Saskatchewan. In W.G.E. Caldwell, Ed., *The Cretaceous System in the Western Interior of North America*, Geological Association of Canada Special Paper No. 13, pp. 235–252.
Sinkankas J. (1976) *Gemstones of North America, Vol. II*. Van Nostrand Reinhold, New York, 494 pp.
Sinkankas J. (1997) *Gemstones of North America, Vol. III*. Geoscience Press, Tucson, AZ, 527 pp.
Stafford P. (1973a) Ammonites and baculites in southern Alberta (part 1). *Gems and Minerals*, No. 424, pp. 32–34.
Stafford P. (1973b) Ammonites and baculites in southern Alberta (part 2). *Gems and Minerals*, No. 425, pp. 27, 42–44.
Stafford P. (1973c) Ammonites and baculites in southern Alberta (part 3). *Gems and Minerals*, No. 426, pp. 30, 31, 41–43.
Tsujita C.J., Westermann G.E.G. (1998) Ammonoid habitats and habits in the Western Interior Seaway: A case study from the Upper Cretaceous Bearpaw Formation of southern Alberta, Canada. *Palaeogeography, Palaeoclimatology, Palaeoecology*, Vol. 144, Nos. 1–2, pp. 135–160.
Vandervelde R. (1991) Ammolite, an organic gemstone from Alberta. In Z.D. Hora, W.N. Hamilton, B. Grant, and P.D. Kelly, Eds., *Industrial Minerals of Alberta and British Columbia, Canada*, British Columbia Geological Survey, Open File 1991-23; and Alberta Geological Survey Information Series 115, pp. 171–172.
Vandervelde R. (1993) Ammolite, an organic gemstone from Alberta. *Canadian Gemmologist*, Vol. 14, No. 2, pp. 53–57.
Voynick S. (1993) Gem ammonite comes of age. *Rock & Gem*, Vol. 23, No. 3, pp. 50, 53–54.
Ward G., Vandervelde R., Paré P. (1982) *Macro-Paleo Bearpaw Formation, Southern Alberta*. Trip No. 11, Field Trip Guidebook, Canadian Society of Petroleum Geologists.
Wight Q. (1993) Canadian Ammolite—The high, dry sea floor yields opal-like material. *Rock & Gem*, Vol. 23, No. 12, pp. 42, 43, 45–47.
Wight W. (1981) "Korite"—Fossil ammonite shell from Alberta, Canada. *Journal of Gemmology*, Vol. 17, No. 6, pp. 406–415.
Wight W. (1995) Canadian gemstones: Old & new. *Canadian Gemmologist*, Vol. 16, No. 3, pp. 82–87.
Wise S.W. (1970) Microarchitecture and mode of formation of nacre (mother-of-pearl) in pelecypods, gastropods, and cephalopods. *Eclogae Geologicae Helvetiae*, Vol. 63, No. 3, pp. 775–797.
Zeitner J.C. (1978) Calcentine is Ammolite is nacre. *Lapidary Journal*, Vol. 32, No. 2, pp. 622–628.

2000 MANUSCRIPT REVIEWERS

Gems & Gemology requires that all articles undergo a peer review process in which each manuscript is reviewed by at least three experts in the field. This process is vital to the accuracy and readability of the published article, but it is also time-consuming for the reviewer. Because members of our Editorial Review Board cannot have expertise in every area, we sometimes call on others in our community to share their intellect and insight. In addition to the members of our Editorial Review Board, we extend a heartfelt thanks to the following individuals who reviewed manuscripts for *G&G* in 2000:

Ms. Dona Dirlam
Ms. Cindy Edelstein
Mr. Israel Eliezri
Mr. Doug Fiske
Dr. Edward J. Gübelin
Ms. Gina Latendresse
Dr. G. Niedermayr
Dr. John Saul
Ms. Hedda Schupak
Dr. Lin G. Sutherland
Mr. Ron Vanderlinden
Dr. Christopher Welbourn

Discovery and Mining of the Argyle Diamond Deposit, Australia

By James E. Shigley, John Chapman, and Robyn K. Ellison

In 1983, the Argyle mine was established as the first major diamond-mining operation in Australia. Almost immediately, it became the world's largest source of diamonds in terms of the volume (carats) produced. The discovery, development, and operation of this mine challenged conventional beliefs about diamond geology, mineral processing, and the marketing of gem diamonds. In its peak year, 1994, the mine produced over 42 million carats (Mct) of rough diamonds, which represented 40% of the world's production. A large proportion of this staggering output consists of small brown-to-yellow—as well as some near-colorless and colorless—rough diamonds. A major cutting industry developed in India to process these diamonds into cut gems. The Argyle mine is also noted for the production of a very limited amount of rare pink diamonds.

The Argyle mine, located in a remote northeastern region of Western Australia, is currently the world's largest producer of diamonds by volume (figure 1). Production in 2000 reached 26.5 million carats (approximately 25% of annual world production), following a peak in 1994 of 42.8 million carats, which was 40% of the diamonds produced worldwide that year. The Argyle mine is known not only for the very large quantity of diamonds it produces, which vary from brown to yellow and from near-colorless to colorless (figure 2), but also for the consistent recovery of a small number of pink diamonds. Prior to 1998, no plans had been finalized for the mine to continue past 2002. In October of that year, however, a decision was made to cut back the 400 m (1,300 ft) high west wall to widen and deepen the pit. With the orebody apparently extending to depth, plans now call for open-pit mining to continue until at least 2006, with a possible transition to an underground operation at that time.

The Argyle mine provides a good example of the modern techniques used both to find viable diamond deposits and to recover the gems on a large scale. Therefore, this article discusses the exploration methods employed to discover the first economic deposits of diamonds in this area of Australia, as well as the mining and recovery techniques used at the mine. The Argyle AK1 pipe represented the first major deposit of diamonds found in lamproite (a kind of volcanic rock similar to kimberlite), the discovery of which called into question prevailing theories of diamond occurrence. We also briefly summarize the gemological characteristics of Argyle diamonds.

The Argyle mine is 100% controlled by Rio Tinto Ltd. (although until late 2000 it was a joint venture with Rio Tinto [56.8%], Ashton Mining Ltd. [38.2%], and the Western Australian Diamond Trust [5%]). It was the first large-scale operation for recovering diamonds in Australia. The ore grade is currently around 3.0 ct per tonne of host rock, which is three to 10 times higher than the typical grade at other primary diamond deposits. (Note: In

See end of article for About the Authors information and acknowledgments.
GEMS & GEMOLOGY, Vol. 37, No. 1, pp. 26–41

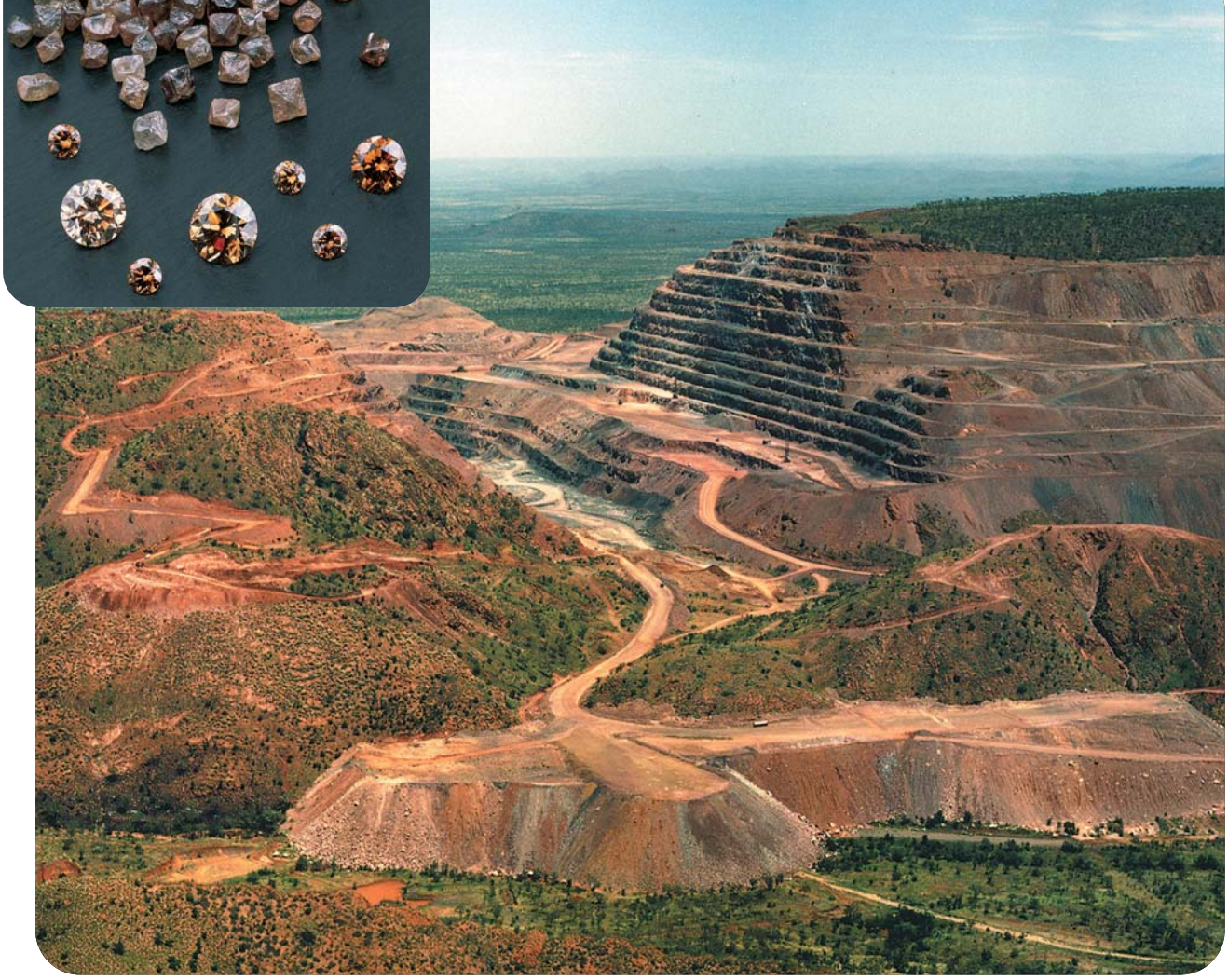

Figure 1. This aerial view of the Argyle mine, looking southwest, shows a portion of the AK1 pit. The shape of the open pit closely follows the outline of the lamproite pipe. In both the foreground and at the opposite end of the pit are dumps where the reddish brown overburden rock has been moved for storage. Since 1985, when mining of the orebody commenced, approximately 550 million tonnes of lamproite ore and overburden rock have been removed from the open pit. Brownish diamonds, such as the crystals and round brilliants shown in the inset, are commonly produced and marketed as "cognac" or "champagne" diamonds. The three largest diamonds weigh 4.11, 4.07, and 2.19 ct; inset photo by Shane F. McClure.

accordance with the usage in other diamond mines throughout the world, volumes of rock are expressed here in metric tonnes, where 1 U.S. short ton = 2,000 pounds = 0.907 metric tonnes.) However, even with this high grade, diamonds comprise only 0.0001% by weight of the ore, so sophisticated ore-processing methods are necessary to extract this very small proportion of diamonds from the very large amount of host rock. In addition, the company conducts its mining activities in an environmentally and socially responsible way.

LOCATION AND TERRAIN

Location and Access. The Argyle mine is situated in the northeastern part of Western Australia, approximately 120 km (75 miles) by road southwest of Kununurra (the nearest town), 540 km (335 miles) southwest of Darwin, and 2,200 km (1,370 miles) northeast of Perth, the state capital (figure 3). The AK1 pipe is located at the headwaters of Smoke Creek in a small valley in the southern end of the Matsu Range, which is the southeastern extension of the Ragged Range (figure 4). Associated alluvial diamond deposits occur along Smoke Creek and Limestone Creek, which drain the AK1 pipe to the north and southeast, respectively. Both drainage systems then turn northeast toward Lake Argyle, 35 km (22 miles) downstream from the mine.

Access to this region is by commercial air flight from Perth or Darwin to Kununurra, and then by a short chartered flight to a landing strip at the mine site. Alternatively, one can travel two hours by vehicle from Kununurra along a paved highway and

Figure 2. A range of colors produced at the Argyle mine can be seen in this selection of rough diamonds. Note also the variety of crystal shapes, including a relatively small proportion of octahedra and macles, and abundant rounded or irregular shapes. These crystals vary from about 0.5 to 1 ct; as such, they are larger than the crystals typically recovered from the mine, which have a mean size of less than 0.1 ct.

then on a dirt road to the site. Access to the mine site is allowed only with prior permission.

Climate and Terrain. In this region of tropical savannah, rainfall averages 700 mm (about 28 inches) per year. Most precipitation occurs in the wet season of January and February, when temperatures can reach 45°C (110°F). Local vegetation is sparse, consisting mostly of occasional small trees along with more numerous bushes and grasses. The

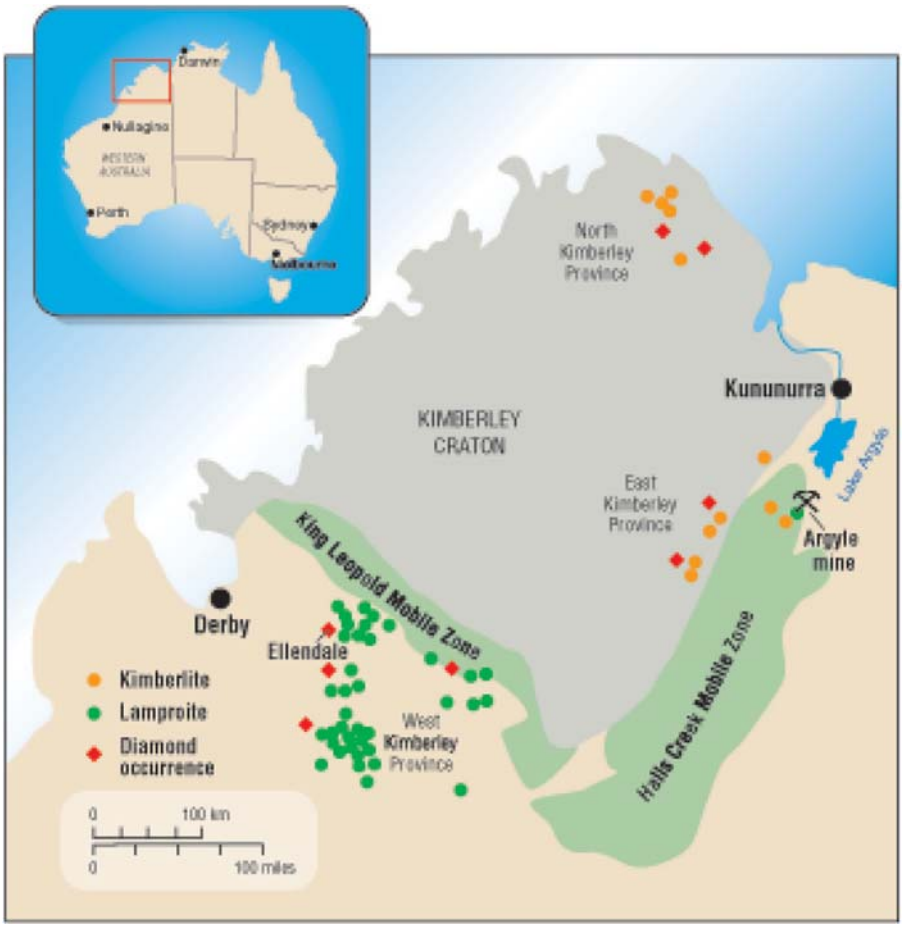

Figure 3. This generalized sketch map shows the locations of kimberlites, lamproites, and diamond occurrences in the Kimberley craton region of Western Australia. The Argyle mine is situated east of the Kimberley craton, near the eastern margin of the Halls Creek Mobile Zone. Other diamond deposits (not yet developed) are located at Ellendale to the southwest of the craton, and at two kimberlites within the northern part of the craton. The first Australian diamonds were found by gold prospectors in alluvial deposits near Nullagine (see inset) in 1895. Adapted from Atkinson et al. (1984b, figure 3B).

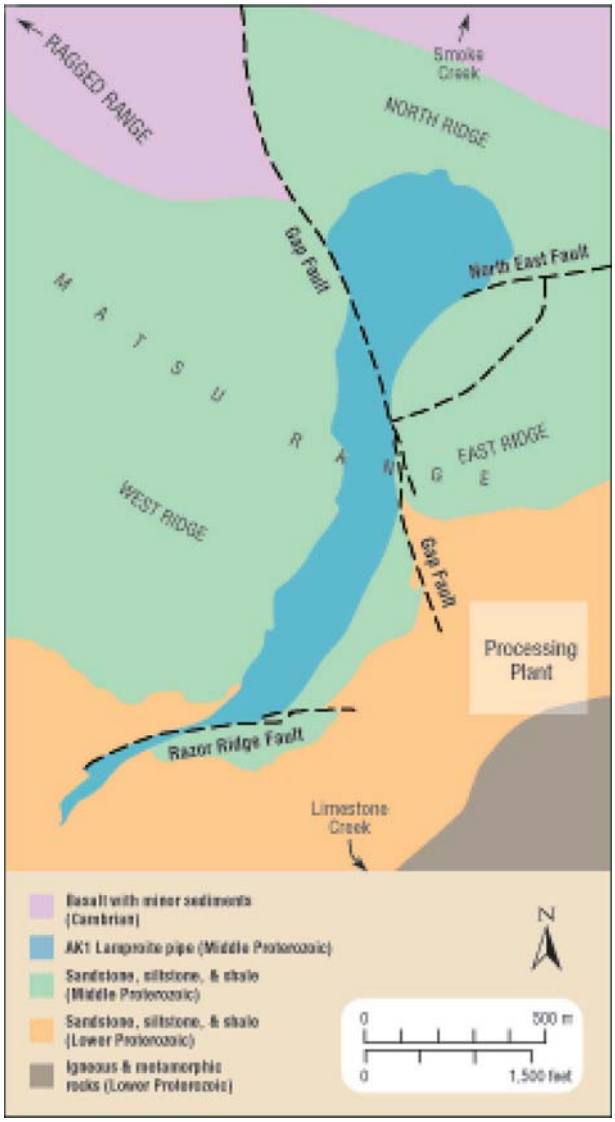

Figure 4. The tadpole-like shape of the Argyle AK1 lamproite pipe, which is broadest to the north and narrowest to the south, is evident in this simplified geologic map. The pipe is located within resistant rocks of the Matsu Range that here form the East and West Ridges.

region is characterized by the presence of bulbous boab trees and abundant termite mounds. Other than the hills of the Matsu and Ragged ranges, much of the terrain surrounding the mine area consists of broad, flat plains. This region contains a few small Aboriginal communities. All materials and supplies must be brought in from Kununurra by truck or aircraft if they cannot be generated at the mine site.

DISCOVERY OF THE ARGYLE DIAMOND DEPOSITS

Exploration for Diamond Host Rocks. In 1895, gold prospectors first found diamonds by accident in stream gravels at Nullagine in Western Australia (figure 3, inset). Many thousands of carats of diamonds were recovered from this and other alluvial deposits in various parts of the country over the next 50 years, but not until the introduction in the 1960s of modern geologic exploration concepts and techniques were diamond-bearing pipes—the primary sources—finally discovered (Geach, 1986; Janse, 1992).

Beginning in the 1970s, as a result of renewed interest in mineral prospecting in Western Australia, the geologically ancient shield areas in this region were selected as prime targets for diamond exploration. A shield area, or craton, is a portion of the continental crust that has been geologically stable (i.e., not involved in mountain building, faulting, deformation, etc.) for billions of years. The geologic settings of the diamondiferous kimberlite pipes in southern Africa were used as models for the selection of shield areas in Western Australia for diamond exploration (see Jaques et al., 1986; Haggerty, 1999).

Although kimberlites were believed to be the only terrestrial source of diamonds at the time, Prider (1960) had suggested that a petrologically related volcanic rock known as lamproite might also host diamonds in this part of Australia. Both the discovery of alluvial diamonds at Nullagine and the occurrence of lamproites along the tectonic margins of the (ironically named) Kimberley craton (in northern Western Australia) were additional reasons for selecting the shield areas of Western Australia for diamond exploration (figure 3). Clifford (1966) had observed that the known diamondiferous kimberlites in southern Africa were restricted in their occurrences to ancient cratons that had been tectonically stable for at least the past 1.5 billion years. This condition was met, at least in part, by the geologic conditions of the Kimberley craton (Deakin et al., 1989).

Following the discovery of several alluvial diamonds in the West Kimberley region along the Lennard River (Ellendale area) in 1969, a consortium of mining companies, collectively known as the Kalumburu Joint Venture (succeeded by the Ashton Joint Venture), began systematic diamond exploration throughout this region. Their objective was to discover an economic diamond deposit that would be amenable to mechanized, large-scale, low-cost,

Figure 5. Two geologists sample stream gravels in a remote portion of the Kimberley region in Western Australia to locate diamond indicator minerals. The size of the region, and its remoteness, meant that a helicopter was needed to reach sites targeted for diamond exploration. Here, the geologists are excavating a heavy-mineral sample from gravel trapped behind a natural rock dam in a creek. A special geologic laboratory was set up in Perth to evaluate the mineral content of such samples.

open-pit mining. Since only minor quantities of alluvial diamonds had been recovered from this region during the previous century, with no primary diamond sources known at the time, these exploration efforts in the Kimberley craton were highly speculative. Nevertheless, early in 1976, geologists from this consortium found certain minerals (such as ilmenite, chromite, chrome diopside, and pyrope garnet) in stream-gravel concentrates which indicated the presence of diamond-bearing host rocks.

To reduce the need for costly bulk-rock sampling, geologists devised rapid evaluation methods to check gravel samples for these diamond indicator minerals (figure 5). Reconnaissance alluvial sampling using these techniques over an area of 200,000 km^2 revealed a classic suite of kimberlite indicator minerals—as well as a different suite of minerals that are now known to be characteristic of lamproites (although their significance was not recognized immediately)—at several locations within and around the Kimberley craton.

Careful geologic fieldwork, combined with airborne magnetometer surveys and subsequent testing for the presence of diamondiferous host rocks, led to the eventual discovery by a number of companies of more than 80 kimberlite and lamproite occurrences within and around the Kimberley craton. To date, however, only one of these occurrences, the Argyle deposit, has been developed into a mine. Other potentially significant diamond occurrences, which at present are being evaluated for their economic viability, are two lamproites located at Ellendale in the West Kimberley province and two kimberlites in the North Kimberley province. In most of these instances, the diamondiferous rocks were discovered in strongly deformed tectonic belts along the margins of the Kimberley craton, and not within the rocks of the craton itself.

Discovery of the Argyle Pipe and Alluvial Deposits. In August 1979, following almost eight years of geologic exploration in the Kimberley region, two diamond crystals were found in a 40 kg sample of gravel collected in Smoke Creek. Further sampling upstream led to the discovery of alluvial deposits along this creek. Then, in early October 1979, the exploration team reached the headwaters of Smoke Creek, which drains a small northward-facing valley in the Matsu Range, and found a large, high-grade primary diamond deposit in an olivine lamproite that is now referred to as the AK1 pipe (figures 4 and 6). The separate Limestone Creek alluvial deposit was identified two years later, after the completion of further gravel sampling in the area.

GEOLOGIC SETTING OF THE ARGYLE MINE

The Kimberley craton consists of a central core of a thick series of nearly flat-lying sedimentary and volcanic rocks that were deposited between 1.9 and 1.6 billion years ago. These rocks form the Kimberley Plateau. They are underlain by a basement of crystalline igneous and metamorphic rocks, which are not exposed on the surface of the plateau. Recent investigations have indicated that the basement is of Archean age, that is, more than 2.5 billion years old (Graham et al., 1999). This central Archean craton is bounded along its southeastern margin by the Halls Creek Mobile Zone (geographically called the East Kimberleys), and along its southwestern margin by the King Leopold Mobile Zone (geographically called the West Kimberleys; again, see figure 3). Diamondiferous kimberlites have been found on the central Archean craton, whereas diamondiferous lamproites have been found in or near the associated mobile zones. This came as a great surprise to geolo-

gists at the time, because—apart from alluvial deposits—significant quantities of diamonds were only known to occur in kimberlites located on Archean cratons (Clifford, 1966; Janse, 1992). The diamondiferous rocks of both types occur as volcanic dikes, pipes, and crater deposits—which are typical modes of emplacement for kimberlite and lamproite magmas (Hawthorne, 1975; Mitchell, 1986, 1989).

Geologic Setting of the Argyle AK1 Pipe. The AK1 olivine lamproite pipe (or diatreme) is located approximately 7 km (4.5 miles) west of the Halls Creek Fault, which forms the eastern boundary of the Halls Creek Mobile Zone (Boxer et al., 1989). This mobile zone is formed by an exposed basement of crystalline metamorphic rocks intruded by later granites, which range in age from 2.5 to 1.8 million years; that is, they are younger than the rocks of the central Archean Kimberley craton. Rocks in the Halls Creek Mobile Zone have been strongly deformed by faulting and folding, and form a landscape of flat plains and low ranges. The northern part of the belt is overlain by northerly dipping sedimentary and volcanic rocks that range in age from 1.5 billion to 500 million years; some of these form the Ragged Range, which rises up to 450 m (1,500 ft) above the basement plain. The Argyle pipe intruded these younger rocks along a pre-existing fault. The diamond deposit was preserved from erosion by resistant outcrops of these rocks, which enclose the upper part of the pipe and the crater. In areas further south, where the host rocks have been eroded, similar pipes and craters have been worn down to a root zone of a few dikes and stringers, such as the Lissadell Road Dike Zone (Janse, 1992). For a discussion of the structures of a pipe and a diatreme, see Kirkley et al. (1991).

Figure 6. This 1983 aerial photograph (looking northeast) shows the valley in the Matsu Range (slightly to the left of center here) where the Argyle AK1 lamproite pipe was discovered after extensive regional exploration for diamonds. Lake Argyle is visible in the distance. The orientation of this photograph, which was taken before diamond-mining operations began, is opposite that of the photo in figure 1. Today, most of this valley floor is occupied by the Argyle open pit.

DESCRIPTION OF THE DIAMOND OCCURRENCE

The AK1 Pipe and a Model for Its Formation. In cross-section, the AK1 pipe exhibits the typical carrot-like structure of a diatreme. When first discovered, the pipe occupied the entire valley floor along Smoke Creek. The pipe itself is not oriented vertically, but is tilted northward at an angle of approximately 30°. Its outline on the surface resembles the shape of a tadpole, with its enlarged "head" to the north and its narrower "tail" elongated in a southerly direction. It is almost 2,000 m (1.2 miles) long, and it varies in width from approximately 600 m (1,950 ft) at the head to 150 m (500 ft) along the tail (see figure 4). This elongate shape is thought to have resulted from post-intrusion faulting and the regional tilting of the pipe.

When found, the AK1 pipe had a surface area of about 50 hectares (~125 acres). However, it is brecciated and fault-bounded on several of its outer contacts, so the original intrusion may have been larger. Radiometric dating (using the rubidium-strontium and potassium-argon methods) of the lamproite rocks within the pipe indicates an emplacement age of 1.178 −0.047 billion years (Pidgeon et al., 1989). The diamonds themselves are age-dated at approximately 1.58 billion years (Chapman et al., 1996). Geologic study has revealed the presence of both tuffaceous and magmatic varieties of lamproite within the pipe (derived from volcanic ash falls and magma crystallization, respectively; Jaques et al., 1986, 1989b,c).

According to a geologic model proposed by Boxer et al. (1989), the lamproite magma that formed the AK1 pipe rose within a zone of weakness in the crust along the mobile belt into overlying quartz-rich sediments. Subsequent interaction of the heated magma with groundwater in these permeable sediments resulted in a series of volcanic explosions

Figure 7. In this view looking northeast from the AK1 lamproite diatreme, one can see the area where initial mining for alluvial diamonds took place, in the loosely consolidated gravels along the drainage system of Smoke Creek.

over an extended period of time, which produced the rocks within the pipe itself. Ejection of large amounts of magma, accompanied by the downward migration of the explosive activity within the pipe, produced a subsidence of the volcanic rocks and surrounding sediments. In turn, this led to the formation of a volcanic crater that eventually filled with groundwater as well as with ash and sediments. More detailed descriptions of the geology of the AK1 pipe can be found in Atkinson et al. (1984a,b), Boxer et al. (1989), Jaques et al. (1986, 1989b,c), Janse (1992), and Smith (1996).

The Associated Alluvial Deposits. As the result of erosion of the orebody over geologic time, diamonds were distributed along the entire length of Smoke Creek (which drains the pipe to the north) from the headwaters (at the pipe) to where the creek enters Lake Argyle (35 km to the northeast; see Deakin et al., 1989). These alluvial diamonds occur in coarse, poorly sorted, massively bedded, and loosely consolidated gravels (figure 7). The diamondiferous areas are divided into the Upper and Lower Smoke Creek deposits, with the former extending the first 2–3 km from the pipe, and the latter extending further downstream. These alluvial beds vary from 1 to 1.7 m (3 to 5 ft) in thickness. Both the Limestone and Gap creeks drain the pipe to the southeast, and their alluvials initially form steep, piedmont fan-type sediments, followed by low terrace and floodplain sediments that can range up to 3.5 m (11 ft) in thickness.

The alluvial deposit contains a range of diamond qualities and sizes, which vary with the distance from the source and the degree of erosion. The ore grade of these alluvial deposits drops off dramatically at distances beyond approximately 10 km downstream from the headwaters of each creek.

ECONOMIC EVALUATION OF THE ARGYLE DEPOSIT

Evaluating Diamond Deposits. As mentioned earlier, diamonds represent only an extremely small percentage of the host kimberlite or lamproite (typically one part per million [5ct/tonne] or less). Determination of the economic viability of a deposit requires an assessment of both the grade of the ore (i.e., how many diamonds it contains), and the average value of the diamonds within the deposit. Both provide a value for each tonne of ore, which is then compared with the costs of recovery and processing to determine if the deposit can be mined economically.

Mining companies face several technical challenges in their attempt to assess the ore grade of a diamond deposit. Since diamonds form discrete crystals that are disseminated at very low concentrations in the host rock, a large amount of material must be sampled (i.e., by large-diameter core-drilling or mechanized excavation) to obtain a statistically significant quantity of diamonds. Such large host-rock samples (each weighing several tonnes) are expensive to excavate and process, especially in remote regions. In addition, numerous drill samples are typically needed to assess the overall spatial extent of the potential orebody.

Evaluating the Argyle Primary and Secondary Deposits. At the AK1 pipe, the mining consortium determined that 2,000 carats would be statistically sufficient to provide an estimate of the value ($/ct) of the diamonds. The evaluation program was conducted between September 1980 and November 1983. First, 182 holes were drilled in a systematic grid pattern both to examine the lamproite orebody and to delineate its outer limits for use in estimating the total amount of ore present (known as the ore reserves). Then, 91 larger-diameter holes were drilled within the orebody to estimate the grade

(i.e., carats of diamonds per tonne) in the ore reserves using standard geostatistical methods.

This evaluation program revealed that only the southern part of the pipe was economically viable. The resulting estimate was that 60 million tonnes of ore, containing 6.8 ct/tonne of diamonds (the proven reserves), and 14 million tonnes at 6.1 ct/tonne (the probable reserves), occurred to a depth of 350 m (1,150 ft) below the surface. These ore grades are the highest known for any primary diamond pipe (a typical grade at other mines—such as at the Premier, Finsch, and Kimberley mines in South Africa—is on the order of 0.5 to 1 ct/tonne).

The final step in the evaluation program involved bulk sampling of the lamproite to identify the best mechanical techniques to liberate the diamonds from the host rock. By the end of 1982, approximately 400,000 carats of diamonds had been recovered from 60,000 tonnes of ore.

During the same period as the evaluation study, a feasibility study was undertaken to establish the most economical plan by which the AK1 orebody could be mined to sustain at least a 20-year mine life. As part of both studies, the associated alluvial deposits were tested by a program of systematic trenching. Representative sediment samples collected from these trenches were processed through a small-scale heavy-media separation plant to recover any diamonds. Prior to the start of mining in early 1983, probable ore reserves in the alluvial deposits were demonstrated to be 2.5 million tonnes, with grades between 3.0 and 4.6 carats of diamonds per tonne.

As the result of the evaluation and feasibility studies, the company decided on a two-phase development program: (1) initial mining, using the small-scale plant, to recover diamonds from both the alluvial deposits and the loose rock on the surface above and around the perimeter of the AK1 pipe; and (2) mining of the lamproite orebody itself. Concurrent with the first phase, construction began on a large-scale commercial recovery plant, so that the mine could operate on a 24-hour-per-day, 7-day-per-week schedule, to process ore recovered during the second phase.

Mining of the alluvial and surface deposits began in 1983. By the end of 1985, more than 17 million carats of diamonds had been produced. At that time, exploitation of the AK1 pipe began, with the expectation that the mine would process 3 million tonnes of ore—and as much as 25 million carats of diamonds—per annum. As of January 2000, the remaining proven AK1 ore reserves were 61 million tonnes of lamproite ore with an average grade of 2.9 ct/tonne.

Removal of Overburden. As mentioned above, the diamonds were first discovered at the mine site in a small valley at the headwaters of Smoke Creek. Initial drilling established that the extent of the lamproite pipe was actually larger than the area of this small valley; portions were overlain by hills of the Matsu Range (the ridges on both sides of the valley seen in figure 1). To widen the pit enough to reach these portions, it was necessary to cut back the sides of these hills at a specific angle. Thus, a very large amount of non-diamond-bearing overburden had to be removed, which formed a crucial component in planning the operation of the mine. It costs just as much to excavate a tonne of waste overburden as it does to remove a tonne of lamproite ore.

Drilling and explosives are used to break up the overburden and ore (figures 8 and 9). A large mechanized shovel loads the material into a truck for

Figure 8. Mobile drill rigs at Argyle make holes for the explosives needed to mine the ore.

Figure 9. At Argyle, explosives are used to break up the lamproite ore and its overburden, so that it can be removed more easily.

transport either to the processing plant if it is ore, or to the waste storage area if it is overburden (figure 10). The trucks can haul 180–240 tonnes of rock per load. Five shovels are currently in operation, each of which costs US$7 million; there are 18 trucks, each of which costs approximately US$3 million.

One of the fortuitous features of the Argyle mine is that until recently much of the extracted ore was located above the surrounding plain, so that a "hill" of ore was gradually leveled as mining progressed, rather than the ore having to be hauled up from a pit. The cost of transporting rock downhill (the recovery plant is located in the plain south of the Matsu Range) is substantially cheaper than hauling it uphill. At the mine's present level within the pit, however, approximately 7.5 tonnes of overburden must be removed to reach one tonne of the diamondiferous ore. Eventually, the cost to recover a carat of diamonds will exceed the value of those diamonds, and the mine will no longer be economic. If the lifespan of the mine is to be extended, alternative recov-

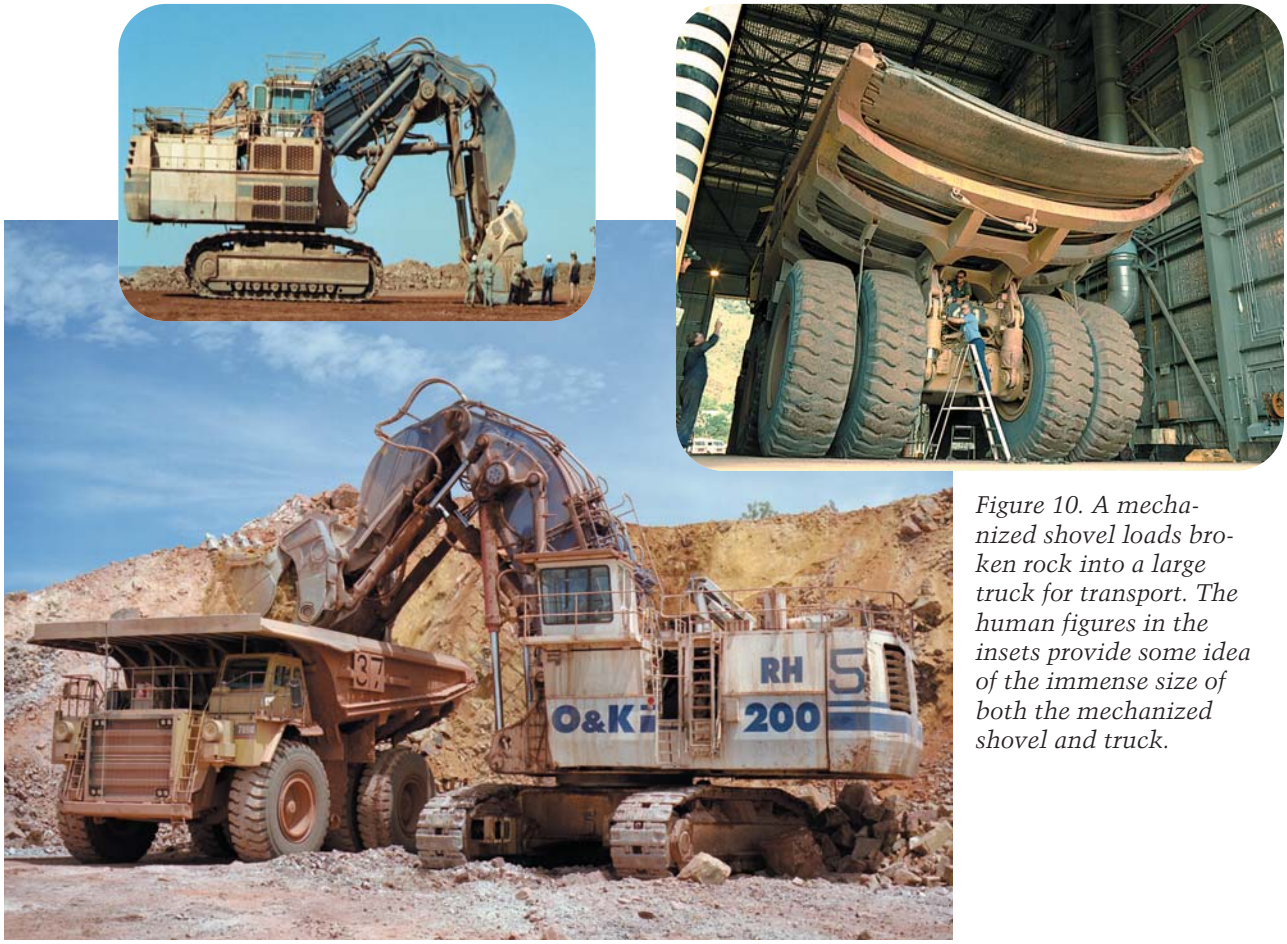

Figure 10. A mechanized shovel loads broken rock into a large truck for transport. The human figures in the insets provide some idea of the immense size of both the mechanized shovel and truck.

TABLE 1. Argyle diamond production from primary (AK1 pipe) and secondary (alluvium) sources, 1982–2000.[a]

Production	1982	1983	1984	1985	1986	1987	1988	1989	1990	1991	1992	1993	1994	1995	1996	1997	1998	1999	2000	**Total**
AK1 pipe																				
Ore processed (Mt)	—	—	—	0.4	3.2	3.5	4.7	4.9	5.1	6.0	6.8	7.0	7.9	8.9	10.2	10.4	11.2	9.5	10.4	110.1
Diamond production (Mct)	—	—	—	1.7	29.2	30.3	34.6	32.8	31.7	33.4	36.6	38.4	39.7	37.5	39.4	38.6	38.9	27.8	25.4	516.0
Alluvium																				
Ore processed (Mt)	0.1	1.1	1.5	1.1	—	—	—	0.8	1.9	1.3	3.5	3.9	4.6	5.3	6.8	5.9	6.3	5.9	4.9	54.9
Diamond production (Mct)	0.3	6.2	5.7	5.3	—	—	—	1.6	2.1	1.6	2.5	2.5	3.1	2.4	2.6	1.6	1.9	1.9	1.1	42.4
Total diamond production (Mct)	0.3	6.2	5.7	7.0	29.2	30.3	34.6	34.4	33.8	35.0	39.1	40.9	42.8	39.9	42.0	40.2	40.8	29.7	26.5	558.4

[a] *Source: Argyle Business Services. Abbreviations: Mct = million carats, Mt = million tonnes; a dash indicates no ore processed or diamonds produced.*

ery methods (such as underground mining) must be used. At the present time, company management is evaluating how best to proceed with underground mining to ensure optimal cost effectiveness.

RECOVERY OF THE DIAMONDS

Table 1 and the bar chart in figure 11 illustrate the enormous quantity of diamonds produced annually from the Argyle mine. Separating diamonds from kimberlite or lamproite ore requires a primarily mechanical, multi-step liberation process (figure 12). In general, the ore must be broken down into progressively smaller pieces (figure 13), until the diamond crystals can be physically removed with little or no damage. At the Argyle mine, this process involves five basic operations:

1. Crushing the ore (in several steps)
2. Scrubbing the broken rock fragments with water to remove dust
3. Screening the ore into specific size fractions
4. Starting from a particular size fraction of the ore, concentrating the diamonds and other heavy minerals (e.g., garnet) using a heavy medium
5. Separating the diamonds from the other heavy minerals by means of X-ray luminescence technology

In the final step, X-rays are used to make the diamonds luminesce. An optical sensor triggers a blast of air to remove each diamond from the concentrate. These X-ray sorters, which were developed specifically for use at the Argyle mine, can detect approximately 200 diamonds per second at peak sorting rates.

Virtually the entire processing operation is mechanized, with almost all of the machines monitored and managed from a central control room. As a result, very few workers (other than maintenance personnel) can be seen around the processing plant outside the central control room and the diamond recovery building.

SOCIAL AND ENVIRONMENTAL ISSUES

Personnel. Development of the Argyle mine was not limited to technical and engineering challenges; there was also the major issue of obtaining a skilled workforce at the mine site. Because of the mine's extreme isolation, it was decided that, rather than construct a new town to house the mine staff and their families, workers would be brought from Perth (a three-hour flight) for a two-week working shift.

Figure 11. This bar chart shows the amount of diamonds produced on an annual basis at Argyle during the period 1982 through 2000.

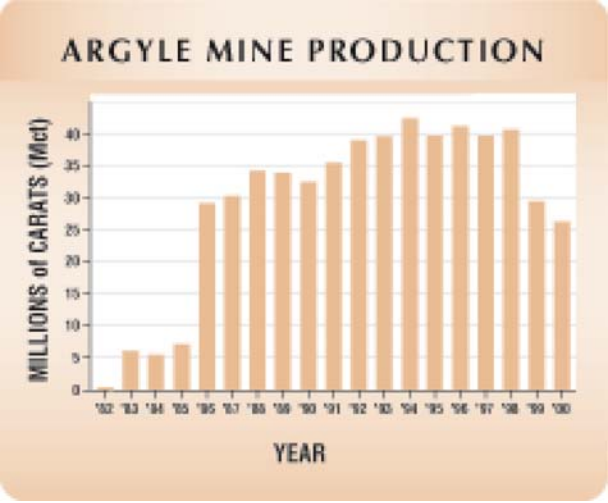

Figure 12. Processing of the diamonds at Argyle is a highly mechanical multi-step process. This view of the processing plant, looking southwest, gives some idea of the size of the operation (which covers 16.3 hectares).

Originally, the mine managers were located at nearby Kununurra and commuted daily by air to the mine; in recent years, this has changed to a weekly commute from Perth. During the mine's peak years, there were some 800 employees. Today, there are some 750 permanent and contract employees and about 300 working on site at any one time. During their two-week shift, workers stay at a permanent village located a short distance from the mine site, where there are both living and recreational facilities. At the present time, mining operations take place on a 24-hour-a-day, 7-day-a-week schedule.

Protecting and Rehabilitating the Local Environment. Efforts to minimize the negative impact of mining operations on the local environment and communities began at the outset and continue to the present time. These efforts include:

1. Minimal disturbance of the local environment (protection of local vegetation, water conservation and reclamation, and regular assessment of water quality in streams and groundwater in the surrounding area)
2. Appropriate consultation with Aboriginal traditional owners
3. Rehabilitation of areas where mining has been completed
4. Limitation of the emission of greenhouse gases
5. Use of hydroelectric power
6. Prompt reporting of any environmental incidents to local authorities

Because of these efforts, the Argyle mine was awarded an ISO (International Standards Organization) 14001 certification in 1997. This provides independent verification that the mine operators are following international best practices with regard to environmental management.

Final Disposition of the Mine Site. Although, as noted above, open-pit mining is planned only until 2006, underground operations could extend the life of the Argyle mine to 2018. Whatever the future operations,

eventually the mine site will have to be decommissioned. This will involve removal of the processing plant and all mining equipment, and rehabilitation of the land used for both alluvial mining and waste rock dumps (with regular future monitoring of this rehabilitated land to ensure that any environmental problems are promptly detected and corrected). Vegetation native to the local area is already being replanted on reclaimed land in order to rehabilitate the environment as much as possible to a condition that existed prior to mining. The open pit will be converted into a lake by gradual filling with groundwater.

DIAMOND SORTING AND VALUATION

After the diamond rough is received at the company offices in Perth, it undergoes a sorting process to prepare it for open-market sale. The prices achieved provide the monetary basis from which government royalties can be determined. The rough diamonds are sorted on the basis of size, shape, color, and "purity" (clarity). For sorting of diamonds on such a large scale, broad quality categories had to be established. An overall price was then assigned to each category. For pieces of rough smaller than 1.5 ct, Argyle (with the assistance of an associated company) developed proprietary automatic machines to sort the diamonds by color into 37 price categories, and by purity (clarity) into 104 price categories. These machines are capable of processing 12,000 to 30,000 diamonds per hour. Pieces larger than 1.5 ct are sorted by hand into a wider variety of categories using 2× head loupes or 10× hand loupes. The skills developed were established over a long period of time, based on expertise recruited by Argyle.

DESCRIPTION OF THE DIAMONDS

Table 2 summarizes typical gemological characteristics of Argyle diamonds (modified and updated from Chapman et al., 1996). Several other researchers have published additional scientific and gemological studies of Argyle diamonds (see Harris and Collins, 1985; Hofer, 1985, 1998; Kane, 1987; Keller, 1990; Tombs, 1990; Kaneko and Lang, 1993; Duval et al., 1996).

Typical Production from the Mine. In terms of percentages and quality categories, production consists of 5% gem, 25% industrial, and the remainder termed *near-gem*, which receive substantial processing to extract a normally low-value polished diamond. The near-gem proportion has increased over time as a result of the skills and technology of the diamond manufacturing companies in India. For the associated alluvial deposits, the percentage of

Figure 13. In a roller coaster–like operation, the crushed lamproite ore moves by conveyor belts between different stages of processing throughout the plant. Photo by James E. Shigley.

TABLE 2. Typical gemological characteristics of Argyle diamonds.[a]

Characteristic	Brown	Near colorless to light yellow	Pink to red[b]
Approximate proportion of total	72%	27%	<<1%
Type	Ia	Ia	Ia or IIa
Nitrogen content	100–500 ppm	500–1000 ppm	10–100 ppm
Nitrogen aggregation	B>A	B>>A	A>>B
Color zoning	Planar in one or more (111) slip planes	None	Planar in one or more (111) slip planes
Anomalous birefringence ("strain")	Banded or cross-hatched (tatami) pattern	May show banded or cross-hatched (tatami) pattern	Banded or cross-hatched (tatami) pattern
UV fluorescence	Dull green (LW>SW)	Blue (LW>SW)	Blue (LW>SW)
UV phosphorescence	Dull yellow or inert	Yellow	Yellow
Visible spectrum	Increasing absorption toward the blue region, with 415, 478, and 503 nm bands	415 nm band	Broad 550 nm band; increasing absorption toward the blue region; weak 415 nm band

[a] *Adapted from Chapman et al. (1996), with recent updates from Argyle.*
[b] *Also seen, <1% of total, are blue and green diamonds.*

Figure 14. In the mid-1980s, a marketing campaign was launched to educate consumers about "champagne" and "cognac" diamonds. This program was based on the development of categories of diamonds using the C1 to C7 scale for increasing amounts of brown color. The seven diamonds shown here represent these categories; they range in weight from 0.48 to 0.56 ct. Photo by Maha Tannous.

gem diamonds is higher relative to the other two categories.

The vast majority of this production consists of small, brown to near-colorless diamonds that are labor intensive to polish because of their size. More than 90% are cut in India, destined for use in the jewelry industry (Sevdermish et al., 1998b). As an indication of the size of the mine's production, we believe that each year's polished output would be sufficient to pavé set the entire surface of a tennis court.

Characteristics of the Rough. The mean size of the Argyle rough is less than 0.10 ct (for crystals larger than 0.8 mm). The largest diamond crystal recovered to date (found in late 1991) weighed 42.6 ct. It has been retained in its rough state and now forms part of the company's diamond exhibit at the mine.

More than 60% of the Argyle diamond crystals are irregular in shape. Macles (twins) comprise about 25%, while 10% are naated or polycrystalline aggregates. The remaining 5% either show some resorption, as evidenced by their rounded dodecahedral shape, or are sharp-edged, planar, octahedral-dodecahedral crystals. Approximately 72% of the diamonds are brown, with most of the remaining stones yellow to near-colorless and colorless. Fewer than 1% are the very rare pink, grayish blue, and green diamonds.

Most Argyle diamonds exhibit evidence of having been plastically deformed following formation in the earth's mantle or during their ascent to the surface. This is apparent in their highly strained character when observed with crossed polarizing filters. The plastic deformation is thought to cause both the brown and pink colors, although the exact origins of these colors are still uncertain (Fritsch, 1998, pp. 34–36, 38–40; Chapman and Noble, 1999). Argyle's rough diamonds are commonly recognized by evidence of etching internally and on their surfaces (i.e., etch channels and hexagonal depressions or pits, as well as frosted surfaces).

Inclusions are found in the vast majority of Argyle diamonds (Jaques et al., 1989a). Graphite is the most abundant inclusion, and is generally seen as black spots. Garnet, olivine, and sulfide minerals have also been identified. A high percentage of the included diamonds contain more than one mineral species.

MARKETING OF ARGYLE DIAMONDS

The discovery of the Argyle orebody was greeted with interest, but also with dismay and uncertainty in some quarters of the jewelry industry. As with the introduction of production from any new mine, there were anxieties about the sudden influx of such a large number of diamonds into the marketplace, especially the impact of Argyle material on existing diamond prices. Based on an understanding of established marketing principles, the company's management implemented a phased marketing strategy that ultimately overcame these concerns.

Nature of the Product. Argyle's marketing challenge has always been closely tied to the nature of the diamonds it produces. At the time of the discovery of the mine in 1979, India was emerging as an important cutting center for diamonds, and manufacturers there were anxious for more material (Sevdermish et al., 1998a,b). India also could provide the affordable labor needed to make the mine's production economic. A relationship with the Indian cutting industry became the platform for Argyle's marketing efforts, which focused on bringing the smaller and mainly colored diamonds to the trade. Between 1983 and 2000, manufacturing of diamonds in India grew 201% in volume and 151% in value; these percentages continue to grow (as reported by the Indian Gem and Jewellery Export Promotion council).

Marketing Brown and Pink Diamonds. With the very large percentage of brown diamonds in its production, the company recognized that initially there would be a high level of resistance to this material at the retail level. By setting up a small manufacturing unit for larger (>0.5 ct) brown diamonds beginning

in the mid-1980s, the management was able to carefully evaluate the gem potential of this kind of diamond. Efforts to use the large production of brown diamonds proved successful with the introduction of a marketing campaign for "champagne" and "cognac" diamonds throughout the mid-to-late 1980s (using what was called a C1 to C7 scale for increasing amounts of brown color—figure 14). For the pink diamonds, Argyle uses four principal categories: pink, purplish pink, brownish pink, and pink "champagne." These colors are in turn graded according to color intensity in a range from very faint to very intense. Today, the Argyle brown and pink diamonds are widely recognized worldwide.

Figure 15. The Argyle mine has become well known for the small but consistent number of pink diamonds it produces annually. These polished Argyle diamonds illustrate the range of pink colors that may be seen, from Fancy pink (the two round brilliants on the left, 0.81 and 0.55 ct) through Fancy Deep pink (the 0.48 ct emerald cut right of center) to Fancy Intense purple-pink (far right, 0.28 and 0.41 ct). Photo by Jennifer Vaccaro.

Sales Agreements and Marketing Efforts. Between 1983 and 1996, most of the rough diamonds were marketed via two sales agreements with De Beers. The first agreement (1983–1991) helped provide industry and investor confidence in the viability of the mine. It also gave company staff members time to establish expertise in the sorting and valuation of their diamonds, as well as in marketing them. Diamond industry analysis conducted during this period laid the foundation for the market intelligence systems that were eventually developed, and they guided Argyle's later efforts to gain a competitive advantage in the marketplace.

Critical to the company's marketing strategy, from as early as 1983, was the capability to sell some of the diamonds directly into the trade. This capability provided both a check and a confirmation for the rough diamond prices received within the contractual agreements. In addition, company management felt that total reliance on a third party between the mine and the consumer might limit their ability to obtain maximum prices for the rough. The company opened a direct sales office in Antwerp in 1985, and a second representative office in Mumbai (Bombay) in 1989 for customer liaison.

This first sales effort through Antwerp was for the near-gem diamonds, which at the time were considered Argyle's least attractive product. In its second contractual agreement with De Beers (1991–1996), the company incorporated the provision for independent sales of a wider range of product categories, which included all of the pink diamonds and a selection of near-gem material. Market research and manufacturing tests had indicated that the unique merits of pink diamonds (figures 15 and 16), before available only sporadically and in very limited quantities, had not been fully exploited. Although the production of pink diamonds at Argyle was also limited, it was consistent. Therefore, the company set out to add value to their overall production by establishing their pink diamonds as the material by which the Argyle mine would be best known.

In 1996, when the second agreement with De Beers had ended, the company began to market its entire production of diamonds through its Antwerp office. Efforts to build product demand lead to several initiatives, at the forefront of which was the launching in 1994 of the Indo-Argyle Diamond Council (IADC), a cooperative agreement with a

Figure 16. Beginning in 1985, the more exceptional pink diamonds from each year's production at the mine were sold individually in special auctions known as "tenders." These three diamonds were sold at the 1998 (top, 1.45 ct Fancy Intense pink), 1999 (bottom left, 0.59 ct Fancy purplish red), and 2000 (bottom right, 0.50 ct Fancy Deep purplish pink) tenders.

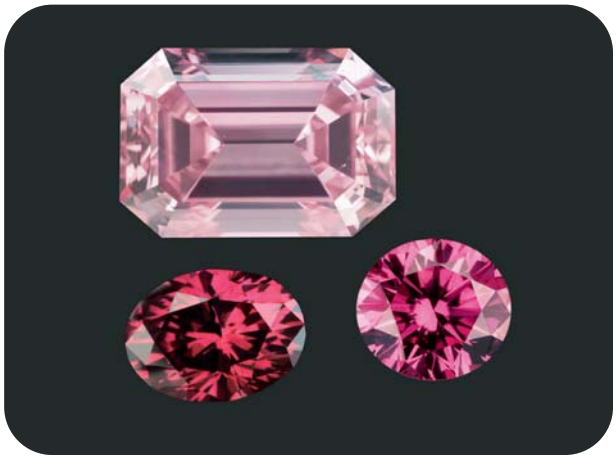

Figure 17. Brownish diamonds, such as the crystals and round brilliants shown here, constitute an important part of Argyle's production. Photo by Shane F. McClure.

number of Indian jewelry manufacturers. Although market research had indicated some reluctance on the part of the U.S. jewelry trade to purchase diamonds and diamond jewelry that originated from Indian manufacturers, Argyle was able to help overcome this reluctance because of its knowledge of the U.S. market and its understanding of dynamics within the trade.

Argyle Pink Diamonds. Beginning in 1985, the more exceptional pink (to red) diamonds from each year's production were sold individually at special auctions known as "tenders." Viewings are held in New York, Sydney, Tokyo, Hong Kong, London and Geneva. These events were held for invited clients. Each was preceded by the distribution of a tender catalogue. The size of these polished pink diamonds averages about one carat; around 40 to 50 carats are sold at these auction events each year (see, e.g., "Argyle Diamond's pink diamond tender 1985–1996," 1997), with prices achieved typically in excess of US$100,000 per carat. To put the true rarity of these special "pink" diamonds into perspective, of every million carats of rough diamonds produced at the mine, a mere one carat is suitable for sale at one of these auctions. Since 1985, more than 700 stones have been offered for sale at the tender at a total weight of almost 550 carats (again, see figure 16).

CONCLUSION

The Argyle mine is a good example of a modern, open-pit mining operation where diamonds are recovered economically on a large scale. Its discovery produced a new understanding among geologists of the conditions of diamond occurrence. As with diamond deposits in other remote regions, development of this mine required innovative solutions for processing the lamproite host rock and constructing the needed infrastructure. In 2000, the mine produced 26.5 million carats of diamonds from approximately 15 million tonnes of lamproite ore processed. Manufacturing of this immense quantity of diamonds, mainly in India, has provided an abundant supply of smaller, mainly brown to near-colorless diamonds for use in less expensive jewelry. The company's "champagne" and "cognac" marketing campaigns stimulated increased sales of brown diamonds in the jewelry trade (figure 17). High-profile auctions of the very rare pink to red diamonds continue to capture trade and consumer attention. ●

ABOUT THE AUTHORS

Dr. Shigley (jshigley@gia.edu) is director of GIA Research in Carlsbad, California. Mr. Chapman is an independent diamond scientist, and Ms. Ellison is a senior business analyst for Argyle Diamond Sales Pty. Ltd., both in Perth, Australia.

Acknowledgments: JES thanks Dr. Jonathan Lew, principal geologist for Rio Tinto Exploration Pty. Ltd. (Western Region, Australia), for his guidance during a visit to the Argyle mine. He also thanks the management of the Argyle mine for access to the mining and recovery operations, as well as for information on mine geology and diamond production. The article benefited from reviews by Dr. A. A. Levinson, Dr. A. J. A. Janse, and R. E. Kane. Unless otherwise indicated, photographs are courtesy of Argyle Diamonds Pty. Ltd.

REFERENCES

"Argyle Diamond's pink diamond tender 1985–1996" (1997) *Australian Gemmologist*, Vol. 19, No. 10, pp. 415–418.

Atkinson W.J., Smith C.B., Boxer G.L. (1984a) The discovery and geology of the Argyle diamond deposits, Kimberley, Western Australia. *Australian Institute of Mining and Metallurgy Conference*, Darwin, Northern Territory, August, pp. 141–149.

Atkinson W.J., Hughes F.E., Smith C.B. (1984b) A review of the kimberlitic rocks of Western Australia. In J. Kornprobst, Ed., *Proceedings of the Third International Kimberlite Conference, Vol. 1—Developments in Petrology 11A, Kimberlites I: Kimberlites and Related Rocks*, Clermont-Ferrand, France, 1982, Elsevier Publishers, Amsterdam, pp. 195–224.

Boxer G.L., Lorenz V., Smith C.B. (1989) The geology and volcanology of the Argyle (AK1) lamproite diatreme, Western Australia. In J. Ross and others, Eds., *Proceedings of the Fourth International Kimberlite Conference—Kimberlites and Related Rocks, Vol. 1, Their Composition, Occurrence, Origin and Emplacement*, Perth, 1986, Geological Society of Australia Special Publication No. 14, pp. 140–169.

Chapman J., Noble C.J. (1999) Studies of the pink and blue coloration in Argyle diamonds. *Gems & Gemology*, Vol. 35, No. 3, pp. 156–157.

Chapman J., Browne G., Sechos B. (1996) The typical gemmological characteristics of Argyle diamonds. *Australian Gemmologist*, Vol. 19, No. 8, pp. 339–346.

Clifford T.N. (1966) Tectono-metallogenic units and metallogenic provinces of Africa. *Earth and Planetary Science Letters*, Vol. 1, pp. 421–434.

Deakin A.S., Boxer G.L., Meakins A.E., Haebig A.E., Lew J.H. (1989) Geology of the Argyle alluvial diamond deposits. In J. Ross and others, Eds., *Proceedings of the Fourth International Kimberlite Conference—Kimberlites and Related Rocks, Vol. 2, Their Mantle/Crust Setting, Diamonds and Diamond Exploration*, Perth, 1986, Geological Society of Australia Special Publication No. 14, pp. 1108–1116.

Duval D., Green T., Louthean R. (1996) *New Frontiers in Diamond—The Mining Revolution*. Rosendale Press, London, 175 pp.

Fritsch E. (1998) The nature of color in diamonds. In G.E. Harlow, Ed., *The Nature of Diamonds*, Cambridge University Press, Cambridge, United Kingdom, pp. 23–47.

Geach C. L. (1986) Diamond exploration in Western Australia. *Geology Today*, Vol. 2, No. 1, pp. 16–20.

Graham S., Lambert D.D., Shee S.H., Smith C.B., Reeves S. (1999). Re-Os isotopic evidence for Archean lithospheric mantle beneath the Kimberley block, Western Australia. *Geology*, Vol. 27, No. 5, pp. 431–434.

Haggerty S.E. (1999) A diamond trilogy: Superplumes, supercontinents, and supernovae. *Science*, Vol. 285, No. 5424, pp. 851–860.

Harris J.W., Collins A.T. (1985) Studies of Argyle diamonds. *Industrial Diamond Review*, Vol. 45, No. 3, pp. 128–130.

Hawthorne J.B. (1975) Model of a kimberlite pipe. *Physics and Chemistry of the Earth*, Vol. 9, pp. 1–15.

Hofer S.C. (1985) Pink diamonds from Australia. *Gems & Gemology*, Vol. 21, No. 3, pp. 145–155.

Hofer S.C. (1998) *Collecting and Classifying Coloured Diamonds: An Illustrated Study of the Aurora Collection*. Ashland Press, New York, 742 pp.

Janse A.J.A. (1992) The Argyle diamond discovery, Kimberley region, Australia. *Exploration and Mining Geology*, Vol. 1, No. 4, pp. 383–390.

Jaques A.L., Lewis J.D., Smith C.B. (1986) *The Kimberlites and Lamproites of Western Australia*. Geological Survey of Western Australia, Bulletin 132.

Jaques A.L., Hall A.E., Sheraton J.W., Smith C.B., Sun S.-S., Drew R.M., Foudoulis C., Ellingsen K. (1989a) Composition of crystalline inclusions and C-isotopic composition of Argyle and Ellendale diamonds. In J. Ross and others, Eds., *Proceedings of the Fourth International Kimberlite Conference—Kimberlites and Related Rocks, Vol. 2, Their Mantle/Crust Setting, Diamonds and Diamond Exploration*, Perth, 1986, Geological Society of Australia Special Publication No. 14, pp. 966–989.

Jaques A.L., Sun S.-S., Chappell B.W. (1989b) Geochemistry of the Argyle (AK1) lamproite pipe, Western Australia. In J. Ross and others, Eds., *Proceedings of the Fourth International Kimberlite Conference—Kimberlites and Related Rocks, Vol. 1, Their Composition, Occurrence, Origin and Emplacement*, Perth, 1986, Geological Society of Australia Special Publication No. 14, pp. 170–188.

Jaques A.L., Haggerty S.E., Lucas H., Boxer G.L. (1989c) Mineralogy and petrology of the Argyle (AK1) lamproite pipe, Western Australia. In J. Ross and others, Eds., *Proceedings of the Fourth International Kimberlite Conference—Kimberlites and Related Rocks, Vol. 1, Their Composition, Occurrence, Origin and Emplacement*, Perth, 1986, Geological Society of Australia Special Publication No. 14, pp. 153–169.

Kane R.E. (1987) Three notable fancy-color diamonds: Purplish red, purple-pink, and reddish purple. *Gems & Gemology*, Vol. 23, No. 2, pp. 90–95.

Kaneko K., Lang A.R. (1993) CL and optical microtopographic studies of Argyle diamonds. *Industrial Diamond Review*, Vol. 53, No. 6, pp. 334–337.

Keller P.C. (1990) *Gemstones and Their Origins*. Van Nostrand Reinhold, New York, pp. 144.

Kirkley M.B., Gurney J.J., Levinson A.A. (1991) Age, origin, and emplacement of diamonds. *Gems & Gemology*, Vol. 27, No. 1, pp. 2–25.

Mitchell R.H. (1986) *Kimberlites: Mineralogy, Geochemistry, and Petrology*. Plenum Publishers, New York.

Mitchell R.H. (1989) Aspects of the petrology of kimberlites and lamproites: Some definitions and distinctions. In J. Ross and others, Eds., *Proceedings of the Fourth International Kimberlite Conference—Kimberlites and Related Rocks, Vol. 1, Their Composition, Occurrence, Origin and Emplacement*, Perth, 1986, Geological Society of Australia Special Publication No. 14, pp. 7–45.

Pidgeon R.T., Smith C.B., Fanning C.M. (1989) Kimberlite and lamproite emplacement ages in Western Australia. In J. Ross et al., Eds., *Proceedings of the Fourth International Kimberlite Conference—Kimberlites and Related Rocks, Vol. 1, Their Composition, Occurrence, Origin and Emplacement*, Perth, 1986, Geological Society of Australia Special Publication No. 14, pp. 369–381.

Prider R.T. (1960) The leucite-lamproites of the Fitzroy Basin, Western Australia. *Journal of the Geological Society of Australia*, Vol. 6, Pt. 2, pp. 71–120.

Sevdermish M., Miciak A.R., Levinson A.A. (1998a) The diamond pipeline into the third millennium: A multi-channel from the mine to the consumer. *Geoscience Canada*, Vol. 25, No. 2, pp. 71–84.

Sevdermish M., Miciak A.R., Levinson A.A. (1998b) The rise to prominence of the modern diamond cutting industry in India. *Gems & Gemology*, Vol. 34, No. 1, pp. 4–23.

Smith R. (1996) Jewel of the Kimberley: Unearthing the world's largest diamond producer. *Australian Geographic*, No. 41, pp. 88–107.

Tombs G.A. (1990) Argyle diamonds. *Australian Gemmologist*, Vol. 17, No. 8, pp. 321–324.

HYDROTHERMAL SYNTHETIC RED BERYL FROM THE INSTITUTE OF CRYSTALLOGRAPHY, MOSCOW

By James E. Shigley, Shane F. McClure, Jo Ellen Cole, John I. Koivula, Taijin Lu, Shane Elen, and Ludmila N. Demianets

Hydrothermal synthetic red beryl has been produced for jewelry applications by the Institute of Crystallography and an affiliated company, Emcom Ltd., both in Moscow. Diagnostic identification features include: a tabular crystal morphology, chevron-like and subparallel or slightly wavy internal growth zoning, sharp absorption bands at approximately 530, 545, 560, 570, and 590 nm due to Co^{2+}, water-related absorption bands between 4200 and 3200 cm^{-1} in the infrared spectrum, and the presence of Co and Ni peaks in EDXRF spectra.

Hydrothermal synthetic red beryl from several sources in Russia has been sold commercially since the mid-1990s, as faceted stones up to several carats (see, e.g., figure 1). This article describes material produced by a private company (Emcom Ltd.) in affiliation with the Institute of Crystallography at the Russian Academy of Sciences in Moscow. The rarity, high value, and commercial interest in natural red beryl from Utah no doubt contributed initially to the goal of producing and marketing a synthetic counterpart. Today, limited demand for this color of synthetic beryl has curtailed production at the Institute of Crystallography, as well as by other producers (pers., comm., 2001: Walter Barshai—Pinky Trading Co., Los Angeles; Alex Grizenko—Russian Colored Stone Co., Golden, Colorado; Uriah Prichard—Morion Co., Brighton, Massachusetts). Nevertheless, synthetic red beryl continues to circulate in the marketplace.

BACKGROUND

Beryl Crystal Chemistry. Pure beryl ($Be_3Al_2Si_6O_{18}$) is colorless. The presence of other elements gives rise to various colors (Fe, Cr, V, and Mn for coloration in both natural and synthetic, plus Ti, Co, and Ni in synthetic beryls; Sinkankas, 1981; Fritsch and Rossman, 1987). These elements substitute for Al. Alkali elements (Li, Na, K, Rb, Cs) can also occur in minor amounts by substituting for Be and Al (Sinkankas, 1981; Aurisicchio et al., 1988; Deer et al., 1997, pp. 378–386); however, these elements do not affect beryl coloration. The beryl crystal structure contains two different sites along "open" channels that can incorporate water molecules (Schaller et al., 1962; Wood and Nassau, 1968; Schmetzer, 1989; Deer et al., 1997). These variations in transition metal, alkali element, and water contents in beryls cause differences in physical properties (such as refractive index, specific gravity, and color), as well as in visible and infrared absorption spectra.

Natural Red Beryl. Gem-quality red beryl occurs at a single locality in the Wah Wah Mountains of southern Utah (see, e.g., Flamini et al., 1983;

See end of article for About the Authors information and acknowledgments.
GEMS & GEMOLOGY, Vol. 37, No. 1, pp. 42–55

Figure 1. These faceted hydrothermal synthetic red beryls (1.46–3.85 ct) are representative of material that has been produced at the Institute of Crystallography and Emcom Ltd. in Moscow. Photo © GIA and Tino Hammid.

Shigley and Foord, 1984). The crystals formed in fractures within devitrified rhyolite lava, probably as a result of the metasomatic reaction between a fluorine-rich gas or vapor phase and potassium feldspar (Aurisicchio et al., 1990; Henn and Becker, 1995). These crystals are often chemically zoned, which can result in an uneven coloration. This is seen as hexagonal orange-red core zones within purplish red rims when the crystals are viewed parallel to the c-axis, and as triangular or hourglass-shaped orange-red core zones within the purplish red rims when the crystals are viewed perpendicular to the c-axis (Shigley and Foord, 1984, pp. 214–215, figures 7 and 8). The color of faceted material ranges from purplish red to red to orange-red. Compared to most other beryls, red beryl is enriched in Mn, Fe, Ti, Rb, Zn, and Sn, and is depleted in Na, K, and Mg. Red beryl is noted for its almost complete absence of water (Nassau and Wood, 1968; Aurisicchio et al., 1990), which is also unique among beryls that typically crystallize in hydrothermal geological environments.

Synthetic Beryls. Growth of synthetic emerald by the flux technique extends back 150 years, while hydrothermal growth of emerald began in the mid-1960s (Nassau, 1976, 1980). Synthetic beryls with colors other than green have been grown by the hydrothermal method only during the past decade. Synthetic pink to red beryls have been reported by Emel'yanova et al. (1965), Taylor (1967), Solntsev et al. (1981), Lebedev et al. (1982, 1983), Platonov et al. (1989), Brown (1990, 1993), Troup et al. (1990), and Fritsch et al. (1992). Henn and Milisenda (1999) described hydrothermal synthetic red beryl from an unstated source in Russia that has many gemological properties in common with the material described here. Although similar in overall appearance, the synthetic product differs in gemological properties from natural red beryl (for descriptions of the latter, see Nassau and Wood, 1968; Schmetzer et al., 1974; Miley, 1980; Flamini et al., 1983; Shigley and Foord, 1984; Aurisicchio et al., 1990; Hosaka et al., 1993; Harding, 1995).

GROWTH CONDITIONS

One of the authors (LD) grew the synthetic red beryl samples examined in this study. The crystals are grown by the so-called regeneration technique from a hydrothermal solution at temperatures of more than 600°C and pressures of more than 2000 bars (Demianets, 1996). Note that these conditions are similar to those reported for growing hydrothermal synthetic emeralds (Bukin et al., 1986, pp. 255–258; Schmetzer, 1988, pp. 157–162). Thin (≤1 mm thick) seed plates of either synthetic colorless beryl or synthetic emerald are used to initiate crystal growth. These seed plates are cut parallel to the dipyramid faces (general Miller form symbol {hk$\overline{2}$il}).

To obtain the desired red to orange-red color, the manufacturers introduce Co and Mn simultaneously into the growth system (along with some Fe and alkaline elements). According to author LD, the typical content of transition metals in a synthetic red beryl crystal is on the order of 1 wt.% Fe (1.28

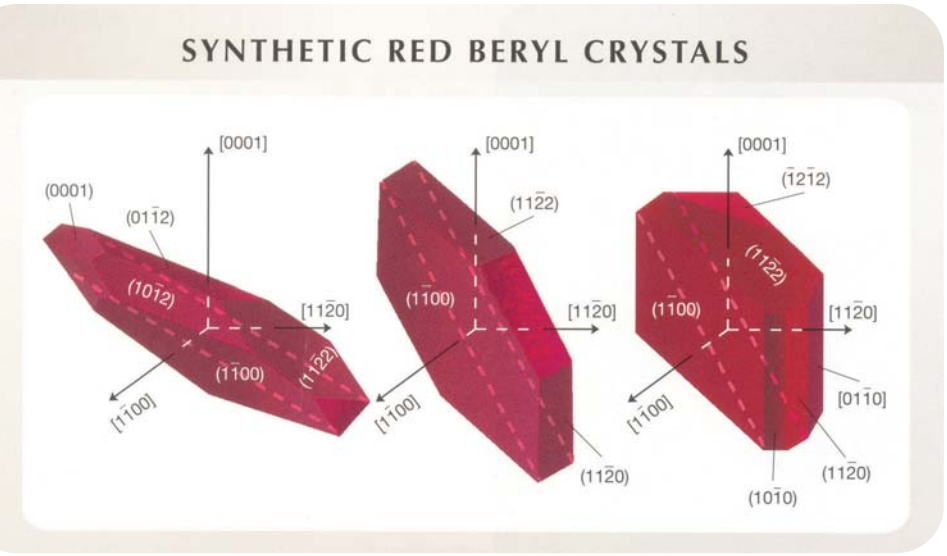

Figure 2. These idealized drawings of three synthetic red beryl crystals illustrate the morphology of this material, which is typical of that seen in other hydrothermally grown synthetic beryls. The crystal faces shown belong to one of the following forms: basal pinacoid {0001}, first-order prism {10$\bar{1}$0}, second-order prism {11$\bar{2}$0}, first-order dipyramid {10$\bar{1}$2}, and second-order dipyramid {11$\bar{2}$2}. Several minor faces that have been known to occur on actual crystals are not shown on these drawings. Zone axes are indicated by the Miller indices shown in brackets. The red dashed line in each drawing represents the seed plate. In the middle drawing, the surface with markings but no Miller index is not a true crystal face, but rather a growth surface that is parallel to the seed plate.

wt.% FeO), 0.12 wt.% Mn (0.15 wt.% MnO), and 0.18 wt.% Co (0.23 wt.% CoO).

The synthetic red beryl crystals are tabular and elongated parallel to the seed plate (figures 2 and 3). They exhibit first- and second-order prisms {10$\bar{1}$0} and {11$\bar{2}$0}, first- and second-order dipyramids {10$\bar{1}$2} and {11$\bar{2}$2}, and sometimes other faces (i.e., {11$\bar{2}$4} and {0001}), depending on the orientation of the seed plate and on the differing growth rates for each crystal face. Researchers at the Institute of Crystallography confirmed the identity of these crystal faces by the single-crystal X-ray diffraction method, using a Rigaku diffractometer. The crystal faces are, for the most part, relatively flat. The surfaces oriented parallel to the seed plate have the highest growth rate and, therefore, exhibit various growth features (mainly growth hillocks and some hopper formations).

MATERIALS AND METHODS

We examined seven rough crystals and 27 faceted specimens of hydrothermal synthetic red beryl loaned by Worldwide Gem Marketing, the company that has sold this material for jewelry purposes on behalf of the Institute of Crystallography. The crystals ranged from 125.7 to 323.9 ct, and the faceted pieces ranged from 0.28 to 3.85 ct (all but three of these were >1 ct). None of the faceted specimens exhibited any remnant of a seed plate.

We tested the rough and polished samples using standard gemological methods. Refractive indices were measured using a Duplex II refractometer. Specific gravity was calculated by the hydrostatic method from weight measurements by means of a Mettler AM100 electronic balance. We did not obtain S.G. measurements for the crystals, because of their large size and the presence of metal suspension wires that would distort the results. Fluorescence to ultraviolet radiation was documented in darkroom conditions with a standard long-wave (366 nm) and short-wave (254 nm) GIA Gem Instruments UV unit. Visible spectra were observed with Beck prism and Discan digital-scanning, diffraction-grating spectroscopes; a calcite dichroscope was used to observe pleochroism. Photomicrographs were taken with Nikon SMZ-U and SMZ-10 photomicroscopes.

Although the synthetic crystals varied in color (purplish red or orange-red), all of the faceted synthetic samples were relatively similar in color (red to orange-red); therefore, we documented representative samples of the latter as described below using advanced instrumentation. Two natural red beryls from Utah also were analyzed for comparison purposes: (1) a 1.95 ct purplish red crystal was polished on opposite sides in an orientation parallel to the c-axis for use in recording visible and infrared spectra, and (2) a 1.50 ct purplish red crystal was used for qualitative chemical analysis.

Absorption spectra in the range 250–850 nm were recorded for three synthetic samples with a Hitachi U4001 spectrophotometer with a 2 nm slit width. To obtain polarized absorption spectra, we prepared an optically oriented flat plate from one of the orange-red synthetic crystals; we then used calcite polarizers to record spectra in orientations both parallel and perpendicular to the c-axis (the optic axis). Unpolarized absorption spectra also were recorded for two faceted synthetic samples.

We documented mid-infrared spectra for four

Figure 3. The morphology of these synthetic red beryl crystals (125.7–323.9 ct) differs significantly from the hexagonal crystal form of natural red beryl (see inset, 2.1 cm tall; photo by Jeff Scovil). Photo © GIA and Tino Hammid.

crystals and one faceted sample of synthetic red beryl with a Nicolet Magna 550 FTIR spectrometer, from 6600 to 400 cm^{-1}, at a resolution of 4 cm^{-1}. To compare our data with those published by Schmetzer and Kiefert (1990) for natural and synthetic beryls, we recorded an infrared transmission spectrum for fragments of one synthetic red beryl crystal. These fragments were embedded in powdered potassium bromide (KBr) and then formed into a thin pellet for analysis. This is a standard procedure that is used to obtain an infrared spectrum from a small quantity of a material, to avoid exceeding the recording range of the detector of the infrared spectrometer. Such a sample produces an "average" infrared spectrum that is independent of crystal orientation.

The spectrum of a plate-like black inclusion seen in one orange-red synthetic crystal was recorded with a Renishaw 2000 Ramascope laser Raman microspectrometer over the range of 100 to 2000 cm^{-1}.

Using two different sets of conditions to optimize the detection of certain elements, we performed qualitative EDXRF chemical analyses with a Tracor Spectrace 5000 instrument on one natural crystal, four faceted synthetic specimens, and three synthetic crystals. For low-atomic weight elements, the conditions were: 15 kV tube voltage, 0.35 mA tube current, a vacuum atmosphere, no filter, and a 200-second counting time. For detecting transition metals, we used: 35 kV tube voltage, 0.30 or 0.35 mA tube current, ambient atmosphere, a thin filter, and a 200-second counting time. While the EDXRF spectra we recorded represent a qualitative chemical analysis, we found that quantitative analyses using the same equipment and standards yielded an estimated detection limit of about 50 ppm for the transition metals in rubies using the second set of analytical conditions.

Quantitative chemical analyses of three faceted synthetic red beryls were obtained with a JEOL 733 electron microprobe at the California Institute of Technology in Pasadena. The operating conditions were: 15 kV beam voltage, 25 nA beam current, 10 micron spot size, minerals or synthetic compounds as standards for the elements analyzed, and the CITZAF data correction procedure.

RESULTS AND DISCUSSION

Visual Characteristics of the Study Specimens. The seven synthetic crystals were similar in morphology and appearance, although they varied in color (five were purplish red, and two were orange–red). All of the 27 faceted samples were red to orange-red. Faceted natural red beryl can show a similar red to orange-red color range when the table is oriented perpendicular to the c-axis (long direction) of the crystal (Shigley and Foord, 1984). However, it is more often red to purplish red, since the table facet is commonly oriented parallel to the c-axis to maximize weight retention.

All seven synthetic crystals were tabular in shape, square in overall cross-section, and elongated in the

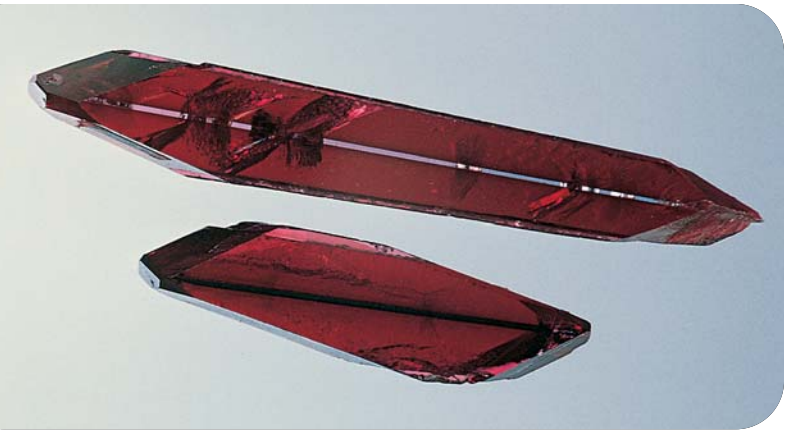

Figure 4. Hydrothermal synthetic red beryl from the Institute of Crystallography is grown from solutions onto thin seed plates of either colorless synthetic beryl (as in the top crystal, 323.9 ct) or synthetic emerald (bottom crystal, 125.7 ct). For the seven crystals we examined, the type of seed plate did not seem to influence the color, shape, or other features of the crystals. Photo © GIA and Tino Hammid.

direction of the seed plate. These plates varied from 0.7 to 1.0 mm in thickness, and extended the entire length of each crystal. Different beryl seed plates were observed: In the five purplish red crystals, two of the seed plates were colorless and three were green; in the two orange-red crystals, one was colorless and the other was green (see, e.g., figure 4). Angles between the c-axis and the seed plate were recorded for five of the crystals: four purplish red—19°, 17°, 17°, and 15°; one orange-red—17°. No obvious color zoning was seen in these crystals, except in one instance where there was a narrow band of lighter color along one outer edge. General comments on the appearance of the crystal faces (which were always present, except as noted below) are as follows:

- First-order prism {10$\bar{1}$0}: these faces, which cover the largest surface area, are relatively smooth and flat (except for very slight growth hillocks). However, on the prism faces along the sides of two crystals, rectangular-shaped depressions and other cavities were observed along the outer edge of the seed plate; these features result from post-growth cleaning in acid.
- Second-order prism {11$\bar{2}$0}: Relatively smooth and flat, these faces are smaller than the first-order prisms.
- First-order dipyramid {10$\bar{1}$2}: These faces are relatively smooth and flat.
- Second-order dipyramid {11$\bar{2}$2}: These large faces are relatively smooth and flat.
- Basal pinacoid {0001}: These faces are flat and very small, or are absent from some crystals.
- Second-order dipyramid {11$\bar{2}$4}: Rarely present, these faces may form flat, very small areas.

There are also rough surfaces that are oriented parallel to the seed plate and perpendicular to the direction of fastest crystal growth. These are not true crystal faces. They exhibit characteristic growth hillocks that are related to the internal chevron-like growth zoning. Similar faces and surface features have been observed on hydrothermal synthetic emerald crystals (Schmetzer, 1988; Sosso and Piacenza, 1995; Schmetzer et al., 1997).

Gemological Properties. The gemological properties of the faceted synthetic red beryls are described below and summarized in table 1.

Refractive Index. Of the 26 faceted samples on which R.I.'s were taken, 24 exhibited values of 1.569–1.573 (n_ε) and 1.576–1.580 (n_ω), with a birefringence of 0.006–0.008. One sample had R.I. values of 1.561 and 1.567, and the other showed 1.582 and 1.588 (both with a birefringence of 0.005); there were no obvious features that might cause these discrepancies. Henn and Milisenda (1999) reported very similar R.I. values of 1.570–1.572 and 1.578–1.580 (birefringence of 0.008) for the synthetic red beryl samples they examined.

The two R.I. values for natural beryls of all kinds generally range from 1.565 to 1.599 and 1.569 to 1.610 (Deer et al., 1997, p. 372). Sinkankas (1981) cited slightly lower ranges of 1.563–1.597 and 1.567–1.602. Higher concentrations of the alkali elements (Li, Na, K, Cs) cause an increase in R.I. values in beryls (Černý and Hawthorne, 1976; Schmetzer, 1988, p. 149; Deer et al., 1997). Published chemical analyses for 29 beryls of various colors (except red; all natural beryls except for one synthetic emerald) indicate Na_2O values of 0.10–2.50 wt.% and K_2O values of 0–0.65 wt.% (Deer et al., 1997, pp. 380–385). In published analyses of natural red beryl, values for these oxides fall in the ranges of 0.03–0.39 wt.% Na_2O and 0.09–0.29 wt.% K_2O; in the hydrothermal synthetic red beryl examined here, the same two oxides varied from 0.06 to 0.12 wt.% and 0.02–0.04 wt.%, respectively (see table 2). The relatively low concentrations of Na and K in both the natural and synthetic red beryls we studied are consistent with their low R.I. values. However, the influence of alkali element concentrations on lowering R.I.

TABLE 1. Properties of hydrothermal synthetic and natural red beryl.

Property	Synthetic	Natural
Source	Institute of Crystallography / Emcom Ltd., Moscow	Wah Wah Mountains, Utah
References	This study (c.f., Henn and Milisenda, 1999)	This study; Shigley and Foord (1984)
Color	Red to orange-red	Purplish red to red to orange-red
Crystal morphology	Tabular, square cross-section, elongated in the direction of the seed plate, which is oriented 15°–19° to the c-axis	Prismatic, hexagonal cross-section, elongated parallel to the c-axis
Crystal forms (and relative occurrence)	{10$\bar{1}$0}, {11$\bar{2}$0}, {10$\bar{1}$2}, {11$\bar{2}$2}—common {0001}, {11$\bar{2}$4}—rare	{0001} and {10$\bar{1}$0}—common {11$\bar{2}$1} and {11$\bar{2}$2}—less common {11$\bar{2}$0}—rare {10$\bar{1}$1}—very rare
Features on crystal faces	Prism {10$\bar{1}$0}, {11$\bar{2}$0}—usually smooth Dipyramid {10$\bar{1}$2}, {11$\bar{2}$2}—usually smooth	Prism {10$\bar{1}$0}—usually smooth Dipyramid {11$\bar{2}$2}—smooth Basal pinacoid {0001}—usually flat
Refractive indices		
n_ε	1.569–1.573	1.564–1.569
n_ω	1.576–1.580	1.568–1.572
Birefringence	0.006–0.008	0.006–0.008
Specific gravity	2.67–2.70	2.66–2.70
Pleochroism		
Parallel to c-axis	Purplish red	Purplish red
Perpendicular to c-axis	Orange-red to orange-brown	Red to orange-red
UV fluorescence	Inert	Inert
Color distribution	Even, except for some brown banding along growth zones	Sometimes even, often zoned with a triangular or hourglass shape (when viewed perpendicular to the c-axis)
Internal growth zoning	Chevron-like and subparallel or slightly wavy patterns (causing a roiled optical effect)	None
Inclusions		
Fluid inclusions	Occasional tiny single- or two-phase inclusions (liquid, or liquid plus gas) along partially healed fractures (rare in faceted material)	Numerous single- or two-phase inclusions (liquid, or liquid plus gas) often along planar or curved fractures or forming "fingerprint" patterns
Solid inclusions	Hematite platelets, tiny triangular inclusions with a dendritic appearance (unidentified), and "nailhead" spicules (both rare in the faceted material examined here)	Tiny grains or crystals of quartz, bixbyite, feldspar, and/or hematite
Other features	Fractures, seed plate, metal wires (in crystals only)	Fractures, sometimes with brown (iron oxide) staining
Distinctive trace elements	Co and Ni	Cs, Sn, and Zn
Visible spectra (spectrophotometer)	Weak bands at 370 and 410 nm; broad absorption between 400 and 470 nm; broad absorption between 480 and 600 with superimposed bands at approximately 530, 545, 560, 570, and 585 nm	Absorption below 400 nm; weak bands at 370, 430, and 485 nm; and broad absorption between 450 and 600 nm (centered at approximately 560 nm)
Infrared spectra	Presence of strong absorption between 4200 and 3200 cm^{-1} (due to water)	Absence of absorption between 4200 and 3200 cm^{-1} (lack of water)

values is probably offset somewhat by the presence of transition metals (e.g., Mn, Fe, Ti) in red beryl. Schmetzer (1988) discussed the opposing effects of alkali elements and transition metals on the optical properties of synthetic emeralds.

Although not an essential component, water is present in most natural beryls in amounts up to 2.7 wt.% H_2O (Deer et al., 1997). Nassau and Wood (1968) cited a range of 0.3–3.0 wt.% H_2O from published analyses of beryls. Černý and Hawthorne (1976) discussed how increasing amounts of water in beryls are accompanied by increasing R.I. values. Nassau and Wood (1968) reported that water is nearly absent (i.e., they could not detect it using infrared spectroscopy) in natural red beryl from Utah, due to the geologic conditions of its formation. Shigley and Foord (1984) reported only 0.36 wt.% H_2O (obtained by a microcoulometric analytical technique) for a single natural red beryl. Again, this very low water content may contribute to the low R.I. values. The synthetic red beryls examined for this study were not analyzed quantitatively for water, but they contained sufficient water for it to be readily detectable by routine mid-infrared spectroscopy techniques, as is typical of any hydrothermally grown synthetic beryl (see Schmetzer and Kiefert, 1990).

TABLE 2. Partial chemical analyses of hydrothermal synthetic and natural red beryl by electron microprobe.[a]

Oxide (wt.%)	Hydrothermal synthetic				Natural				
	This study[b]	This study[b]	This study[b]	Henn and Milisenda (1999)[c]	Flamini et al. (1983)[d]	Shigley and Foord (1984)[e]	Aurisicchio et al. (1990)[f]	Aurisicchio et al. (1990)[g]	Harding (1995)[h]
SiO_2	65.37	65.54	65.79	66.08	64.71	66.80	66.18	64.84	67.17
TiO_2	0.02	0.01	n.d.	0.05	0.28	0.40	0.25	0.52	0.29
Al_2O_3	16.79	16.99	17.01	16.96	17.75	17.60	16.51	18.14	16.75
Cr_2O_3	0.03	0.04	0.03	0.02	n.r.	n.r.	n.r.	n.r.	n.r.
FeO	1.48	1.47	1.32	1.62	1.46	1.80	2.63	1.96	2.81
MnO	0.03	n.d.	0.01	0.18	0.18	0.30	0.73	0.27	0.82
CoO	0.30	0.26	0.30	0.31	n.r.	n.r.	n.r.	n.r.	n.r.
MgO	0.12	0.15	0.15	0.03	0.40	0.10	n.r.	0.27	n.r.
CaO	n.a.	n.a.	n.a.	n.r.	n.r.	n.r.	n.r.	n.r.	0.13
Na_2O	0.06	0.12	0.08	0.06	0.39	0.03	n.d.	0.20	n.r.
K_2O	0.03	0.04	0.02	0.01	0.09	0.10	n.d.	0.29	0.10
Cs_2O	n.a.	n.a.	n.a.	n.r.	0.21	0.25	n.r.	0.56	n.r.
SnO_2	n.a.	n.a.	n.a.	n.r.	n.r.	0.02	n.r.	n.r.	n.r.
ZnO	n.a.	n.a.	n.a.	n.r.	n.r.	0.08	n.d.	n.r.	n.r.
Total[a]	84.23	84.62	84.71	85.32	85.47	87.48	86.30	87.05	88.07

[a]*Notes: n.d. = not detected, n.r. = not reported, n.a. = not analyzed for. Electron microprobe analyses do not include BeO, Li_2O, and H_2O, so the data presented here do not total 100 wt.%. Ni was not analyzed by electron microprobe in this study.*
[b]*Average of three analyses of one sample.*
[c]*Average of seven analyses of one sample.*
[d]*Average of 17 analyses of one crystal.*
[e]*One analysis of the purplish red rim of a color-zoned crystal.*
[f]*One analysis of the red rim of a color-zoned crystal (analysis #3 of crystal #1).*
[g]*One analysis of the red rim of a color-zoned crystal (analysis #12 of crystal #2).*
[h]*Average of three analyses of one polished sample.*

Specific Gravity. All 27 faceted synthetic red beryls had S.G. values in the range 2.67–2.70. Henn and Milisenda (1999) reported S.G. values of 2.63–2.65 for their study samples. For synthetic emeralds of all kinds colored by Cr or V, Sinkankas (1981) reported a maximum S.G. range of 2.65–2.71. Taylor (1967) reported S.G. values of 2.67–2.68 for pink Co-colored synthetic beryl, and Brown (1993) indicated 2.685 for a Ti-doped hydrothermal synthetic beryl. For comparison, natural beryls of all kinds have a maximum S.G. range of 2.63–2.92 (Sinkankas, 1981; Deer et al., 1997). Schmetzer (1988) discussed how increasing concentrations of alkali elements and transition metals in beryls are accompanied by increasing S.G. values. As mentioned above, the synthetic red beryl examined here is deficient in alkali elements, but it contains greater amounts of the transition metals relative to most natural beryls.

Polariscope Reaction. Each of the 27 faceted synthetic red beryls exhibited typical double refraction with a uniaxial optic figure. The orientation of the optic axis varied from nearly parallel to nearly perpendicular to the table facet; however, most were oriented with the c-axis at no more than about 20° from the plane of the table. These variations result from the tabular crystal shape, coupled with the desire to maximize weight retention during faceting without including portions of the seed plate.

Pleochroism. When viewed with a dichroscope, all 27 faceted samples of synthetic red beryl exhibited moderate to very strong, purplish red (n_e) and orange-red to orange-brown (n_w) dichroism (figure 5).

Absorption Features Seen with a Desk-Model Spectroscope. The spectra of each of the faceted synthetic red beryls displayed the same general pattern of absorption features: a broad region of absorption below 400 nm, a broad region of absorption from about 420 to 470 nm, a region of absorption from about 400 to 600 nm containing a narrow (slightly diffuse) absorption band of moderate intensity centered at about 530 nm, two strong sharp bands at about 545 and 560 nm, and two weak sharp bands at about 570 and 590 nm.

Figure 5. The synthetic red beryls studied showed moderate to very strong dichroism. When viewed table-down, this 0.75 ct triangle shape displayed purplish red and orange-brown pleochroic colors. Photomicrograph by James Shigley; magnified 3×.

This pattern is quite different from the spectrum of the natural red beryl we examined, which showed an intense region of absorption below about 450 nm and a broad absorption between about 540 and 580 nm. Thus, the presence of several diffuse-to-sharp absorption bands between 530 and 590 nm (due to Co^{2+}) is distinctive of this hydrothermal synthetic red beryl.

Internal Characteristics. Examination of the crystals and faceted samples of synthetic red beryl with a binocular microscope revealed the following features:

1. Prominent internal growth zoning (figure 6) was oriented at an oblique angle to the seed plate. According to Schmetzer (1988), this kind of zoning in hydrothermal synthetic beryls arises from the growth of a number of subparallel "crystallites" at an oblique angle to the seed plate. Their intersection produces chevron-like microstructures, which are best seen when the sample is viewed perpendicular to the plane of the seed plate. He noted that this internal growth zoning also gives rise to a roiled optical effect.
2. A subparallel or slightly wavy pattern (sometimes brownish) was best seen when the samples were examined parallel to the seed plate direction (figure 7); it is related to the internal growth zoning mentioned above. When the samples were viewed with crossed polarizers, a strain pattern that mimics this growth zoning was evident (figure 8).
3. Remnants of the metal wire used to suspend the crystals during growth may be present at one or both ends of the crystals; these were not seen in the faceted samples.
4. Occasional small, partially healed fractures—usually planar or curved in shape, but sometimes in more complicated patterns—contained tiny liquid

Figure 6. The most distinctive visual feature of the hydrothermal synthetic red beryls examined was chevron-like internal growth zoning. From observations in the original crystals, we know that this zoning is oriented along the direction of crystal growth at a high, oblique angle to the plane of the seed plate. Photomicrographs by James Shigley; left—magnified 3×, right—magnified 9×.

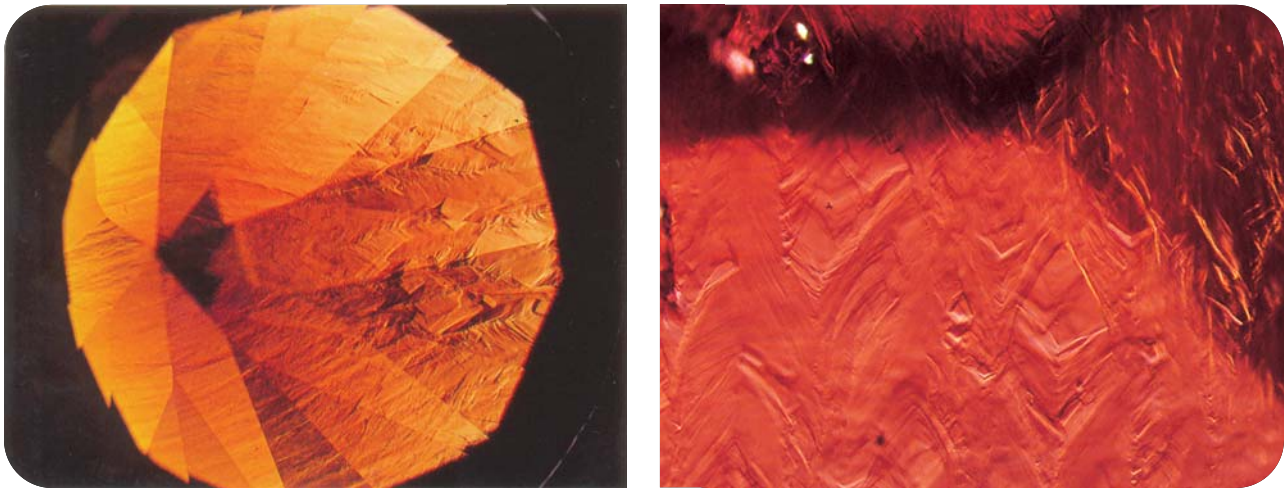

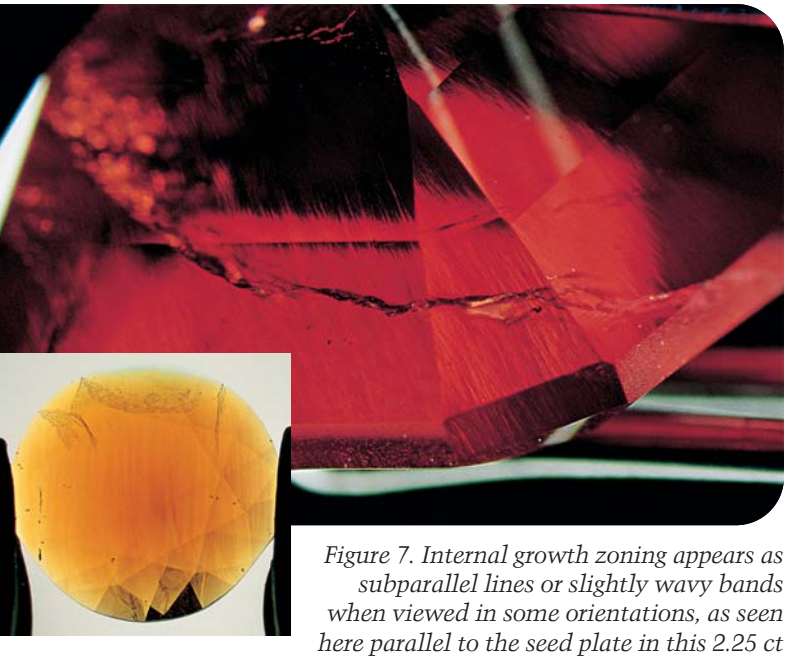

Figure 7. Internal growth zoning appears as subparallel lines or slightly wavy bands when viewed in some orientations, as seen here parallel to the seed plate in this 2.25 ct faceted synthetic red beryl. (Photomicrograph by Shane Elen; magnified 4×.) When immersed in water, the subparallel or slightly wavy growth banding in some of the faceted specimens had a slightly brownish appearance (see inset); several partially healed fractures are also visible. (Photomicrograph by James Shigley; magnified 2×.)

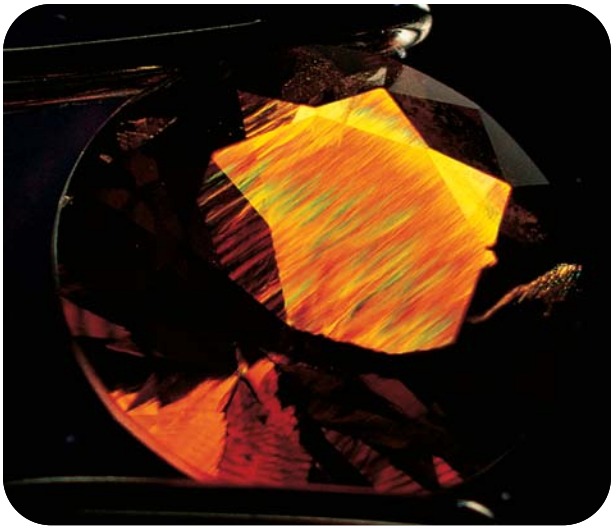

Figure 8. When this 2.59 ct faceted synthetic red beryl was viewed with crossed polarizers, the strain pattern was seen to follow the banded growth zoning. Photomicrograph by Shane Elen.

or liquid-and-gas inclusions (figure 9). In general, these fractures were absent from the faceted material, presumably because they were excluded during fashioning.

5. Occasional isolated liquid-and-gas inclusions (figure 10) and rare solid inclusions were seen in the synthetic crystals. A few tiny triangular inclusions were noted along the edge of the seed plate in several crystals, but they could not be identified because of their size, orientation, and location (figure 11). A prominent opaque black platelet in one of the synthetic red beryl crystals was identified by Raman analysis as hematite (figure 12).
6. Occasional "nailhead" spicules were present near the seed plate (figure 13). Some were hollow and others contained two phases (liquid and gas); they were "capped" by a colorless or a colored solid inclusion that, again, we were unable to identify by Raman analysis because of their nature and location.

Figure 9. Some synthetic red beryl samples contained small, partially healed fractures composed of numerous tiny liquid or liquid-and-gas inclusions along lines or forming small "fingerprint" patterns. Although often planar, some partially healed fractures displayed curved shapes. Photomicrographs by James Shigley; magnified 8× (left) and 14× (right).

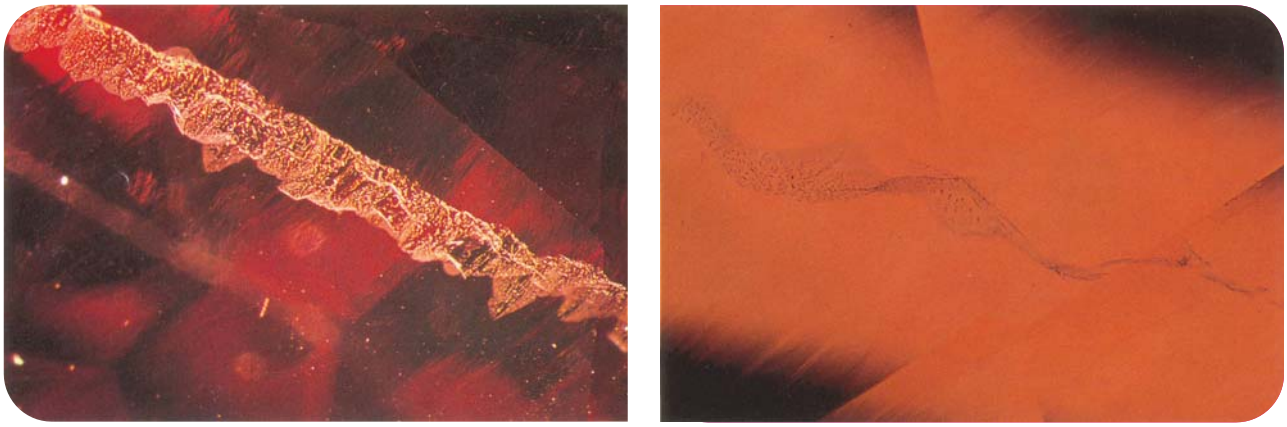

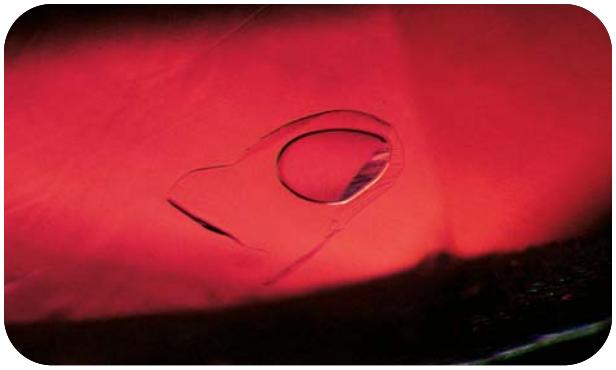

Figure 10. Isolated two-phase fluid (liquid and gas) inclusions were seen in several of the synthetic red beryl crystals, but less frequently in the faceted samples. Photomicrograph by John I. Koivula; magnified 25×.

Figure 11. A few triangular-shaped inclusions were seen in several of the synthetic red beryl crystals along seed-plate boundaries. Because the seed plate and adjacent areas are removed during faceting, such inclusions are unlikely to occur in cut stones; they were not present in the faceted specimens examined for this study. Photomicrograph by James Shigley; magnified 20×.

Although none of the faceted samples we examined contained remnants of the seed plate, the metal suspension wire, or any large fractures, such features have been reported in hydrothermal synthetic emeralds and could be present in other faceted samples of hydrothermal synthetic red beryl.

It is important to note that almost all of the inclusions that have been reported in natural red beryl (see, e.g., Shigley and Foord, 1984; table 1) are quite different from those seen in its synthetic counterpart.

Chemical Composition. The electron microprobe analyses in table 2 are of synthetic and natural red beryls from this study and elsewhere. In addition to the elements shown in this table, we detected the presence of Cu, Ni, and Rb in the synthetic material, and Cu, Ga, and Rb in a natural red beryl using EDXRF (figure 14). The most diagnostic elements for identifying synthetic red beryl are Co and Ni. Neither of these elements was detected by the highly sensitive emission spectrography technique in a natural red beryl (Shigley and Foord, 1984, p. 216), nor have they been reported elsewhere for the natural material. Using EDXRF, we also found Cr in a synthetic red beryl, but minute amounts of this element have been detected in natural red beryl (Shigley and Foord, 1984).

Absorption Spectroscopy. Polarized visible spectra for an orange-red synthetic and a purplish red natural beryl are presented in figure 15. Several features are shown in the synthetic red beryl spectrum polarized parallel to the c-axis (figure 15A; attributed causes shown in parentheses, after Solntsev et al., 1981):

1. Weak bands at about 370 nm (Fe^{3+}) and 410 nm (Ni^{3+})
2. A strong broad absorption region between 400 and 470 nm (maximum at about 450 nm, due to Co^{2+})
3. A strong broad absorption region from 480 to 600 nm (maximum at about 560 nm), with a weak band at about 525 nm and superimposed sharp peaks at 545, 560, 570, and 585 nm (all due to Co^{2+})

The two regions of strong absorption (centered at about 450 and 560 nm) are of approximately equal intensity in the spectrum in figure 15A. In the spectrum polarized perpendicular to the c-axis (figure 15B), the absorption region centered at 450 nm is much more intense. These spectra are comparable to those for synthetic beryls published by Emel'yanova

Figure 12. This opaque black inclusion was identified as hematite by Raman analysis. Photomicrograph by James Shigley; magnified 15×.

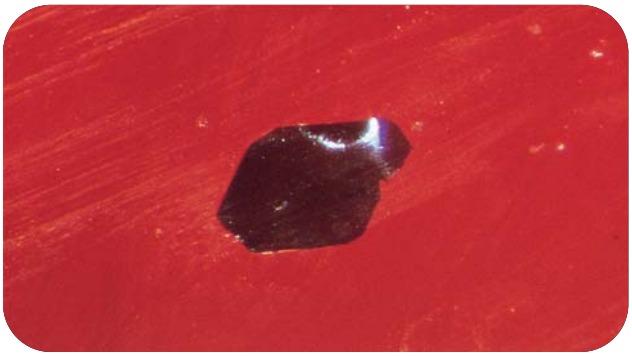

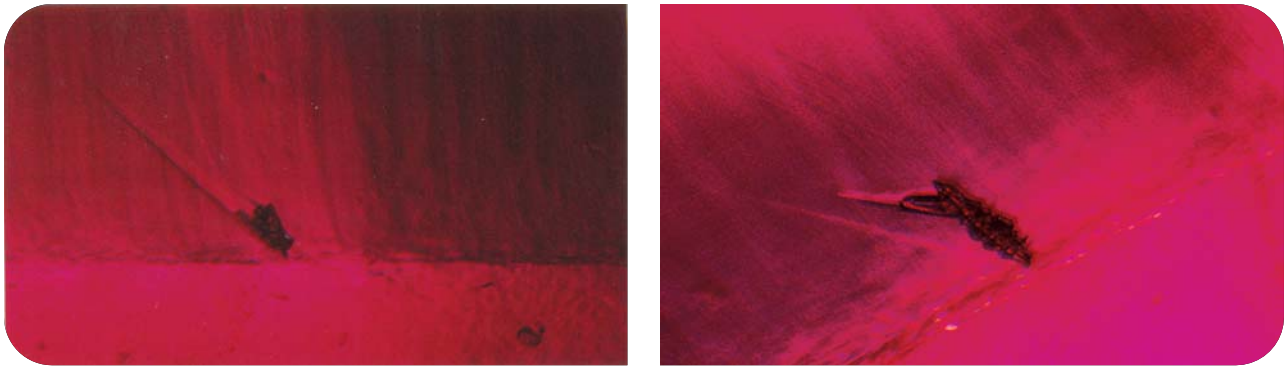

Figure 13. "Nailhead" spicules were occasionally observed in the crystals, near the seed plate. They are formed by an unknown solid phase and an associated hollow tube filled with a liquid (left), and sometimes with a gas bubble (right). Photomicrographs by John I. Koivula; magnified 40×.

et al. (1965), Lebedev et al. (1982, 1983), and Henn and Milisenda (1999, figure 2; except that, in their spectrum polarized parallel to the c-axis, the absorption region centered at 560 nm is more intense than the one centered at 450 nm).

For the natural red beryl, the spectrum polarized parallel to the c-axis (figure 15C) exhibits the following features (for comparison, see Solntsev et al., 1981; Shigley and Foord, 1984):

1. Increasing absorption below 400 nm (Fe^{3+})
2. A weak peak at about 430 nm (Fe^{3+})
3. A broad intense region of absorption from 450 to 600 nm (centered at about 560 nm; Mn^{3+})

Figure 14. EDXRF spectra of an orange-red hydrothermal synthetic red beryl (A and B) and a natural purplish red beryl crystal from Utah (C and D) show notable differences in chemical composition. Analytical conditions were optimized to detect low-atomic-weight elements (A and C) and transition metals (B and D). Peaks resulting from instrumental artifacts are not labeled, and should be ignored. The distinctive elements in the synthetic red beryl are Co and Ni.

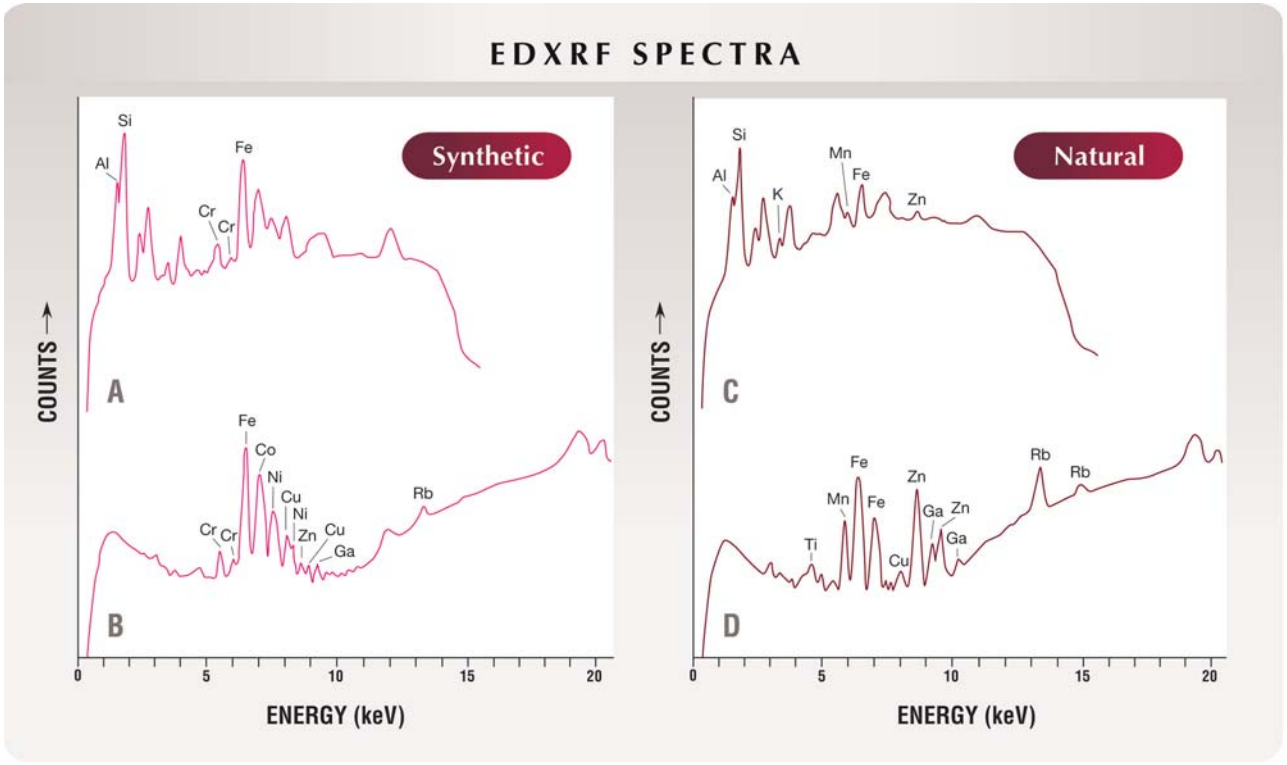

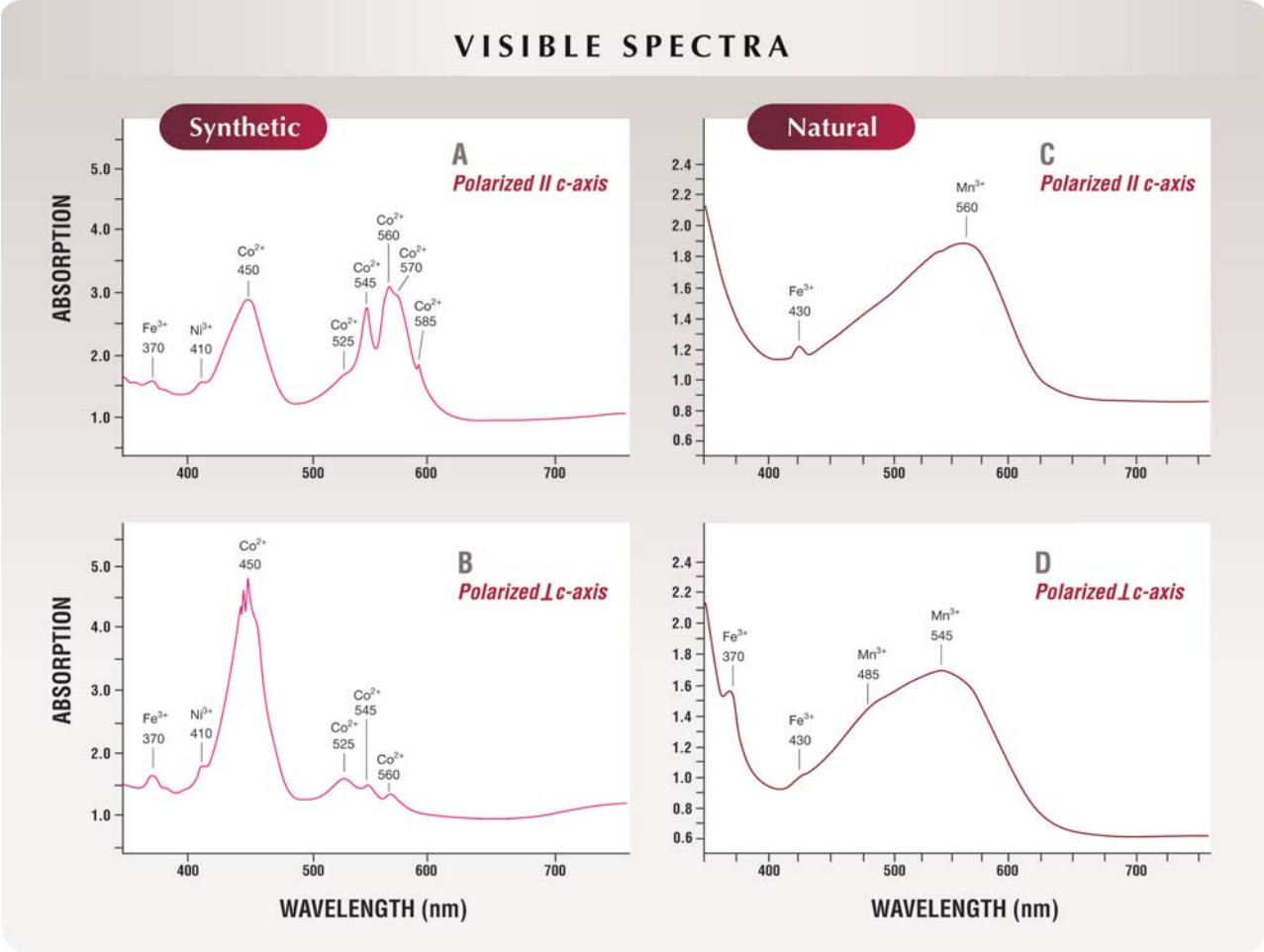

Figure 15. These polarized visible absorption spectra of synthetic (A and B) and natural (C and D) red beryl reveal distinctive differences in the two materials. Note in particular the prominent Co-related absorption bands between about 530 and 590 nm in the synthetic material. Spectra A and B were recorded for a polished fragment (2.7 mm thick) taken from an orange-red synthetic crystal. Spectra C and D were recorded for an oriented natural purplish red crystal from Utah, on which a flat surface had been polished parallel to a prominent prism face (3.2 mm thick).

The spectrum polarized perpendicular to the c-axis (figure 15D) displays a similar pattern, but with these additional features:

1. A weak band at about 370 nm (Fe^{3+})
2. A weak band at about 485 nm (Mn^{3+}) on the shoulder of the intense broad band that is mentioned above
3. An intense broad band that is centered at about 545 nm

For either natural or synthetic red beryl, a visible spectrum recorded using unpolarized light will exhibit the more intense of these spectral features. In particular, the diagnostic series of Co^{2+} absorption bands would be present at approximately 530, 545, 560, 570, and 590 nm (due to Co^{2+}) in the synthetic sample.

Infrared Spectroscopy. A comparison of mid-infrared (6000–400 cm^{-1}) spectra for representative natural and synthetic red beryls (figure 16) reveals absorption features that have been reported previously in hydrothermal synthetic beryls (see Schmetzer and Kiefert, 1990; Henn and Milisenda, 1999). The natural crystal displays almost no absorption features above 2300 cm^{-1}, except for several weak features between about 3000 and 2800 cm^{-1}. In contrast, the synthetic red beryl displays spectral features at about 5300 cm^{-1}, a very strong region of absorption between 4200 and 3200 cm^{-1}, and a series of weaker features from 3300 to 2300 cm^{-1}. The absorption between 4200 and 3200 cm^{-1} has been attributed to the presence of water in beryl (Wood and Nassau, 1968; Aurisicchio et al., 1994). This latter feature in the spectrum of

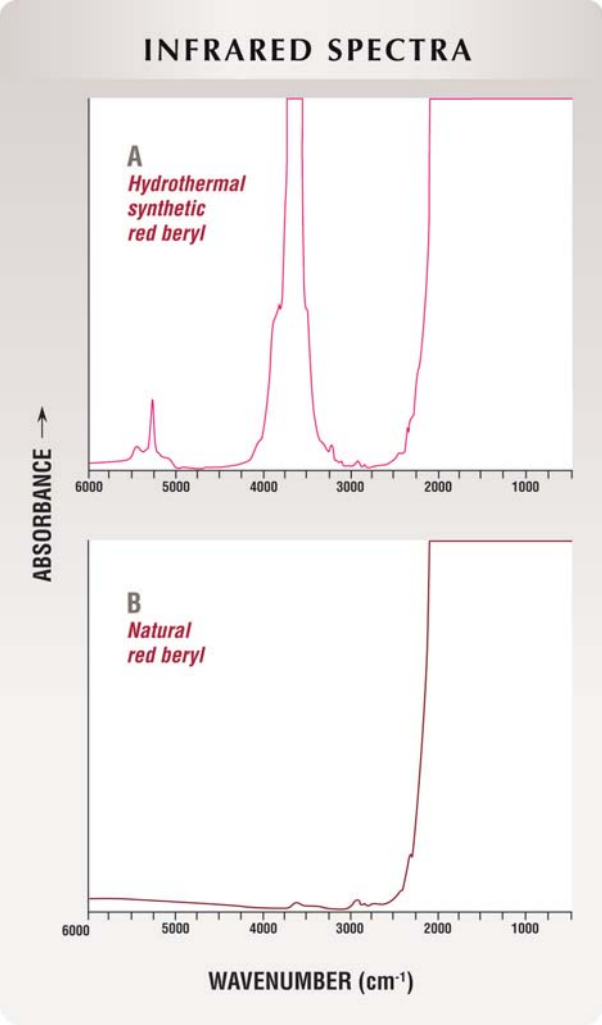

Figure 16. In these mid-infrared absorption spectra, strong absorption between 4200 and 3200 cm^{-1} is diagnostic of the synthetic red beryl (A). This absorption, which is due to water, is virtually absent in the spectrum of natural red beryl (B).

synthetic red beryl, and its absence in the spectrum of the natural counterpart (which contains very little water), is the most distinctive difference in infrared spectra, and it provides immediate proof that the material is a hydrothermal synthetic.

Schmetzer and Kiefert (1990) grouped natural and synthetic emeralds into five categories based on the relative intensities of the water-related mid-infrared bands at 3694, 3592, and 3655 cm^{-1} (which they labeled as bands A, B, and C, respectively). The relative intensity ratio of these three bands in the synthetic red beryl is A>B>>C. This result is consistent with the group II spectrum type, which Schmetzer and Kiefert (1990) suggested is typical of other low alkali-bearing synthetic beryls and synthetic emeralds grown in Russia.

CONCLUSION

Although natural red beryl remains a rare and relatively expensive gem material, its synthetic counterpart is also attractive but has not attained widespread demand. Synthetic red beryl has a distinctive tabular crystal morphology, chevron-like or wavy internal growth zoning, and several strong absorption bands between 530 and 590 nm due to coloration by Co^{2+}. Overall, inclusions were rare in the synthetic red beryls examined for this study, but occasional single- or two-phase fluid (liquid or liquid-gas) and spicule inclusions were seen. In addition, the presence of Co and Ni is proof that the material is synthetic, as are water-related absorption bands between 4200 and 3200 cm^{-1} in the infrared spectra. ●

ABOUT THE AUTHORS
Dr. Shigley (jshigley@gia.edu) is director, Dr. Lu is research scientist, and Mr. Elen is supervisor of analytical equipment at GIA Research in Carlsbad, California. Mr. McClure is director of identification services, and Mr. Koivula is chief research gemologist at the GIA Gem Trade Laboratory in Carlsbad. Ms. Cole is collection curator at GIA in Carlsbad. Dr. Demianets is head of the Department of Crystal Growth from Solutions at the Institute of Crystallography, Russian Academy of Sciences, Moscow. She supervised the production of the synthetic red beryl described in this article.

Acknowledgments: The authors thank Evgeni Vertkov of Worldwide Gem Marketing Corp., Huntington Beach, California. Sam Muhlmeister, a research associate at the GIA Gem Trade Laboratory (GTL), Carlsbad, helped with EDXRF analysis. Mike Moon, formerly of GIA Research, helped with collection of spectroscopic data. Dr. Chi Ma of the Division of Geological and Planetary Sciences, California Institute of Technology, Pasadena, carried out the electron microprobe analyses. Dr. Ilene Reinitz of the GIA GTL in New York provided helpful suggestions. The authors also thank Dr. Karl Schmetzer and two unidentified reviewers for their useful comments, and Kennecott Exploration Co. for the donation of two natural red beryl crystals analyzed as part of this study.

REFERENCES

Aurisicchio C., Fioravanti G., Grubessi O., Zanazzi P.F. (1988) Reappraisal of the crystal chemistry of beryl. *American Mineralogist*, Vol. 73, No. 7/8, pp. 826–837.

Aurisicchio C., Fioravanti G., Grubessi O. (1990) Genesis and growth of the red beryl from Utah (U.S.A.). *Atti Della Accademia Nazionale dei Lincei, Rendiconti Lincei, Scienze Fisiche e Naturali*, Series 9, Vol. 1, No. 4, pp. 393–404.

Aurisicchio C., Grubessi O., Zecchini P. (1994) Infrared spectroscopy and crystal chemistry of the beryl group. *Canadian Mineralogist*, Vol. 32, Part 1, pp. 55–68.

Brown G. (1990) Biron synthetic pink beryl. *Australian Gemmologist*, Vol. 17, No. 6, pp. 219–221.

——— (1993) Australian titaniferous synthetic beryl. *Journal of the Gemmological Association of Hong Kong*, Vol. 16, pp. 5–6.

Bukin G.V., Godovikov A.A., Klaykhin V.A., Sobolev V.S. (1986) Growth of emerald single crystals. *Growth of Crystals*, Vol. 13, pp. 251–260.

Černý P., Hawthorne F.C. (1976) Refractive indices versus alkali contents in beryl: General limitations and applications to some pegmatitic types. *Canadian Mineralogist*, Vol. 14, Part 4, pp. 491–497.

Deer W.A., Howie R.A., Zussman J. (1997) *Rock-forming Minerals, Vol. 1B, Disilicates and Ring Silicates*. The Geological Society, London.

Demianets L.N. (1996) Regeneration growth of some hexagonal (trigonal) crystals under hydrothermal conditions. *Collected Abstracts, International Union of Crystallography, 12th Congress and Assembly*, Seattle, Washington, August 8–17.

Emel'yanova E.N., Grum-Grzhimailo S.V., Boksha O.N., Varina T.M. (1965) Artificial beryl containing V, Mn, Co, and Ni. *Soviet Physics—Crystallography*, Vol. 10, No. 1, pp. 46–49.

Flamini A., Gastaldi L., Grubessi O., Viticoli S. (1983) Sulle caratteristiche particolari del berillo rosso dell'Utah. *La Gemmologia*, Vol. 9, No. 1/2, pp. 12–20.

Fritsch E., Rossman G.R. (1987) An update on color in gems. Part 1: Introduction and colors caused by dispersed metal ions. *Gems & Gemology*, Vol. 23, No. 3, pp. 126–139.

Fritsch E., Muhlmeister S., Birkner A. (1992) A preliminary spectroscopic study of the Biron synthetic pink titanium-beryl. *Australian Gemmologist*, Vol. 18, No. 3, pp. 81–82.

Harding R.R. (1995) A note on red beryl. *Journal of Gemmology*, Vol. 24, No. 8, pp. 581–583.

Henn U., Becker G. (1995) Rote Berylle aus Utah, USA–Neue Beobachtungen. *Zeitschrift der Deutschen Gemmologischen Gesellschaft*, Vol. 44, No. 2/3, pp. 55–60.

Henn U., Milisenda C.C. (1999) Synthetische rote Berylle aus Russland. *Gemmologie: Zeitschrift der Deutschen Gemmologischen Gesellschaft*, Vol. 48, No. 2, pp. 97–104.

Hosaka M., Tubokawa K., Hatushika T., Yamashita H. (1993) Observations of red beryl crystals from the Wah Wah Mountains, Utah. *Journal of Gemmology*, Vol. 23, No. 7, pp. 409–411.

Lebedev A.S., Ilyin A.G., Klyakhin V.A. (1982) Hydrothermally grown beryls of gem quality. *Morphology and Phase Equilibria of Minerals*, International Mineralogical Association, Meeting, Vol. 2, pp. 403–405 (in Russian).

——— (1983) Variétés de béryl "gemme" hydrothermal. *Revue de Gemmologie a.f.g.*, No. 76, pp. 4–5.

Miley F. (1980) An examination of red beryl. *Gems & Gemology*, Vol. 16, No. 12, pp. 405–408.

Nassau K. (1976) Synthetic emeralds: The confusing history and current technology. *Journal of Crystal Growth*, Vol. 35, pp. 211–222.

——— (1980) *Gems Made by Man*. Chilton Book Co., Radnor, PA.

Nassau K., Wood D.L. (1968) An examination of red beryl from Utah. *American Mineralogist*, Vol. 53, No. 5/6, pp. 801–806.

Platonov A.N., Taran M.N., Klyakhin V.A. (1989) On two colour types of Mn^{3+}-bearing beryls. *Zeitschrift der Deutschen Gemmologischen Gesellschaft*, Vol. 38, No. 4, pp. 147–154.

Schaller W.T., Stevens R.E., Jahns R.H. (1962) An unusual beryl from Arizona. *American Mineralogist*, Vol. 47, No. 5/6, pp. 672–699.

Schmetzer K. (1988) Characterization of Russian hydrothermally-grown synthetic emeralds. *Journal of Gemmology*, Vol. 21, No. 3, pp. 145–164.

——— (1989) Types of water in natural and synthetic emerald. *Neues Jahrbuch für Mineralogie Monatshefte*, No. 1, pp. 15–26.

Schmetzer K., Kiefert L. (1990) Water in beryls—A contribution to the separability of natural and synthetic emeralds by infrared spectroscopy. *Journal of Gemmology*, Vol. 22, No. 4, pp. 215–223.

Schmetzer K., Bank H., Berdesinski W. (1974) Eine seltene rote Varietät der Mineralart Beryll. *Zeitschrift der Deutschen Gemmologischen Gesellschaft*, Vol. 23, No. 2, pp. 139–141.

Schmetzer K., Kiefert L., Bernhardt H.-J., Beili Z. (1997) Characterization of Chinese hydrothermal synthetic emerald. *Gems & Gemology*, Vol. 33, No. 4, pp. 276–291.

Shigley J.E., Foord E.E. (1984) Gem-quality red beryl from the Wah Wah Mountains, Utah. *Gems & Gemology*, Vol. 20, No. 4, pp. 208–221.

Sinkankas J. (1981) *Emerald and Other Beryls*. Chilton Book Co., Radnor, PA.

Solntsev V.P., Kharchenko E.I., Lebedev A.S., Klyakhin V.A., Ilyin A.G. (1981) Nature of color centers and EPR of a manganese-activated beryl. *Journal of Applied Spectroscopy*, Vol. 34, No. 1, pp. 111–115.

Sosso F., Piacenza B. (1995) Russian hydrothermal synthetic emeralds: Characterization of the inclusions. *Journal of Gemmology*, Vol. 24, No. 7, pp. 501–507.

Taylor A.M. (1967) Synthetic cobalt beryl. *Journal of Gemmology*, Vol. 10, No. 8, pp. 258–261.

Troup G.T., Hutton D.R., Pilbrow J.R. (1990) Electron paramagnetic resonance and fluorescence of Ti^{3+} in Australian Biron synthetic beryl. In *Abstracts, Australian Institute of Physics, 14th Condensed Matter Physics Meeting*, Wagga Wagga, New South Wales.

Wood D.L., Nassau K. (1968) The characterization of beryl and emerald by visible and infrared absorption spectroscopy. *American Mineralogist*, Vol. 53, No. 5/6, pp. 777–800.

Gem Trade **LAB NOTES**

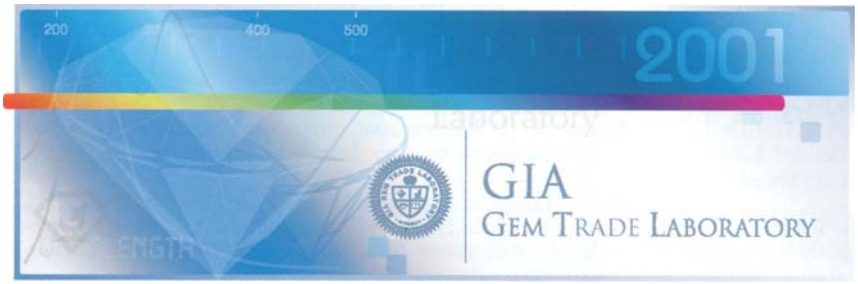

Editors

Thomas M. Moses, Ilene Reinitz, Shane F. McClure, and Mary L. Johnson
GIA Gem Trade Laboratory

Contributing Editors

G. Robert Crowningshield
GIA Gem Trade Laboratory, East Coast

Karin Hurwit, John I. Koivula, and Cheryl Y. Wentzell
GIA Gem Trade Laboratory, West Coast

Unusual ANDRADITE GARNET

The East Coast lab recently was given the opportunity to examine, for a limited time, a transparent, very dark red, round-brilliant-cut stone (figure 1, far left) that weighed 5.73 ct and measured approximately 11.51 × 11.32 × 6.50 mm. According to the client, Jeffrey Hayat of Gem Demantoid in New York City, the stone was recovered from a mine in Namibia (exact locality not disclosed) that produces andradite garnet in a wide variety of colors, ranging from orange to yellow to (demantoid) green (again, see figure 1). Yellowish green to brown andradites from Namibia were described in the Fall 1997 Gem News section (pp. 222–223).

Standard gemological testing revealed an R.I. over-the-limits of the standard refractometer (that is, greater than 1.81) and a specific gravity of 3.86, both of which are consistent with andradite garnet. When viewed between crossed polarizers, the stone showed snake-like bands and strain colors, both in patterns and sections, as well as multiple directions of growth. The stone did not fluoresce to either long- or short-wave ultraviolet radiation. The desk-model prism spectroscope revealed a 420 nm cutoff, which—like the features indicated above—is typical for andradite garnet. Confirmation that the stone was andradite was provided by Raman analysis.

Microscopic examination revealed some fractures and fingerprints, as well as a group of aligned acicular crystals (several of which were bent at one end to a new set of parallel orientations). Also present near these inclusions were some irregularly shaped crystals. A few small cavities seen on the crown were most likely the result of crystals that were pulled out during the cutting process. Although some color banding was visible with darkfield illumination, immersion of the stone in methylene iodide revealed a distinct yellow bodycolor and strong straight, angular, red-brown color banding (figure 2). This banding, which is not commonly seen in andradite garnet, accounted for the stone's unusual dark red color.

The gemological properties and

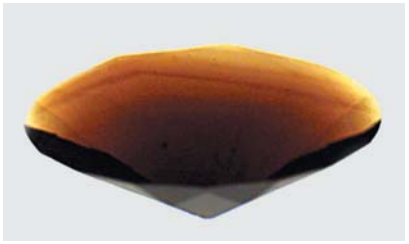

Figure 2. Immersion in methylene iodide made it easy to distinguish between the yellow bodycolor of the 5.73 ct andradite and its straight, angular, red-brown color banding.

Figure 1. The transparent, very dark red 5.73 ct round brilliant on the far left was identified as andradite garnet. The Namibian mine that produced this unusual red andradite also produces andradite garnets within their previously known range of colors (here, 0.82–3.29 ct).

Editor's note: The initials at the end of each item identify the editor(s) or contributing editor(s) who provided that item. Full names are given for other GIA Gem Trade Laboratory contributors.

Gems & Gemology, *Vol. 37, No. 1, pp. 56–63*

Figure 3. This 3.03 ct synthetic apatite showed a color change from purple-pink in incandescent light (left) to violetish blue in fluorescent light (right).

Raman analysis confirmed the client's original suspicion about the garnet's identity. The dark red color and strong color zoning are quite unusual for andradite, however.

Wendi M. Mayerson

SYNTHETIC APATITE

The West Coast laboratory recently received a call asking if we had ever seen a color-change apatite. None of the laboratory staff had seen or heard of such material. The caller said that a stone he had acquired as part of an old private gem collection was supposed to be one, so he sent it to us for examination.

When we received the sample, the first thing we noticed was its unusual color. In incandescent light, it was a very pleasing, medium-toned purple-pink. In fluorescent light, the color became an equally pleasing violetish blue (figure 3). To the best of our knowledge, these colors—like the color change—had never been reported for apatite.

Standard gemological testing of the 3.03 ct sample produced refractive indices of 1.630–1.637 (with a corresponding birefringence of 0.007), a specific gravity of 3.22, a uniaxial optic character, no fluorescence to long-wave—and a weak orange to short-wave—UV radiation, and numerous sharp lines in the desk-model spectroscope. The pleochroism was weak, and the pleochroic colors varied depending on which light source was used.

These properties are consistent with apatite, except for the spectrum. It is well known that blue and yellow apatites typically show a rare-earth spectrum, but this primarily consists of a small group of lines centered around 580 nm. This stone showed no fewer than 30 discrete lines across the spectrum, with major clusters around 520 and 580 nm. This fact alone aroused our suspicions about the sample's authenticity.

Microscopic examination revealed clouds throughout the sample in a vaguely chevron-like pattern that was somewhat reminiscent of the growth structure seen in some hydrothermal synthetics (figure 4). However, it was not a hydrothermal product because the most telling inclusions were several elongated gas bubbles, some of which had a thready appearance similar to that seen in some synthetic spinels (figure 5). These inclusions were clearly not natural, which led us to conclude that the piece was a synthetic apatite—the first synthetic apatite submitted to the laboratory for identification.

To acquire more information on this material, we performed qualitative chemical analysis via energy-dispersive X-ray fluorescence. EDXRF revealed that, in addition to phosphorus and calcium as major elements, there was a relatively large amount of neodymium present. A small amount of strontium also was detected. This chemistry is consistent with that reported in a Winter 1992 Gem News item (p. 277) for a color-change synthetic apatite that was being grown for laser applications. *SFM*

Figure 4. These clouds in synthetic apatite, which have a vaguely chevron-like pattern, are somewhat reminiscent of synthetics grown by the hydrothermal process, although that turned out not to be the case for this sample. Magnified 20×.

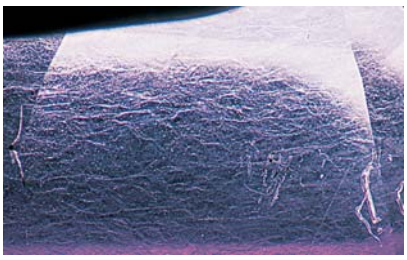

Figure 5. Elongated, thready gas bubbles in this color-change apatite proved its synthetic origin. Magnified 20×.

Unusual BERYL-and-Glass Triplet Imitating Emerald

Last fall, the East Coast laboratory received a transparent green emerald-cut stone that was prong set in a simple white metal pendant with a small transparent near-colorless round brilliant above it (figure 6). The emerald cut measured approximately 10.00 × 8.00 × 6.35 mm. The client who submitted the piece received it as a gift approximately 40 years ago and had been told it was an emerald. Although initial testing resulted in a refractive

Figure 6. The transparent green imitation emerald (10.00 × 8.00 × 6.35 mm) in this pendant was identified as an assemblage consisting of a colorless beryl crown of undetermined origin and a green glass pavilion joined by a colorless layer of cement.

Figure 7. Immersion in water eliminates the optical illusion of this assembled emerald imitation, and the true colors of the crown and pavilion can be seen.

index of 1.582–1.591 for the crown, typical for emerald, further observation using a standard gemological microscope revealed multiple gas bubbles aligned in a single plane parallel to the table of the stone. This was our first indication that the emerald cut was an assemblage.

The fact that this piece was an assemblage was not surprising in itself, since there are several relatively common types of assembled stones imitating emeralds in today's market, some of which have been used since the end of the 19th century (see, e.g., E. B. Misiorowski and D. M. Dirlam, "Art Nouveau: Jewels and jewelers," Winter 1986 *Gems & Gemology*, pp. 209–228). However, the typical assembled emerald simulant consists of a colorless crown and pavilion (commonly made of quartz, beryl, or synthetic spinel) that are joined by a green cement layer. This combination produces an optical illusion in which it appears that the crown and pavilion are green and the cement layer is colorless, even when viewed from the side. Immersion reveals the true colors of the assembled parts (see, e.g., Winter 1986 Lab Notes, pp. 236–238; Summer 1994 Gem News, p. 131). The emerald cut in this pendant showed the same optical effect when viewed from the side; yet when we immersed it in water, we were surprised to discover that the specimen had a *colorless* crown attached by *colorless* cement to a *green* pavilion (figure 7).

Our next step was to determine the identity of each component of this assemblage. First, we placed the entire piece on its side in a polariscope. We then rotated the piece 360° between crossed polarizing filters. Consistent with the refractive indices we had ascertained, the crown "blinked," which indicated that it was a doubly refractive material. Since we already had determined that the crown was colorless, this meant that it must be colorless beryl. Our second surprise was that the pavilion did not blink, even when checked in three directions. It also did not show pleochroism, which confirmed that it was isotropic (singly refractive). Since the mounting prevented access to the pavilion with a standard refractometer, we used a small, vintage (1940s) "Gem Refractometer." The resulting R.I. of 1.49, along with the results we obtained from testing an inconspicuous spot with hardness points under magnification, confirmed that the pavilion was made of glass.

This assemblage proved to be unusual for two reasons. First, its face-up green color was the result of reflection off a green pavilion, rather than reflection off a green cement

Figure 8. Viewed table-up with darkfield illumination, this 1.34 ct diamond shows only a few small inclusions and the faint outline of a cloud of "pinpoints." Magnified 15×.

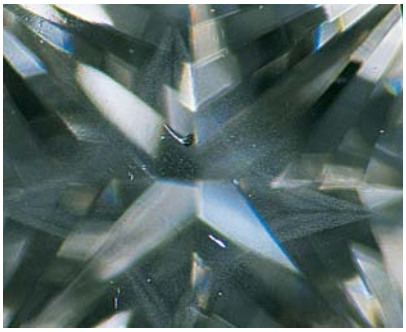

Figure 9. When the diamond was viewed in the same position as in figure 8, but with fiber-optic illumination, a bright and beautiful stellate cloud became visible. Magnified 15×.

layer. Second, its crown and pavilion consisted of two entirely different materials. The conclusion in the resulting gem identification report read as follows: "Triplet consisting of a colorless beryl crown and a green glass pavilion, joined together with colorless cement." The following comment also was included: "The natural or synthetic origin of this beryl is currently undeterminable."

Wendi M. Mayerson

DIAMOND

With a Hidden Cloud Formation

Darkfield is the standard illumination for clarity grading diamonds with a gemological microscope, and today's gemological microscopes are manufactured with highly efficient built-in darkfield systems. Darkfield illumination is uncomplicated, effective, and provides a consistency that is extremely important in determining the nature and number of internal features in a diamond.

However, darkfield is not the only method of illumination useful in the examination of polished diamonds. For example, polarized light will reveal strain in diamonds that would not be visible under darkfield conditions. A fiber-optic illuminator may also reveal features that were not seen in darkfield.

We recently saw an excellent example of the benefits of using a fiber-optic light source in a 1.34 ct diamond sent to the West Coast laboratory for grading. When viewed table-up in darkfield conditions, the diamond seemed to contain only a few small inclusions as well as the faint outline of a cloud composed of tiny "pinpoints" (figure 8). However, when illuminated through the side with a fiber-optic light probe and viewed in the identical table-up position, this same diamond appeared entirely different. The "faint cloud" observed with darkfield illumination turned out to be a bright and beautiful stellate cloud of octahedral form (figure 9), which seemed to add an almost magical quality to the interior of this diamond.

While it is important for economic and business reasons to maintain the efficiency of the diamond-grading process, sometimes exploring outside the parameters of traditional diamond-grading practice can be quite rewarding. It is hard to believe that the owners of this or any similar diamond would not want to know that their diamond was host to such a spectacular cloud formation. It is important for all gemologists to keep in mind that just because you don't see it, that doesn't mean it isn't there. Note, too, that features seen with such sources of illumination do not contribute to the clarity grade of the diamond, which is determined solely by features seen with darkfield.

JIK and Maha Tannous

With Pseudo-Dichroism

In the day-to-day business of diamond grading, the color grading of fancy-color diamonds presents certain problems and challenges for the gemological laboratory. One of these is how to deal with color zoning. A case in point is the strongly color-zoned 0.24 ct diamond shown in figure 10, which appeared brownish pink face up.

Figure 10. This 0.24 ct color-zoned diamond appeared brownish pink when viewed face-up.

The grader had to determine the relative influence of each of the color components, brown and pink, in order to establish which of the two was dominant and, therefore, would be designated the priority color. One factor that can affect the final outcome is color zoning. While not all fancy-color diamonds show color zoning, those that do present special challenges; in addition, the difficulty of determining the final color increases as the zoning becomes more prominent.

When examined through its pavilion in two different viewing directions (180° apart) the diamond appeared to be essentially brown with only a slight influence of a pink component (figure 11, left). When this

Figure 11. When viewed from certain directions through the pavilion, the diamond shown in figure 10 appeared a slightly pinkish brown (left). When the diamond was rotated approximately 90° (right), the color observed through the pavilion changed dramatically to a much more intense pink, which gave the appearance of pseudo-dichroism. Strong color zoning was also visible. Both magnified 10×.

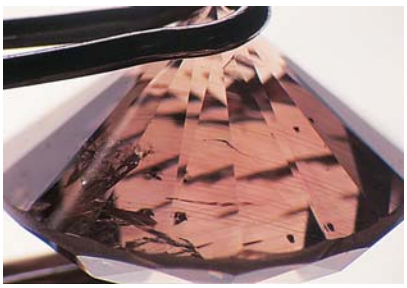

same stone was rotated 90° from either of these positions, the dominant color was an obvious pink that appeared only slightly brownish. We also noticed that the color in these alternate views was strongly zoned and uneven in its distribution (figure 11, right). This change of color with viewing direction created the illusion of dichroism in the diamond. Since true dichroism is impossible in a singly refractive mineral such as diamond, this pseudo-dichroism was attributed to the very strong directional color zoning, which is not often encountered in diamonds.

At the GIA Gem Trade Laboratory, color grades for fancy-color diamonds are assessed through the crown and table facets only (see, e.g., J. King et al., "Color grading of colored diamonds in the GIA Gem Trade Laboratory," Winter 1994 *Gems & Gemology*, pp. 220–242), so this pseudo-dichroism did not affect the color call of brownish pink. In instances where the face-up appearance shows distinctly different colors, those colors are noted on the reports.

JIK and Maha Tannous

SYNTHETIC DIAMOND
With Distinctive Surface Features

The East Coast lab recently received, for origin-of-color determination, two stones that displayed very unusual surface features. One, a 0.75 ct orange-yellow cut-cornered rectangular brilliant, exhibited a stippled surface—with what appeared to be numerous small whitish pits—on several of its large pavilion facets (figure 12). The other, a 0.52 ct orangy yellow round brilliant (figure 13, left), had numerous large cavities on its table. Both had the gemological properties of diamond.

However, magnification of the 0.75 ct stone at a relatively low power (10×) revealed color zoning that followed an hourglass pattern, a cloud of small highly reflective inclusions, and larger opaque inclusions. Using a desk-model spectroscope, we found several fine absorption bands throughout the green area of the spectrum. The sample fluoresced a very weak orange, with a square zone of strong greenish yellow under the table, to both long- and short-wave UV radiation. The color zoning, inclusions, spectrum, and fluorescence were all typical of synthetic diamond. The large pavilion facets had the rough appearance of large, "unpolished" natural diamond surfaces, but they did not show any of the growth or dissolution features that one would expect to see on such "naturals." Higher magnification revealed that the stippling was actually the result of the faceting process, in the course of which a cloud of small highly reflective flux inclusions was exposed on the surface. The stone's weak attraction to a magnet verified that the pinpoints in the cloud were a metallic flux, thereby confirming that this was a synthetic diamond.

Higher-magnification examination of the surface features of the 0.52 ct stone provided some important clues to its origin. The noncrystalline shape of the features (figure 13, center), along with the fact that they were cavities (voids) and not surface-reaching inclusions (figure 13, right), suggested that they were the result of flux inclusions that had been dissolved by an acid. Washing in acid is a common procedure after diamond cutting. Unlike the 0.75 ct synthetic diamond, the color zoning in this stone, while uneven, did not follow an obvious hourglass pattern. Only examination through the bezel facets provided us with the visual clue of a partial cubic growth structure, which suggested synthetic origin. The strong magnetic reaction (in response to the remaining, wholly included flux) confirmed that this diamond was also synthetic.

Although the surface features of both synthetic diamonds were somewhat unusual, the other properties were consistent with those previously noted for this material (see, e.g., J. E. Shigley et al., "A chart for the separation of natural and synthetic diamonds," Winter 1995 *Gems & Gemology*, pp. 256–265).

Akira Hyatt and Thomas Gelb

Figure 12. Note the cloud of small highly reflective flux inclusions in this 0.75 ct orange-yellow synthetic diamond. Magnified 30×.

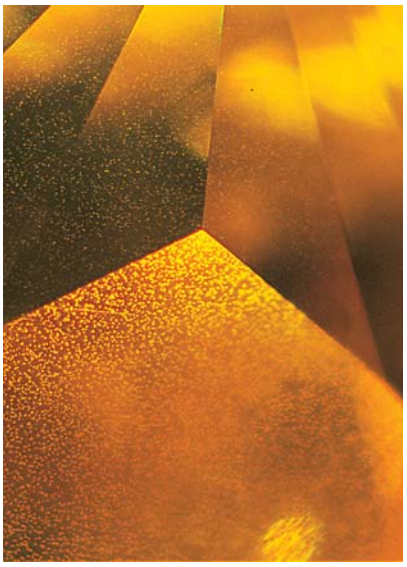

Another MUSGRAVITE

In the Summer 1997 Gem News section (pp. 145–147), the editors described the first example of faceted musgravite they had seen. Since that time, many people have submitted stones to the laboratory for testing in the hopes that they would prove to be musgravite, which has become highly sought after as a collector's stone. Until recently, all of those stones turned out to be taaffeite. The separation of these two minerals is difficult, because their physical and optical properties overlap to such a degree that it is impossible to distinguish them completely with standard gemological testing.

A few months ago, gem collector James Houran sent our West Coast

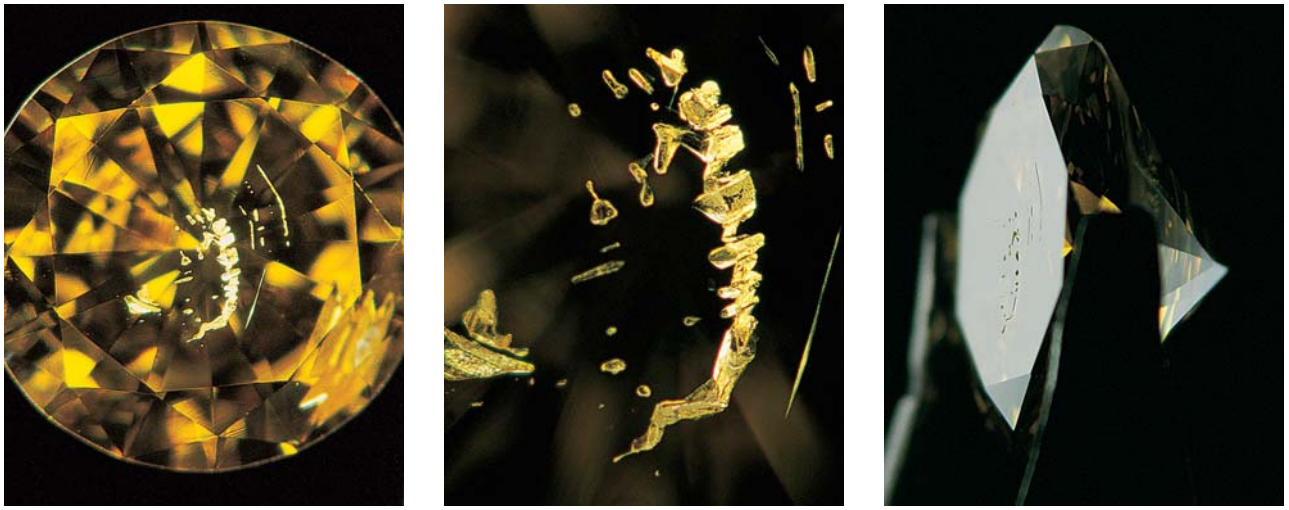

Figure 13. Left: Large cavities were visible on the table of this 0.52 ct orangy yellow synthetic diamond at relatively low magnification (15×). Center: At higher magnification (45×), it is evident that these cavities are amorphous rather than crystalline in shape. Right: Examination with reflected light confirmed that the cavities were not related to surface-reaching inclusions but were probably the result of flux inclusions that had been dissolved during an acid cleaning after polishing (magnified 15×).

lab a stone that had been represented to him as green taaffeite, a color we had not seen in that gem species. The 0.36 ct cushion mixed cut was actually greenish gray (figure 14). Standard gemological testing revealed refractive indices of 1.719–1.726 (birefringence 0.007), a specific gravity of 3.61, no pleochroism or UV fluorescence, and a band at 460 nm in the desk-model spectroscope. These properties were within the range for taaffeite, but the R.I. and birefringence were relatively high compared to those noted in the majority of taaffeites we had seen. Checking the literature, we found that these were the exact optical properties reported for musgravite in the above-mentioned Gem News item. To confirm this identification, we performed more-sophisticated tests on the stone.

Qualitative chemical analysis by EDXRF revealed magnesium and aluminum as the primary components, with relatively high concentrations of iron and zinc, and smaller amounts of manganese, calcium, and gallium. This chemistry is consistent with taaffeite and musgravite, $BeMg_3Al_8O_{16}$ and $(Mg,Fe,Zn)_2BeA_{16}O_{12}$, respectively (Gaines et al., *Dana's New Mineralogy*, 8th ed., John Wiley & Sons, New York, 1997, p. 309; Be and O are not detectable with EDXRF). However, even though higher levels of iron and zinc have been noted previously in musgravite, this chemistry is not distinctive of either mineral.

In 1998, L. Kiefert and K. Schmetzer published a study describing the separation of taaffeite and musgravite using Raman analysis ("Distinction of taaffeite and musgravite," *Journal of Gemmology*, Vol. 26, No. 3, pp. 165–167). We had used this method on several stones submitted to the lab in the past that were represented as musgravite. In those cases, the spectra always showed a match for taaffeite, and this identification was subsequently confirmed by X-ray diffraction analysis. This time, however, the Raman spectra matched the published results for musgravite, and X-ray diffraction analysis verified the identification. This was the first opportunity we have had to confirm in our laboratory the usefulness of Raman spectroscopy in distinguishing musgravite from taaffeite.

Figure 14. This 0.36 ct greenish gray musgravite is only the second faceted example of this mineral species seen at the GIA Gem Trade Laboratory.

This was only the second example of faceted musgravite to come through our laboratory (and only the fourth reported, to our knowledge). It was also particularly useful, in that the test results were consistent with the previously published high-end refractive index and birefringence for musgravite as well as with the published

Figure 15. Note the broad range of natural colors in this five-strand necklace of natural saltwater pearls (3.75–10.30 mm).

distinction of this mineral using Raman spectroscopy. *SFM*

PEARLS
Natural Five-Strand Pastel Necklace

Given the recent rise in popularity of a broader range of pearl colors, we were intrigued by a necklace that was submitted to the East Coast lab. The five-strand necklace contained a total of 518 pearls, ranging from approximately 3.75 to 10.30 mm, of various shapes and colors (figure 15). The strands were graduated in length and attached by a diamond clasp. Using the standard gemological tests of X-radiography, X-ray fluorescence, and magnification, we determined that all were saltwater pearls of natural origin and color.

The worn condition of the pearls indicated that the necklace was an older piece, and as such it displayed an unusually broad range of pastel colors. These included the oranges, yellows, and pinks that are so popular today in Chinese freshwater cultured pearls (see, e.g., Fall 1998 Lab Notes, pp. 216–217, and the cover and p. 102 of the Summer 2000 issue of *Gems & Gemology*). It also displayed cooler hues such as blues and violets. In addition, there were several greenish yellow pearls, and even one pearl with a stronger saturation that appeared similar to what might be considered a "pistachio" color today.

The asymmetrical, if not somewhat random, placement of the various pearls made for a visually engaging piece that was further enhanced by the diamond clasp. The clasp was composed of a single very light brown marquise-cut diamond surrounded by near-colorless baguettes and triangular cuts. The color of the marquise worked well with this necklace, complementing the hues and tones of the various pearls. *Akira Hyatt*

QUARTZITE
Bangle Dyed Three Colors to Imitate Jadeite

In December 2000, the East Coast lab received for identification a translucent bangle bracelet that was a mottled lavender, green, and orange. It measured approximately 74.75 × 14.20 × 8.20 mm (figure 16). Carved from a single piece of gem material, such bracelets are commonly made of jadeite or nephrite, since their exceptional toughness is required to give the piece durability.

Standard gemological testing revealed a spot refractive index of 1.54 on the crystalline aggregate material. This did not match the R.I. of either jadeite (1.66) or nephrite (1.61). Microscopic examination of each color region revealed dye concentrations in fractures and in between individual grains; the dye concentrations overlapped in those areas where two colors appeared to meet (figure 17). Although we did not see any distinct lines with

Figure 16. This tri-colored, dyed, and impregnated quartzite bangle bracelet is effective as a simulant of high-quality jadeite.

a desk-model prism spectroscope, the green area revealed a dark absorption in the far red (680–700 nm). The lavender areas fluoresced a medium pink to long-wave UV radiation, and the whole bracelet fluoresced a medium-strong bluish white to short-wave UV. Testing with a Fourier-transform infrared spectrometer (FTIR) confirmed that the bracelet was not jadeite and suggested quartz. More importantly, this spectrum indicated that the bracelet had been polymer impregnated.

Figure 17. At 50× magnification, the dye concentrations in the bracelet shown in figure 16 can be seen to overlap where the colors appear to meet.

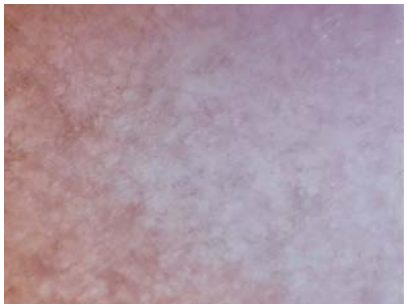

Identification of the bracelet as dyed quartzite was not surprising, since this metamorphic rock—formed by the silica cementation of quartz grains—is one of the most familiar jadeite simulants in today's market (see, e.g., R. Kammerling et al., "Some common—and not so common—imitations of jade," *Journal of the Gemmological Association of Hong Kong*, Vol. 18, 1995, pp. 12–19). Quartzite is also commonly dyed a variety of colors to imitate various types of jadeite (see Summer 1991 Gem News, p. 122; Winter 1987 Lab Notes, p. 234; and Summer 1987 Lab Notes, pp. 106–107).

What was somewhat surprising was that the bracelet had been polymer impregnated. Jadeite is often "bleached" with acids to remove staining, a process that weakens its structure by dissolving and removing random grains. As a result, bleached jadeite is usually impregnated with polymers to restore durability and improve luster. Such an impregnation may also add color if a dye has been mixed into the polymer. Quartzite should not need to be impregnated, even after "bleaching," because quartz is not soluble in the acids used for jade bleaching. In the case of this bracelet, the impregnation may have been merely a way to carry the dye into the quartzite. Alternatively, the piece may have been polymer impregnated precisely to deceive—not only the casual observer, but also the advanced gemological tester—by giving a polymer signal on the spectrometer. Because there are only slight distinctions in the infrared spectra of jadeite and quartz, a tester who was looking only for evidence of treatment might overlook the subtle differences. Although we reported on an impregnated dyed green quartzite cabochon in the Summer 1995 Lab Notes (pp. 125–126), this was the first tri-colored dyed and impregnated quartzite bangle examined in our lab.

Wendi M. Mayerson

PHOTO CREDITS
Elizabeth Schrader took figures 1, 2, and 16. Maha Tannous supplied figures 3, 10, and 14. Shane F. McClure provided figures 4 and 5. Jennifer Vaccaro supplied figures 6 and 7. John I. Koivula took figures 8, 9, and 11. Vincent Cracco provided figures 12 and 13. Akira Hyatt supplied figure 15. Wendi Mayerson took figure 17.

GEM NEWS International

This issue marks the introduction of the Gem News International (GNI) section in *Gems & Gemology*. We have restructured the Gem News section as GNI to truly reflect the international nature of our discipline. This section will provide a forum for brief communications and specific coverage of new localities, new materials, and new techniques/instrumentation, as well as the conference reports and many other interesting developments that our readers have come to anticipate. The editorship of GNI has been assumed by Brendan Laurs, senior editor of *Gems & Gemology*. In addition, we have added three more contributing editors from the world's major gemological laboratories.

As before, items from other contributors are welcome. Author bylines are provided for contributing editors and outside authors (with affiliation and e-mail, where available, on the first entry if more than one entry is provided). Items without bylines were prepared by the section editor or other *G&G* staff. All contributions should be sent to Brendan Laurs at blaurs@gia.edu (e-mail), 760-603-4595 (fax), or GIA, 5345 Armada Drive, Carlsbad, CA 92008.

DIAMONDS

White House Conference on "Conflict" Diamonds. In an effort to ensure political stability and eliminate human rights abuses in certain African countries, the outgoing U.S. Presidential administration convened the "White House Diamond Conference: Technologies for Identification and Certification" in Washington, D.C., on January 10. This one-day conference addressed the need to eliminate conflict diamonds (e.g., those mined from rebel-controlled areas in Angola, the Democratic Republic of the Congo, and Sierra Leone) from international commerce. The objective was to determine if technology is in place—or could be developed and perfected within the next five to 10 years—to identify or track rough and polished diamonds from specific regions of origin through the jewelry trade to the consumer. This goal should be accomplished without disrupting or penalizing the legitimate diamond trade, including the economies of African countries that depend on legitimate diamond exports, such as Botswana, Namibia, and South Africa. According to current estimates, conflict diamonds account for less than 4% of the world's rough diamond production.

The conference brought together 132 participants from governments, the diamond industry, companies with specialized technologies, academia (including museums), and humanitarian nongovernmental organizations (e.g., Global Witness, Amnesty International). Most of the participants were policy makers, scientists, and engineers from the U.S. Also present were technical personnel from Canada, Great Britain, Belgium, and Israel, as well as diplomatic representatives of countries involved in the diamond trade.

A plenary "background" session explained the complexities of the diamond industry to conference participants who were not involved in the trade. Recurrent themes were:

- The long-term harm that negative publicity associated with conflict diamonds could cause the jewelry industry
- The recognition that, with the knowledge presently available, it is not possible to certify the country of origin of individual diamonds, either rough or polished
- The difficulty of completely eliminating trade in conflict diamonds in impoverished societies where corruption exists.

The World Diamond Council (represented by Eli Izhakoff) strongly supports a global rough-diamond certification program, such as the proposed "System for International Rough Diamond Export and Import Controls," as the only feasible approach to the conflict diamond problem at this time (to view a copy of the document, visit www.worlddiamondcouncil.com). Yet the intricacies of the diamond "pipeline" (described by Jeffrey Fischer of the Diamond Manufacturers and Importers Association of America), in which diamonds mined in 22 countries often

GEMS & GEMOLOGY, Vol. 37, No. 1, pp. 64–78

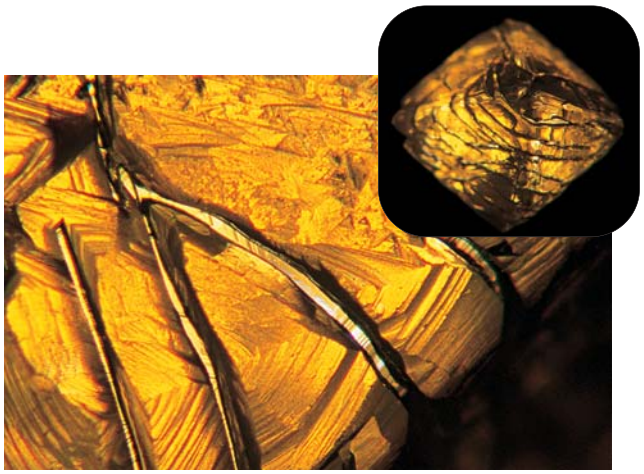

Figure 1. At a recent White House conference on "conflict" diamonds, scientists grappled with methods of determining the country of origin of rough and polished diamonds. Some experts have classified the geographic origin of rough diamonds by observing their external morphology. Note the complex features on the surface of this 1.03 ct diamond (see inset) from the Sewa River in Sierra Leone. Photos courtesy of Thomas Hunn Co., Grand Junction, Colorado.

go through numerous mixings and trans-border crossings before they reach the cutting factory, makes any control system a challenge. The Belgian High Diamond Council (HRD, represented by Mark van Bockstael) recently helped implement a prototype certification program for legitimate diamonds from Angola and Sierra Leone.

The following session, on measuring chemical and physical properties of diamonds to determine their country of origin, focused on diamond formation in the Earth's interior and subsequent transport to the surface (Prof. Stephen Haggerty, University of Massachusetts), chemical and isotopic analyses (Prof. Roberta Rudnick, University of Maryland), and spectroscopic characteristics (Prof. Lawrence Taylor, University of Tennessee). Notwithstanding the possibilities suggested by many advanced and sophisticated techniques and instruments (e.g., determinations of trace elements and C, N, O, and S isotopes in diamonds and their inclusions by various forms of mass spectrometry), no chemical or physical method is sufficiently definitive to be practical for determining the country of origin of a diamond.

Dr. Jeff Harris (University of Glasgow) noted that experts can sometimes classify the geographic origin of some rough diamonds with a high degree of confidence on the basis of external morphology (see, e.g., figure 1)—particularly with "run of mine" parcels. However, mixing of rough diamonds from different sources can defeat the authenticity of such determinations. The likelihood of recognizing rough diamonds from Angola and Sierra Leone is also severely hampered by the fact that the vast majority of the conflict diamonds in these countries are alluvial in origin, so they probably originate from several primary sources (possibly in neighboring "nonconflict" countries).

The task of determining a diamond's country of origin becomes quite daunting when the actual magnitude of the diamond trade is realized. One of us (JES) informed the conference participants that over 800 million polished diamonds enter the market annually, and the vast majority are small stones weighing about 2–3 points on average (mostly cut in India). Furthermore, all the potentially useful methods to analyze the chemical or physical properties of diamonds or their inclusions require expensive equipment, highly trained personnel, and lengthy timeframes. A large database of information about the chemical and physical properties of diamonds from each producing country (and mine) would be required to make such techniques definitive, and no such database (or collection of diamonds from which it could be developed) yet exists.

Since there is currently no method to chemically or physically "fingerprint" diamonds for provenance, the final morning session on technologies to support a global certification program became more relevant. Simon Pitman represented the De La Rue company, which has been in the business of supplying secure and authenticated products (e.g., securities and bank notes) for over 200 years. In cooperation with the Belgian HRD, this company is now engaged in developing the secure certification necessary for the movement of legitimate diamonds from Angola and Sierra Leone. The De La Rue methods appear to employ technologies similar to those used by the U.S. Secret Service (represented by Dr. Antonio Cantu) to combat counterfeiting or alteration of legitimate currency and documents.

Several novel suggestions were presented for "tagging" (i.e., uniquely identifying) individual diamonds. Instrumentation manufactured by Gemprint Corp. (represented by Hermann Wallner) records the reflections of laser light on or through a fashioned diamond. According to Mr. Wallner, the reflection pattern for each diamond is unique (because of slight differences in the angles between polished faces) and can be stored in a database to help track a diamond after polishing. At present, however, this technique is not applicable to rough diamonds, and the Gemprint "signature" may be altered if the diamond is repolished. Sarin Technologies (represented by Zeev Leshem) offered the possibility that individual rough stones could be uniquely identified and subsequently tracked by "mapping" their surfaces with proprietary proportion measurement machines. Also of interest was the concept (called Gemtrac) proposed by 3Beams Technologies (represented by Dr. Jayant Neogi) to brand and track diamonds from the mine to the consumer. In this scenario, individual diamonds would be given a "bar code" at the mine—either directly on the rough diamond, or encapsulated in a biodegradable polymer that would also hold the diamond. This means of identification would accompany the diamond through the polishing stage and eventually to the consumer. All transactions involving the diamond would be stored in a central database.

For the second half of the conference, participants were divided into four groups based on their expertise, and then reassembled for final discussions. The "Chain of

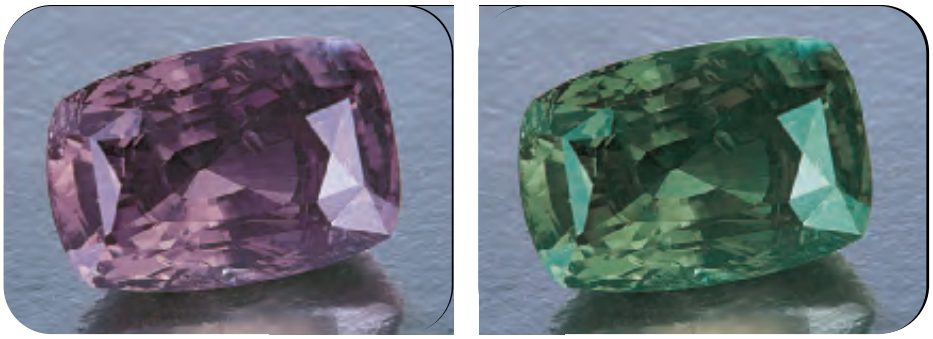

Figure 2. This 6.0 ct alexandrite from Madagascar shows a distinct color change from purple in incandescent light (left) to green in daylight-equivalent fluorescent light (right). Courtesy of Evan Caplan, Los Angeles; photo by Maha Tannous.

Custody" group discussed methods to expand certification programs globally in a practical and cost-effective manner, without penalizing legitimate producers or burdening the entire industry with increased costs. The "Tagging Technologies" group observed that the proposed suggestions for tagging individual diamonds (see above) were probably not yet practical. However, the group considered the laser tagging of individual large and valuable stones as a possible alternative.

The "Spectroscopic Analysis" group recognized that reference diamonds from specific mines and countries are not available for study, and that without such diamonds it is not possible to determine if there are locality-specific diagnostic spectroscopic features. One member of the group (Prof. George Rossman, California Institute of Technology) presented an imaginative method for determining the latitude from which a diamond originated and, by inference, the country in which it was mined. This technique uses the hydrogen and oxygen isotopic composition of clays found on the surface (e.g., within minute crevices) of rough diamonds. However, a thorough cleaning of a diamond (to remove the clay) or treating the specimen with clay from a different locality could defeat this approach.

The "Chemical Analysis" group also noted the need for reference diamonds from specific mines and countries. There is potential for characterizing parcels using physical features (e.g., morphology, color, inclusions), perhaps assisted by studies of chemical characteristics of individual diamonds, but much more work is needed. Also, identifying chemical variations in diamonds will require very sensitive and expensive techniques such as ion microprobe analysis and laser ablation mass spectrometry; these are also somewhat destructive. Although the use of bio-tracers, pollen, and other materials that might be retained on the surface of a rough diamond was mentioned, they are likely to have limited utility. It will be difficult to prove that the data provided by any of the chemical methods from a single diamond is absolutely unique to a deposit or country of origin.

In conclusion, no definitive scientific means exists today to identify the country of origin of a diamond. Although "tagging" systems are available that could help document the movement of diamonds from mine to market, none of the methods suggested thus far is practical for dealing with the millions of carats of rough diamonds mined each year. It appears that the only hope to deal with conflict diamonds in the near future rests with a multinational certification system (such as the World Diamond Council proposal mentioned above) that authenticates the movement of legitimate diamonds.

Alfred A. Levinson
University of Calgary, Alberta, Canada
levinson@geo.ucalgary.ca

James E. Shigley
GIA Research, Carlsbad

TUCSON 2001

Once again, the numerous gem and mineral shows in Tucson, Arizona, revealed several interesting new and unusual items among the thousands of rubies, emeralds, sapphires, and other gems seen in this vast marketplace every year. Among the highlights this year were a 23.23 ct tsavorite garnet from Tanzania (see below), a 6.0 ct alexandrite from Madagascar with a distinct green-to-purple color change (figure 2), a 270 ct opal from Lightning Ridge, Australia (figure 3), and platinum- or gold-coated drusy materials (see below). We also took this opportunity to acquire more information on materials seen in the trade over the years that are not well known. *G&G* thanks our many friends who shared material with us this year.

DIAMONDS

Update on GIA's diamond cut research. At the Tucson Convention Center on February 4, GIA Research Associate Al Gilbertson and Manager of Research and Development Dr. Ilene Reinitz presented some preliminary findings from the next stage in GIA's ongoing study of the influence of proportions on the appearance of round-brilliant-cut diamonds. Their presentation focused on three main topics: (1) three-dimensional modeling of a light ray's path through a polished diamond; (2) the effect of "panorama"—that is, lighting conditions and all objects in proximity to the diamond, including the observer—on diamond appearance; and (3) how sharp contrasts in the panorama can affect the appearance of

fire, such as the number and variety of "chromatic flares"—single occurrences of colored spectral light, either one color or a band of colors—that emerge from the diamond. GIA will continue to publish findings from their cut project in future issues of *Gems & Gemology*.

COLORED STONES AND ORGANIC MATERIALS

Cultured abalone pearls from California. At the GJX show, Pearls of Passion International (Davenport, California) exhibited an assortment of 10–14 mm cultured abalone mabe pearls (see, e.g., figure 4). Their first commercial harvest, in early 1999, yielded a few hundred cultured abalone pearls, but in 2000 production increased to tens of thousands of cultured pearls. The company's success is credited to two decades of research and development on Pacific Coast abalone.

The *Haliotis rufescens*, or red abalone, is the only species used to culture California abalone pearls on the Davenport pearl farm, which is located 120 km (75 miles) south of San Francisco. The land-based operation consists of 2,000,000 abalone that are bred and nurtured to maturity for insertion of the nucleus at three years of age.

Figure 3. This 270 ct opal from Lightning Ridge, Australia, was mined about 30 years ago, but exhibited in Tucson for the first time this year. Note the interesting feather-like patterns of the play-of-color. Courtesy of Opex Opal, Santa Barbara, California; photo by Robert Weldon, © GIA.

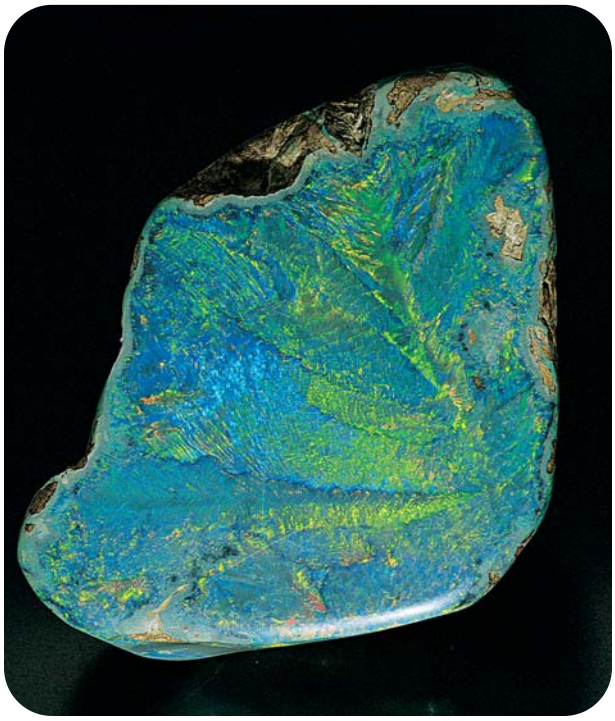

Figure 4. Cultured abalone mabe pearls from California are being commercially farmed using Haliotis rufescens*, or red abalone. These mabes show some of the colors produced (11–13 mm in diameter). Courtesy of Pearls of Passion International; photo by Angelique Crown.*

Nucleation is performed year-around, as is harvesting after an average cultivation period of 18 to 24 months. Although the implantation techniques are proprietary, the nuclei consist of fashioned pieces of shell or hardened polymer, and are attached to the interior of the abalone's shell without surgery (which could jeopardize the animal's health). After implantation, the abalone are housed in tanks and fed a mixture of local sea kelp. To ensure the optimal growing conditions of their natural environment, the water temperature is kept at 10°–13°C (50°–55°F) by circulating 2,000 gallons of fresh seawater throughout the nursery per minute.

The nucleus is retained during harvesting, when the cultured mabes are cut from the shell and rounded into calibrated sizes (10–14 mm) or freeform designs. Typically, a separate disk fabricated from abalone shell is attached to the back of each cultured pearl to finish the assembly, although some of the cultured mabes used in closed-back jewelry designs do not have the shell backing. Of the harvested cultured pearls, 25% represent top quality, with a consistent nacre thickness between 0.5 and 2.0 mm on every piece. No treatments or enhancements are used to achieve the high natural luster and lively magenta, blue, violet, and green body colors. To differentiate their cultured abalone pearls from other pearl products, the company plans to introduce a branding strategy this June.

Angelique Crown
Eclat, La Jolla, California
eclat@gemkey.com

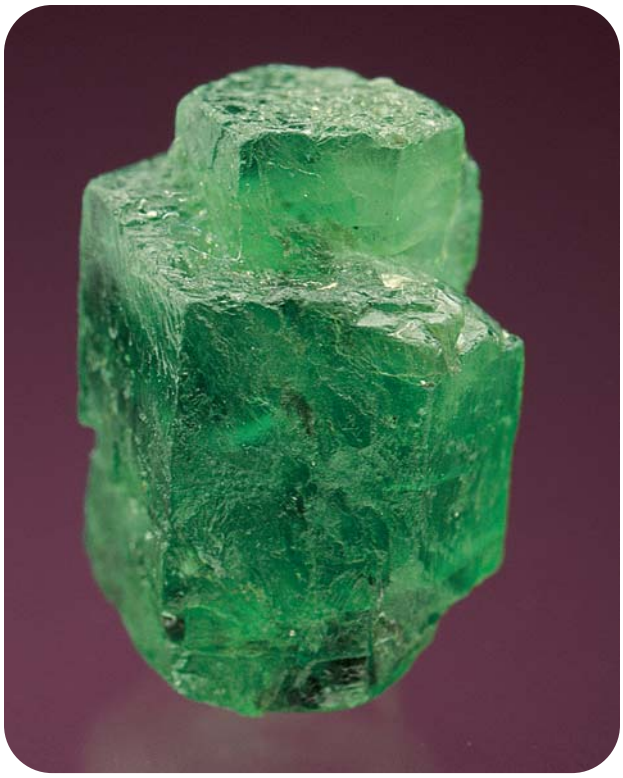

Figure 5. This Afghan emerald crystal (4.02 ct) was recently mined at Korgun, Laghman Province. Courtesy of Dudley Blauwet Gems; photo by Jeff Scovil.

Benitoite mine sold. At this year's Tucson Gem & Mineral Society (TGMS) show, rumors were confirmed that the world's sole commercial source of gem benitoite has been sold to a new mining group. The Benitoite Gem mine was purchased last November by Benitoite Mining Inc., Golden, Colorado. Company president Bryan Lees told GNI editor Brendan Laurs that negotiations for the property were initiated with past-owners William Forrest and Elvis "Buzz" Gray—who have been working the mine on a part-time basis for more than three decades—after AZCO Mining dropped its option in early 2000.

We have since learned that Benitoite Mining initiated work at the mine in March 2001. Next year, the company plans to expand the existing open pit in search of new lode material, while building a new, larger, washing plant for processing the eluvial reserves and old tailings. The new plant will capture the small pieces of gem rough that were overlooked in the past, and the company intends to create a market for melee-size faceted stones. Benitoite mineral specimens will be sold through the affiliated Collector's Edge company in Golden, Colorado.

Figure 6. These emeralds (0.38–2.04 ct) were recently recovered during bulk sampling at the new Piteiras emerald deposit in Minas Gerais, Brazil. Courtesy of Seahawk Minerals Ltd.; photo by Maha Tannous.

Emeralds from Laghman, Afghanistan. For many years, Afghanistan has supplied modest amounts of high-quality emeralds from mines in the Panjshir Valley (see, e.g., G. Bowersox et al., "Emeralds of the Panjshir Valley, Afghanistan," Spring 1991 *Gems & Gemology*, pp. 26–39). Recently, emeralds have also been found to the southeast in Laghman Province, which is famous for gem-bearing pegmatite deposits of tourmaline, spodumene, aquamarine, and morganite. According to Dudley Blauwet (Dudley Blauwet Gems, Louisville, Colorado), there are two emerald localities—Lamonda and Korgun. At Lamonda, large (up to 3 × 4 cm) semitransparent crystals are produced, and associated minerals on some specimens suggest that these emeralds formed in a granitic pegmatite, rather than in hydrothermal veins as in the Panjshir Valley. At Korgun, about 4–5 kg of smaller crystals were reportedly produced last summer, some of which are gemmy and have saturated color (see, e.g., figure 5). Syed Iftikhar Hussain (Syed Trading Co., Peshawar, Pakistan) had about 25 faceted emeralds from Laghman, with the largest weighing 1.39 ct. Most of the stones were lightly included and their green color showed moderate saturation.

First production of emeralds from Piteiras, Brazil. Representatives from Seahawk Minerals Ltd. showed *G&G* editors several polished emeralds (figure 6) from the new Piteiras property in Minas Gerais. Piteiras is situated between the Belmont mine to the northwest, where emeralds were first discovered in this region in 1976, and the Capoeirana mining area to the southeast (see D. S. Epstein, "The Capoeirana emerald deposit . . .," Fall 1989 *Gems & Gemology*, pp. 150–158). This emerald-bearing belt lies approximately 14 km southeast of the city of Itabira.

The Piteiras deposit was discovered in October 1998; bulk-sample testing is now underway to determine the feasibility of underground mining (figure 7). Geologic mapping, geochemical soil sampling, pitting, and systematic core drilling have defined an emerald-bearing phlogo-

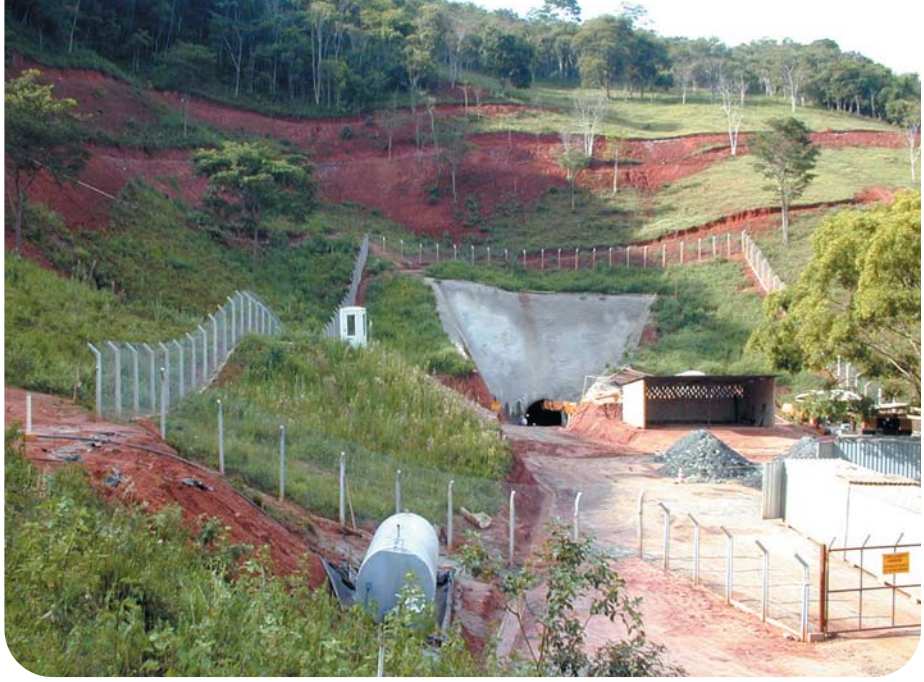

Figure 7. From the tunnel shown here, the emerald-bearing "blackwall zone" at Piteiras is being explored by underground bulk sampling. Courtesy of Seahawk Minerals Ltd.

pite/biotite "blackwall zone" over an area of 200 × 800 m with possible extensions. This zone, with a thickness ranging from 0.5 to more than 10 m, is the site of intense contact metasomatism between ultrabasic rocks (a source of chromium) and adjacent alumino-silicates (a source of beryllium).

Of 45 core holes drilled by Seahawk, 36 intersected the blackwall zone and 18 of these contained emerald crystals or emerald fragments. A crystal recovered from one such core yielded a fine-color 2.44 ct faceted oval, as well as a 4.6 ct cabochon.

A 3,000 ton bulk sample is being excavated from beneath the southeastern section of the mining property. Shortly before the Tucson show, a 538-gram aggregate of emeralds in phlogopite schist was recovered at the entrance of the newly established ramp. This aggregate yielded 725 carats of rough and preformed emeralds that are being faceted (again, see figure 6) and polished as cabochons.

Jan Kanis
55758 Veitsrodt, Germany

Educational iolite. When visiting the Tucson shows, the Interstate 10 corridor is a particularly good place to search for unusual gemology-related items such as out-of-print books, used and unusual instruments, and gems appropriate for educational purposes. Many dealers also set up temporary "shops" in the many hotels paralleling the freeway.

At one of these hotels, *Le Mineral Brut* from St. Jean Le Vieux, France, offered a variety of interesting gem materials from Madagascar. These included well-polished specimens of copal containing both insects and arachnids (see, e.g., Spring 2000 Gem News, pp. 67–68), polished samples of "Ocean Jasper" (see, e.g., Spring 2000 Gem News, p. 69), and a large selection of transparent precision-cut iolite blocks which were displayed on a light table.

All gemologists are familiar with the distinctive pleochroism shown by iolite, which is ofen used to teach this property in the classroom. This dramatic pleochroism is clearly visible in the block pictured in figure 8, which weighs 8.25 ct and measures 11.25 × 8.96 × 6.56 mm. The dark blue color projecting through the top of the block is in stark contrast to the light brown to near-colorless sides. To those unfamiliar with the visual effects of pleochroism, this gives a first impression that the blue surface may have been coated or painted blue.

John I. Koivula and Maha Tannous
GIA Gem Trade Laboratory, Carlsbad
jkoivula@gia.edu

"Hte Long Sein" jadeite. Several deposits in northern Myanmar produce jadeite, but one locality near Lonkin is the source of a relatively new type called "Hte Long Sein" (figure 9), which means "full green" in Burmese. Although this deposit was discovered in 1994, large-scale mining by the Myanmar government and a private enterprise did not start until 1997. Since 1999, a wide variety of Hte Long Sein jadeite products have entered the Hong Kong market, including carved butterflies, leaves, beadwork, and bangles. This is the first year the material was shown in Tucson, by Mason-Kay Inc. (Denver, Colorado) at the AGTA show.

Hte Long Sein jadeite generally has a bright green color but poor transparency, which is due to abundant fine internal fractures. The transparency can be increased by cutting the material into thin slices, and lower-quality material is commonly impregnated with an epoxy resin (easily detected by infrared spectroscopy). Hte Long Sein jadeite also has the following properties, as determined by this contributor: coarse- to medium-grained granular texture, generally with no preferred orientation of the crystals; S.G. of 3.30–3.31; R.I. of 1.66; appears green with the Chelsea color filter; inert to both long- and short-wave UV radiation; infrared and Raman spectra are similar to those of typical green jadeite.

Electron microprobe analyses (performed at the Mineral Deposit Research Institute at the China Academy of Geological Science and at The Testing Centre of the China University of Geosciences in Wuhan) indicate that

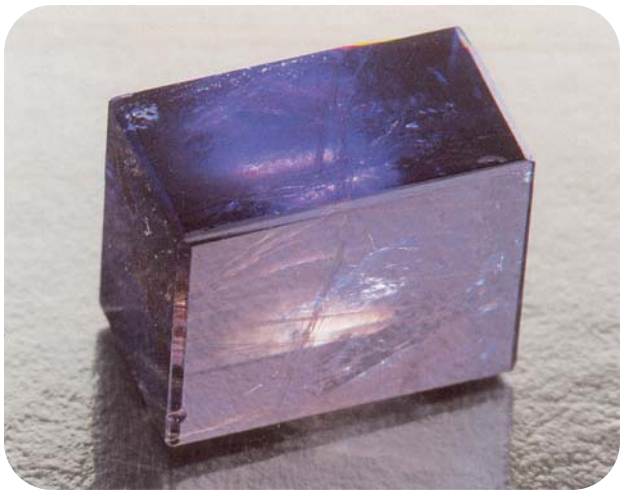

Figure 8. This 8.25 ct rectangular block of iolite was carefully oriented to display its distinctive pleochroism. Photo by Maha Tannous.

this jadeite contains up to 2.61 wt.% Cr_2O_3, which provides the bright green color.

C. M. Ou Yang
Hong Kong Gems Laboratory
cmouyang@my.netvigator.com

Editor's note: Further information on very thin pieces of dark green jadeite jade—possibly from this source—can be found in the Fall 1995 Lab Notes, pp. 199–201, and Winter 1995 Lab Notes, pp. 266–267.

Kunzite from Nigeria. Although famous for its recent production of tourmaline and spessartine (see, e.g., Gem News: Winter 1998, pp. 298–299, and Winter 1999, p. 216), Nigeria also produces several other gemstones, among them spodumene (kunzite). Dudley Blauwet had an attractive rough-and-cut pair of transparent pink Nigerian kunzite (figure 10) that reportedly was recovered last fall near the Niger/Kaduna border. Bill Larson of Pala International (Fallbrook, California) estimates that about 2 kg of gemmy Nigerian kunzite have been produced over the past two years.

"Rainbow" obsidian from Jalisco, Mexico. Although this material has been known for several years (see, e.g., Summer 1993 Gem News, p. 133, and Spring 1997 Gem News, p. 63), Larry Castle of Carved Opal and Obsidian, Austin, Texas, was marketing large quantities of cleverly carved "rainbow" obsidian in a novel double-heart pattern (figure 11).

A recent study by J. L. Greller and G. Ulmer ("Sheen and 'rainbow' obsidians: An electron microprobe study," *Geological Society of America Abstracts with Program, Northeastern Section*, Vol. 30, No. 1, 1998, p. 22) indicated that the iridescent colors are caused by oriented rods of augitic pyroxene. The "rainbow" results from layers of different iridescent colors of obsidian. Each layer has a single color—perhaps related to the size, orientation, and number of the pyroxene rods—which in the better qualities produces alternating colors of iridescent violet, blue, green, yellow, orange, and pink. Orientation of the rough is critical to revealing the iridescence. In addition, when samples are cut at a shallow angle (e.g., 10°) to the layers, the various colors appear parallel to one another. Thus, cutting of the material as high-domed cabochons or spheres produces concentric patterns. By manipulating the material in this fashion, lapidaries in Mexico produced the unusual double-heart pattern illustrated in figure 11.

Robert E. Kane
Helena, Montana
rekane@compuserve.com

New production of Indonesian opal. An array of attractive Indonesian opals, some set in 22K yellow gold jewelry, were exhibited at the TGMS show by Pelangí-Dharma Mulia, an opal mining, cutting, and jewelry-making company in Jakarta, Indonesia. The company owns 11 hectares (about 27 acres) of opal-bearing land in the

Figure 9. "Hte Long Sein" jadeite, from a relatively new source in Myanmar, is typically carved in very thin pieces that show a rich green color. Courtesy of C. M. Ou Yang.

Banten area of West Java. Irwan Holmes, an American consultant for the company, told GNI editor Brendan Laurs that the opal was mined over the past year, and represented some of the best material recovered so far from his (and other) deposits. Mr. Holmes estimated that the Banten area yielded nearly 1,000 carats of fine-quality opal last year, from approximately 10 active mines, each of which produces a different type of opal.

Both white opal and various types of "hydrophane" opal (e.g., light, dark, and "golden") were being exhibited (figure 12). Although black opal is also recovered at one of the deposits, it was not being sold because much of it is unstable. The white opal is translucent to semitransparent, with an intense play-of-color. According to Mr. Holmes, this material typically is stable, although occasional samples develop a white cloudiness after cutting. The material marketed as "hydrophane" is semitransparent to opaque and shows intense play-of-color that reportedly disappears when the opal is immersed in water; the play-of-color returns after the stones dehydrate (typically within one hour in an air-conditioned room). This is opposite to the behavior commonly associated with hydrophane opal (see, e.g., R. Webster, revised by P. G. Read, *Gems—Their Sources, Descriptions, and Identification*, 5th ed., Butterworth Heinemann, 1994, p. 246), such as that found in Australia.

Australian prehnite returns. Although prehnite from Australia has been seen in the gem trade for nearly two decades, this year at the Tucson Intergem show we noted significant quantities of attractive material (see, e.g., figure 13). Jay Lennon of Jayrock, Adelaide, Australia told GNI editor Brendan Laurs that the material had been stockpiled from alluvial deposits on aboriginal land near Wave Hill over the past 20 years. This remote locality in the Northern Territories is several hundred kilometers east of the nearest town, Catherine. The supplier of the material recently sold some of his stock to Mr. Lennon, who was delighted in the opportunity since collecting the prehnite reportedly has been illegal for the past five years.

Australian prehnite typically is greenish yellow to yellow. The prominent radial fibrous structure of this aggregate material gives rise to a moonstone-like appearance in some stones. Gemological properties (obtained from one sample by Shane McClure, GIA Gem Trade Laboratory director of Identification Services) were: semitransparent to translucent; R.I. of 1.618–1.641; S.G. of 2.91; weak dull yellow fluorescence to long-wave UV radiation, and weak orange to short-wave; aggregate reaction in the polariscope; no spectrum seen with the desk-model spectroscope. Note that both refractive indices may sometimes be seen in an aggregate material that is very compact, with an exceptionally small grain size.

According to Mr. Lennon, gem-quality prehnite is very rare: a 400 kg parcel of rough might be expected to yield just 6 kg of translucent tumbled stones and 4 kg of semitransparent beads. In addition to tumbled stones and

Figure 10. Small amounts of kunzite have recently been found in gem-rich Nigeria. The crystal shown here is 5.7 cm high, and the cushion-cut stone weighs 12.29 ct. Courtesy of Dudley Blauwet Gems; photo by Jeff Scovil.

Figure 11. The double-heart pattern in this "rainbow" obsidian from Mexico (7.5 × 4.2 cm) is produced by carving the material so that parallel layers of different colors are cleverly exposed. Photo by Maha Tannous.

Figure 12. These attractive opals originated from the Banten area of West Java, Indonesia. Clockwise from the top, the samples weigh 48.04, 7.03, 2.55, 2.64, and 11.30 ct. Courtesy of Pelangí-Dharma Mulia; photo by Elizabeth Schrader.

beads (both polished and faceted), Mr. Lennon had numerous freeform cabochons as well as a few faceted stones. All of the stones were hand polished in India.

"Yosemite" topaz. Its general lack of brilliance in faceted form relegates colorless topaz to the status of a less-than-popular gem material. It is now routinely irradiated and heated to create a more desirable blue color, but is rarely used in its natural colorless state. This year, however, we saw a beautiful exception to this rule. The 59.73 ct colorless topaz shown in figure 14 was among the small works of natural gem art on display in Tucson.

The lapidary, Kevin Lane Smith of Tucson, took advantage of the natural surface etching on this topaz.

Figure 13. Significant quantities of attractive prehnite reappeared in Tucson this year. The largest stone shown here weighs 28.61 ct, and the pear shape weighs 15.32 ct. Courtesy of Jayrock; photo by Maha Tannous.

The result is a dramatic natural art scene that looks like a landscape you might see in California's Yosemite National Park.

The Winter 1996 Gem News (p. 283) also featured naturally etched scenes that were incorporated into fashioned quartz and beryl. However, this is the first time we have seen colorless topaz used in this creative manner.

John I. Koivula and Maha Tannous

Colored tourmaline from northern Pakistan. Large quantities of gem tourmaline have been produced in Afghanistan, but thus far neighboring Pakistan has yielded little of this popular gem mineral for faceting. The country's most prolific pegmatites, in the Gilgit-Skardu area of northern Pakistan, typically produce aquamarine, brownish topaz, and schorl, although some deposits also have green and bicolored pink-green tourmaline crystals that are typically too included for faceting. Lesser-known pegmatites in the Azad Kashmir area yield spessartine garnet and some colored tourmaline. Another pegmatite district in the Chitral area has produced mainly aquamarine. (For an overview of these pegmatite deposits, see A. H. Kazmi and M. O'Donoghue, *Gemstones of Pakistan—Geology and Gemmology*, Gemstone Corporation of Pakistan, Peshawar, 1990).

Recently, some unusual gemmy yellow to greenish yellow tourmalines were mined in northern Pakistan, in the vicinity of the world's ninth highest mountain, Nanga Parbat (8,125 m/26,657 feet). We know of two dealers who were carrying this material in Tucson—Dudley Blauwet at the TGMS show and Syed Iftikhar Hussain in the Best Western Executive Inn. During a recent buying trip to Pakistan, Mr. Blauwet told us, he saw small parcels of yellow (see, e.g., figure 15), light pink, and bicolored green-pink tourmaline, reportedly from new deposits northeast of Nanga Parbat between Astor and the Raikot Bridge, which is on the Karakorum Highway. A few of the crystals were transparent enough for faceting. Mr. Hussain had 2–3 kg of greenish yellow to yellowish green tourmalines from this area that were mined in July and August 2000 (see, e.g., figure 16). Most were cabochon-grade, although some were facetable. The largest crystals recovered reportedly were up to about 7 cm. Gemological properties measured on one 16.07 ct crystal by GNI editor Brendan Laurs are as follows: color—yellow-green to green-yellow, R.I.—1.63 (spot), S.G. (measured hydrostatically)—3.09, inert to short- and long-wave UV radiation, and inclusions consisting of partially healed fractures, "feathers," and dust-like clouds.

Although quantities of colored tourmaline from Pakistan remain limited so far, pegmatites in the Astor–Raikot Bridge area show interesting potential for future gem production.

Fashioning the "Green King of Africa" tsavorite. Recently a remarkable suite of tsavorites was faceted from a single piece of rough, just in time for the Tucson show. This entry

provides some background on the difficult decisions faced by the cutter when dealing with large rough such as this.

Late in December 2000, a miner offered this contributor a 192 ct piece of tsavorite that was reportedly found in the tailings of the old Titus tsavorite mine in Tanzania. The stone had a heavily included and cracked surface, and appeared at first glance to have only a small central portion of facetable quality. If the rough was sawn in the directions shown in figure 17, the miner estimated, it could produce a single 12 ct cushion-cut gem and about 20–30 carats of smaller, lower-quality stones.

However, this contributor suspected that the rough had a much larger gem concealed within. After purchasing the stone, business partner Avi Meirom and I began a series of examinations which included immersing the stone in baby oil, tea, and at one point, a glass of whiskey. The cracks on the surface of the rough were misleading, because they did not penetrate the full depth of the stone. Therefore, we decided to saw the stone in entirely different directions from those proposed by the miner. We believed that the largest gem-quality portion was on the area seen on the left of side A in figure 18 (also seen in the lower part of side B). To liberate this area for cutting, three sawcuts would be needed (A, B, and C), each penetrating just part way into the stone (figure 19). Additional cuts were required to obtain the other gemmy portions. Cuts A and B were done with a very thin saw blade (0.1 mm) at relatively low speed with plenty of water. The blade was actually bent slightly along the major crack in the B direction.

After slicing and preshaping, we obtained a clean cushion preform weighing 28.8 ct. Final faceting yielded an exceptional 23.23 ct gemstone (figure 20). The rough also yielded a 6.80 ct pear and 18.32 carats of other gems weighing 1–3 ct. The total yield of the 192 ct piece of tsavorite rough was 41.50 ct, or 21.6%.

Menahem Sevdermish
Menavi Quality Cut, Ramat Gan, Israel
smenahem@netvision.net.il

Highlights from the TGMS Show and Mineralogical Symposium. As part of the four-day TGMS show, the Friends of Mineralogy, the Tucson Gem and Mineral Society, and the Mineralogical Society of America host an annual mineral symposium. The purpose of the symposium is to bring together amateur collectors and professional mineralogists to exchange information—this year, on Russian gems and minerals. Abstracts were published in the January-February 2001 issue of the *Mineralogical Record*.

The following presentations contained interesting gemological information. Dr. Dmitry Belakovsky, curator of the Fersman Mineralogical Museum in Moscow, provided an overview of famous localities—past, present, and future. He focused on two notable periods of collecting: In the middle of the 18th century, the great Siberian expeditions found aquamarine, tourmaline, heliodor, and topaz. Then, in the second quarter of the 20th century, geologic

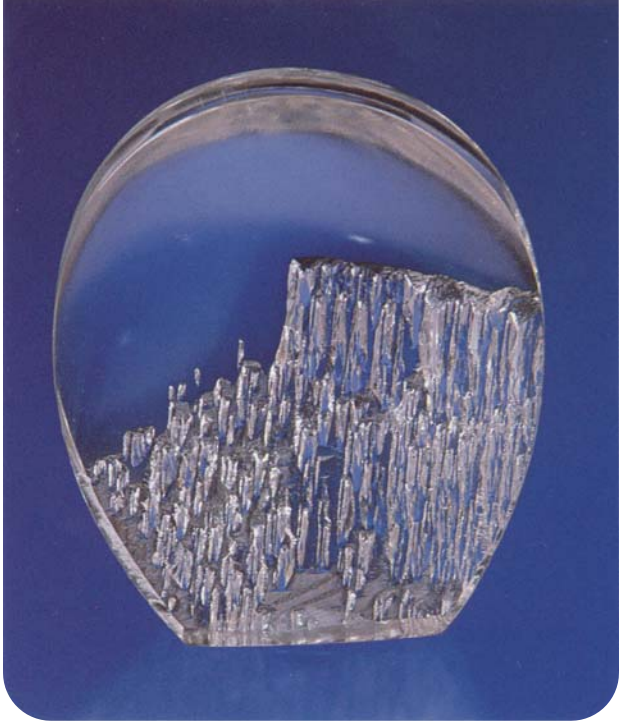

Figure 14. The natural etch patterns on the surface of this polished topaz (32.67 × 25.0 × 7.1 mm) produce a scene reminiscent of Yosemite National Park. Photo by Maha Tannous.

expeditions to the northern Ural Mountains and Siberia, the Central Asian Republics, and the Kola Peninsula located more gem and mineral deposits. As a result, about 200 important mineral localities are known in the former Soviet Union. Dr. Belakovsky concluded by pointing out that military and economic collapse have resulted in the closure of many important localities. In addition, the complications of mining licenses and export requirements make it difficult to export gems and minerals today.

An interesting talk authored by Drs. William (Skip) Simmons, Karen Webber, and Alexander Falster of the University of New Orleans focused on tourmaline from the Malkhanskiy pegmatite district of the Transbaikal region of south-central Siberia. Seven pegmatites are currently being mined for rubellite and polychrome

Figure 15. Yellow tourmaline crystals such as this one (5.1 cm long) were recently mined from a new area in northern Pakistan. Photo by Dudley Blauwet.

Figure 16. Northern Pakistan is also the source of these yellowish green tourmalines. The largest crystal measures 3.5 cm tall. Courtesy of Syed Trading Co.; photo by Jeff Scovil.

tourmaline. Electron microprobe analyses of the tourmaline revealed elbaite compositions with a significant liddicoatite component in some samples.

Dr. Peter Lyckberg presented three lectures on gem deposits in Russia, the Ukraine, Kazakhstan, and Tajikistan. For each region, he reviewed mining during the past few decades. He also clarified an often-mislabeled locality, Sherlovaya Gora in the Transbaikal region of Siberia, Russia. Called the greatest gem beryl producer in Russia, it is a greisen deposit that has been confused with another pegmatite locality in the Adun Chelon Mountain Range, which also produces beryl, but with different characteristics.

A new gem map of Russia and adjacent countries was available at the TGMS show. Although printed in Russian, it is accompanied by a guide in English. The map and guide can be purchased from Mineralogical Almanac (minbooks@online.ru), P.O. Box 368, Moscow, Russia 103009.

Other gem and jewelry highlights on display at the TGMS show were:

- More than 60 Fabergé pieces from several collectors and dealers
- Fabergé memorabilia including invoices for two Imperial eggs, early catalogs, and photographs of the Fabergé workshops
- The Mackay emerald necklace, featuring the largest cut emerald (168 ct) in the National Gem Collection at the Smithsonian Institution
- Large gemmy aquamarine crystals from southern India, including the 10 kg crystal pictured in the Fall 2000 GN section (additional crystals on display weighed 2.3 kg, 650 g, and 280 g)
- A 2,750 ct treated-color blue topaz, fashioned by Dr. Artmura Kirk and donated to the Virginia Polytechnic Institute and State University.

Next year, the 48th Tucson Gem & Mineral Society show will feature minerals and art from Africa.

Dona M. Dirlam
GIA Library and Information Center, Carlsbad
ddirlam@gia.edu

Faceted vesuvianite from California. Although small quantities of polished yellow-green vesuvianite (idocrase) from northern California have been around for years, this year's TGMS show saw the commercial availability of faceted material (see, e.g., figure 21). The historic deposit—east of Paradise on the Feather River—was reopened three years ago by these contributors and Ben Halpin. The deposit consists of pods and lenses of massive vesuvianite within sheared serpentine, and is one of the original localities for a yellow-

Figure 17. The miner proposed sawing the tsavorite rough in these directions, to yield a cushion-shape estimated at 12 ct and additional smaller gems that would total about 30 carats.

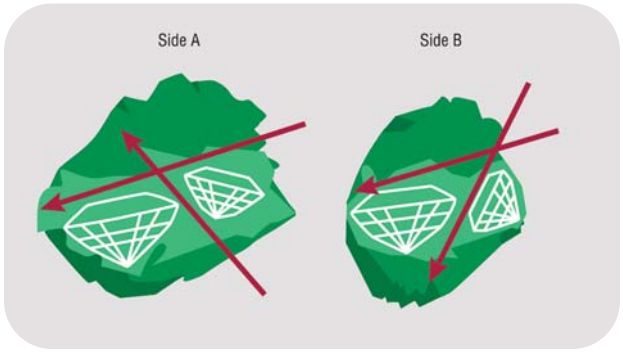

Figure 18. A careful examination of the tsavorite revealed a much larger gem concealed within, so it was decided to saw the gem in entirely different directions.

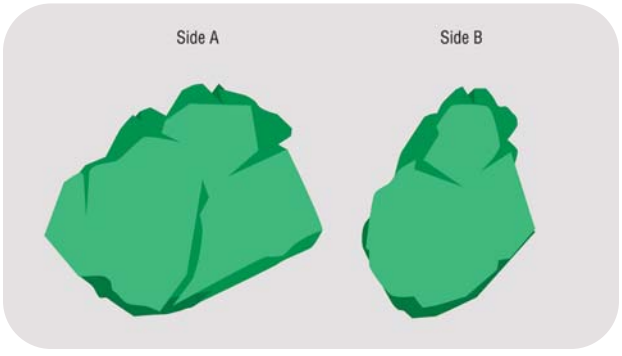

green variety of vesuvianite sometimes known as "Californite" or "Pulga jade." In addition to cabochons, as this vesuvianite is typically seen, about 250 carats of faceted stones recently have been cut, ranging from 0.1–3 ct. More faceted vesuvianite is expected this summer from a 10 kg parcel of rough that is presently being cut. An additional 10–20 kg of rough is being cleaned and processed for future cutting. The yield of faceted stones is typically just one-quarter of 1%, and of cabochons, approximately 5%.

Gemological properties (obtained from one sample by Shane McClure) were: R.I. of 1.71; S.G. of 3.36; inert to long- and short-wave UV radiation; aggregate reaction in the polariscope; strong 464 nm band visible with a spectroscope; and a hazy appearance due to the aggregate structure. The material exhibited in Tucson was the first to be commercially recovered in several decades, and mining will resume in May 2001. The deposit shows strong potential to supply commercial quantities of gem vesuvianite for years to come.

Anders Karlsson and
Roger Smith (saladinsmith@earthlink.net)
Orion Gems, Carmel, California

SYNTHETICS AND SIMULANTS

Opal imitations. Among the unusual synthetics and simulants seen at Tucson was a semi-transparent synthetic opal triplet (see, e.g., figure 22) that consisted of a thin slab of synthetic opal sandwiched between two pieces of transparent glass (R.I. of 1.515): a dome top and flat base. (More commonly, opal triplets are opaque, because a black chalcedony or onyx base is used.) A variety of shapes were available, in sizes from 5 × 3 mm to 20 × 15 mm. Also seen were opal triplet beads ranging from 4 to 12 mm. Probably intended for use as ear studs, these beads were composed of glass that had a very small, thin, two-layered patch consisting of opal (represented as natural) attached to a dark gray- or black-coated glass. As shown in figure 22, the glass was very effective in reflecting the play-of-color from the thin slice of opal in the patch.

Wendi M. Mayerson
GIA Gem Trade Laboratory, New York
wmayerson@gia.edu

Phillip G. York
GIA Education, Carlsbad

Figure 19. Using a fine blade, the tsavorite was carefully sawn to preserve the large facetable area on the left.

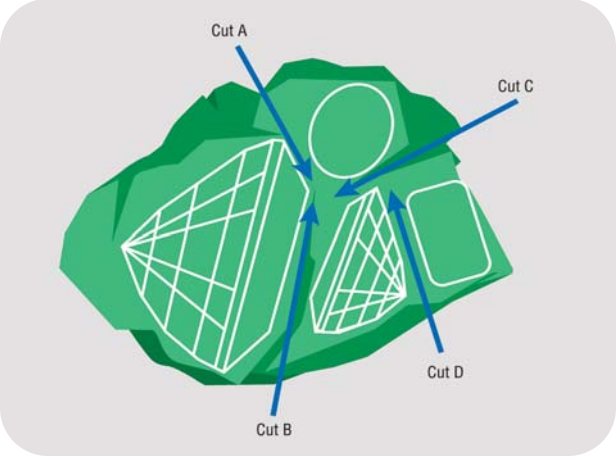

Figure 20. The 23.23 ct "Green King of Africa" is shown here, together with several other stones (1.05–6.80 ct) cut from the same rough. Courtesy of Menavi Quality Cut Ltd.; photo by Maha Tannous.

Green flame-fusion synthetic sapphire. Green is an uncommon color for gem sapphires—whether natural or synthetic—but this year, significant quantities of green flame-fusion synthetic sapphires were being sold by one distributor at the GLDA (Gem and Lapidary Dealers Association) show. Robert Silverman of Lannyte (Houston, Texas) had several dozen faceted examples, as well as numerous boules (see, e.g., figure 23). He stated that this green synthetic sapphire has been grown in Europe for at least the past two years, but this was the first time it had been cut and made available to the trade in the U.S. The color ranged from green to bluish green, with the latter being more common.

The faceted green synthetic sapphires are usually in the 2–3 ct range. Larger samples are not readily available, because the boules are of limited size (typically not more than 50 mm long and 20 mm wide), and are color zoned with a pale exterior. During growth of the boules, the melt initially crystallizes into dark "cobalt" blue synthetic sapphire, but according to Mr. Silverman, the color changes to green shortly after crystallization. Typically, one end of each boule (i.e., the last part of the boule to crystallize) retains a small portion of blue color (again, see figure 23). Previous studies of green synthetic sapphire have documented Co^{3+} or a combination of Co^{3+} and V^{3+} as the color-causing agents (see, e.g., Spring 1995 Lab Notes, pp. 57–58).

Figure 21. Commercial quantities of faceted vesuvianite debuted in Tucson this year. The stones shown here weigh 0.41–3.31 ct. Courtesy of Roger Smith; photo by Maha Tannous.

TREATMENTS

Platinum coating of drusy materials. Again this year, drusy gemstones were very popular at the Tucson gem shows. The newest addition to the drusy family, "platinum drusy," has a platinum coating reportedly applied via vapor deposition onto a black drusy surface. The material was seen at the booths of Maxam Magnata Designer Drusy (Tucson, Arizona) and Rare Earth Mining Co. (Trumbull, Connecticut); the latter was marketing it as "Tucsonite." According to literature provided by Maxam Magnata, the surface material typically consists of dyed black quartz (commonly known as black onyx in the trade) from Brazil.

In some pieces, the platinum coating had been polished off the smooth rim surrounding the drusy crystal surface, creating the illusion of pavé diamonds surrounded by a bezel (figure 24). The pieces were marketed in pairs (of various shapes) for earrings and in larger free-form pieces for pins and necklaces.

A similar material also was available that had been coated with 23K yellow gold. Because both the gold and the platinum finishes are coatings, and thus should not be directly buffed or polished, it was recommended to jewelers that the metal mounting be cleaned prior to setting. After mounting, water and a soft toothbrush are the cleaning materials of choice.

Wendi M. Mayerson and Phillip G. York

Figure 22. This 14 ¥ 10 mm cabochon (left) is a synthetic opal triplet. The 5 mm bead on the right derives its rich color from a thin slice of reportedly natural opal on a black-coated glass base. Photo by Maha Tannous.

MISCELLANEOUS

An attractive way to display loose gemstones. This year, several exhibitors at Tucson were using a convenient device for displaying gemstones of various sizes and shapes. The "Gem Clipper" comes in three sizes, for holding faceted stones that are 4–9 mm, 7–15 mm, and 13–19 mm (figure 25). It is available with a variety of different bases. The clip that holds the stone is made from flexible stainless steel with a high spring tension. This design allows it to be used as a stand-alone display or as a tool for picking up and examining the gemstone.

Micromosaics from natural gemstones. Micromosaics were introduced in the 18th century as diminutive imitations of wall mosaics found at Herculaneum and Pompeii in ancient Italy. They became particularly popular as elements in the "archeological style" jewelry that was fashionable in the 19th century. The tiny tiles, or *tesserae*, used to make micromosaic images were traditionally made of glass. Although micromosaics were out of fashion for most of the 20th century, interest in them has grown in the last decade due to a greater interest in antique jewelry.

The micromosaic technique has been revived and brought to a new level by a group of Russian artists based in Moscow. Victor Kuzmishchev and Elena Koroleva, among others, use gemstones in place of glass to create a wide range of original compositions and copies of old masterpieces, as well as portraits, landscapes, and icons (see, e.g., figure 26). Their booth at the GLDA show exhibited a number of very fine micromosaic plaques and three-dimensional objects, which incorporated 55 kinds of natural gem materials, including topaz, aquamarine, and other beryl. The tesserae range from 0.15 × 0.15 × 0.7 mm to 0.7 × 0.7 × 0.7 mm, and it takes 300–500 tesserae to fill an area of just 1 cm^2.

Elise B. Misiorowski
Jewelry Historian, Los Angeles
elisemiz@aol.com

ANNOUNCEMENTS

***Leigha* theft.** On February 6, a theft occurred from Arthur Lee Anderson's Gem Arts booth after the closing of the GJX show in Tucson. Among the items stolen were pieces

Figure 23. These green flame-fusion synthetic sapphires were reportedly grown in Europe. The faceted examples weigh 2.17 and 1.80 ct, and the split boule measures 40 ¥ 16 mm. Note the dark blue area on the left end of the boule. Courtesy of Lannyte; photo by Maha Tannous.

from Mr. Anderson's gem sculpture *Leigha*, which was featured in the Spring 1998 issue of *Gems & Gemology* (pp. 24–33). The arms, legs, skirt, and base of the statue were stolen, along with photos that chronicled the making of the statue and showed the finished work. Mr. Anderson is offering a $5,000 reward for the return of the pieces. Anyone with knowledge of these items' whereabouts may contact intermediary John Brady at 520-623-4353.

Figure 24. The glittering appearance of these pieces results from a thin coating of platinum that has been applied over drusy gem materials. The two smaller pieces measure approximately 11.5 mm in maximum dimension. Photo by Maha Tannous.

Conferences

Fourth Oxford Conference on Spectrometry. Held June 9–13 at Davidson College in Davidson, North Carolina, this conference is expected to draw a large group of scientists in the field of spectrometry, color science, appearance measurements, and related areas. Call Dr. Art Springsteen at 602-525-4479, or e-mail arts@aviantechnologies.com.

Figure 25. A range of sizes and designs are available for the "Gem Clipper," a device to display loose gemstones. Shown here are a 3.40 ct topaz (right), an 8.58 ct amethyst (middle), and a 3.37 ct tsavorite (left). Photo by Maha Tannous.

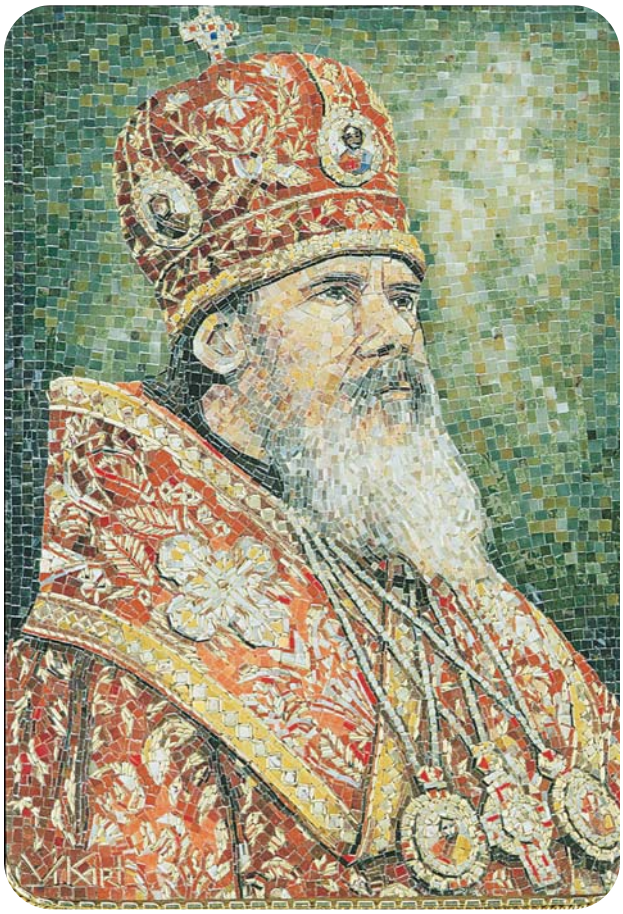

Figure 26. This micromosaic portrait of the leader of the Russian Orthodox church measures 48 × 63 mm, and is constructed of several natural gem materials. Tesserae of gold have been used to enhance the richness of the piece. Courtesy of Vikart, Moscow, Russia; photo by Robert Weldon.

FIPP 2001. The *11th International Gemstones Show* and the *13th Open Air Precious Stones Show* will be held July 4–8 at the Teófilo Otoni City Hall in Minas Gerais, Brazil. The shows will feature conferences, mining tours, and 220 gem exhibitors. Fax 55-33-3522-1662 or e-mail geabr@uai.com.br.

Jewelry 2001. The *22nd Annual Antique & Period Jewelry and Gemstone Conference* will be held July 14–22 at Adelphi University in Garden City, Long Island, New York. This conference will emphasize jewelry of the 18th through 20th centuries and its identification through the understanding of stone cutting, jewelry making techniques, and stylistic influences. A wide variety of hands-on seminars and demonstrations will be offered. Visit www.jewelrycamp.org, call 212-535-2479, or e-mail jwlrycamp@aol.com.

Diamond 2001. The *12th European Conference on Diamond, Diamond-Like Materials, Carbon Nanotubes, Nitrides & Silicon Carbide* will take place September 2–7 in Budapest, Hungary. The program will include growth technologies, as well as advanced characterization techniques, of natural and high pressure grown synthetic diamond, silicon carbide, and other materials. Visit http://www.diamond-conference.com or e-mail e.reed@elsevier.co.uk.

Exhibits

Gold of Africa Museum. AngloGold has opened the world's first museum dedicated to African gold. Located in the historic Martin Melck House in Cape Town, South Africa, it features a permanent collection of more than 350 gold objects from Ghana, the Ivory Coast, Mali, and Senegal. These 19th and 20th century pieces, ranging from crowns to jewelry, were purchased recently from the Barbier-Mueller Museum in Geneva. Visit www.anglogold.com (see November 23, 2000 press release and Photo Library).

Romancing the Stone: The Many Facets of Tourmaline. Now through January 20, 2002, at the Harvard Museum of Natural History in Cambridge, Massachusetts, this exhibition features an extensive collection of tourmaline. Visitors can see an array of crystals and fine jewelry, while learning about the natural history of tourmaline and its ornamental and practical uses. Visit www.hmnh.harvard.edu/tourmalines.html or call 617-495-3045.

Programa Royal Collections. On display at the Museo de las Ciencias Príncipe Felipe in Valencia, Spain, the Programa Royal Collections features two major compilations: the Royal Collection and Art Natura. The Royal Collection contains over 200,000 carats of cut gemstones in both classical and fancy shapes, many of which weigh more than 1,000 carats. Art Natura contains over 100,000 carats of small sculptures and carvings made of gem materials. These two exhibitions will be on display for the next five years, along with additional temporary exhibitions. Visit http://elindice.com/FinanzasyNegocios/GemologiayMetales or e-mail prc.aeie@maptel.

ERRATUM

In the Winter 2000 gem localities article by Shigley et al., the caption for figure 28 (p. 310) should have included the following information: "Photo © Tino Hammid and Christie's Hong Kong." Our apologies for the omission. Also, on p. 302 and p. 319 of this article, the famous nephrite jade area in the Liaoning Province is Xiu Yan County, rather than Xiu Lan County. We thank Sophia Cui at the China University of Geoscience for this correction.

GEMS & GEMOLOGY Challenge

The following 25 questions are based on information from the four 2000 issues of *Gems & Gemology*. Refer to the feature articles and "Notes and New Techniques" in those issues to find the **single best answer** for each question; then mark your choice on the response card provided in this issue. (Sorry, no photocopies or facsimiles will be accepted; contact the Subscriptions Department—dortiz@gia.edu—if you wish to purchase additional copies of this issue.) Mail the card so that we receive it no later than Monday, August 6, 2001. Please include your name and address. All entries will be acknowledged with a letter and an answer key **after the due date.**

Score 75% or better, and you will receive a GIA Continuing Education Certificate. If you are a member of the GIA Alumni Association, you will earn 5 Carat Points toward GIA's Alumni Circle of Achievement. (Be sure to include your GIA Alumni membership number on your answer card and submit your Carat card for credit.) Earn a perfect score, and your name will also be featured in the Fall 2001 issue of *Gems & Gemology*. Good luck!

1. What diamond type can be changed from brown to greenish yellow by HPHT processing?
   A. Type IIa
   B. Type IIb
   C. Type Ia
   D. Type Ib

2. The most common type of treatment (aside from dyeing) used for gems continues to be
   A. irradiation.
   B. heat treatment.
   C. diffusion treatment.
   D. fracture filling.

3. Which of these analytical techniques could not be considered "mature" to gemologists in the 1990s?
   A. Isotopic studies
   B. Ultraviolet-visible spectroscopy
   C. Electron microprobe analysis
   D. X-ray fluorescence spectrometry

4. If bead-nucleated Chinese freshwater cultured pearls do become common in the future, their nature will be readily identifiable by
   A. Fourier-transform infrared spectroscopy.
   B. magnification.
   C. X-radiography.
   D. X-ray diffraction.

5. Most of the corundum mined from the Jegdalek deposit in east-central Afghanistan is
   A. ruby.
   B. pink sapphire.
   C. blue sapphire.
   D. bicolored blue and red-to-pink corundum.

6. The emphasis on fancy-color diamonds in jewelry during the 1990s was primarily due to the greater availability of fancy brown, yellow, and pink diamonds from
   A. Australia.
   B. Canada.
   C. Brazil.
   D. Russia.

7. The larger size of Chinese freshwater cultured pearls over the last several years can be attributed primarily to
   A. a longer cultivation period and the use of younger mussels.
   B. the change from the *Hyriopsis cumingi* mussel to the *Cristaria plicata*.
   C. the use of mantle-tissue nuclei.
   D. the use of reject cultured pearls as nuclei.

8. In Myanmar's Jade Tract, miners often can identify the occasional jadeite boulder by
   A. its slightly sticky feel.
   B. the distinct ringing sound it makes when struck with a metal tool.
   C. its greater heft than other types of rock in the conglomerate.
   D. all of the above.

9. Spectral features due to single substitutional nitrogen atoms in a nominally type IIa diamond provide an indication of
   A. fracture filling.
   B. HPHT treatment.
   C. irradiation.
   D. a surface coating.

10. The purple to purplish red color of chromium-bearing taaffeites is a function of the relative amounts of chromium and _____ present.
   A. cobalt
   B. titanium
   C. iron
   D. manganese

11. A new laser treatment for diamonds, which typically does not have a surface-reaching drill hole, works best on
   A. small inclusions.
   B. inclusions deep within a stone.
   C. dark inclusions near the surface.
   D. light inclusions far from the stone's surface.

12. Diagnostic inclusions, in the form of _____, were documented in Tairus hydrothermal synthetic emeralds in the 1990s.
   A. iron oxides
   B. platinum platelets
   C. flux "fingerprints"
   D. chromite

13. Evidence that a near-colorless type IIa diamond has been HPHT treated can be provided by a combination of
   A. photoluminescence spectra and inclusions.
   B. graining and cathodoluminescence.
   C. X-ray topography and infrared spectra.
   D. infrared spectra and graining.

14. The most significant amethyst-producing country of the 1990s was
   A. Zambia.
   B. Uruguay.
   C. Brazil.
   D. Canada.

15. Diamonds filled with Oved's new XL-21 glass formulation are characterized by
   A. a strong flash effect.
   B. the "Oved" logo inscribed on a bezel facet.
   C. the detection of Pb and Bi by EDXRF analysis.
   D. all of the above.

16. Which imitation rough was most common in the 1990s?
   A. Imitation diamond crystals
   B. Imitation ruby crystals
   C. Imitation sapphire crystals
   D. Imitation emerald crystals

17. Which significant technological challenge of the 1980s remained in the 1990s?
   A. Identifying synthetic diamonds by their fluorescence
   B. Determining origin of color for green diamonds
   C. Identifying GE POL diamonds
   D. Characterizing diamond fillers

18. HPHT-treated greenish yellow to yellowish green diamonds may show
   A. chalky greenish yellow fluorescence.
   B. strong green "transmission" (luminescence to visible light).
   C. fractures with etched, frosted textures or partial graphitization.
   D. all of the above.

19. Most of the shell jewelry discovered at archeological sites on the island of Antigua was manufactured from the _____ shell.
   A. queen conch
   B. nautilus
   C. abalone
   D. thorny oyster

20. The _____ effect of one gem material overlaid on another was introduced to the jewelry world in the 1990s.
   A. "optic dish"
   B. "drusy"
   C. "Mystère"
   D. "trompe l'oeil"

21. Gem-quality haüyne is rarely seen in jewelry because of
   A. its high specific gravity and low luster.
   B. its rarity and low hardness.
   C. its treatment with paraffin wax.
   D. its popularity as a collector's stone.

22. X-ray diffraction analysis identified lazurite and _____ as the principal minerals in samples of first-grade lapis lazuli from both Chile and Afghanistan.
   A. wollastonite
   B. barite
   C. pyrite
   D. calcite

23. The first major demantoid garnet locality outside of Russia was discovered in _____ in the mid-1990s.
   A. Namibia
   B. Tanzania
   C. China
   D. Madagascar

24. The most important factor in the evaluation of Burmese jadeite is
   A. diaphaneity.
   B. texture.
   C. color.
   D. cut.

25. Sapphires from the Antsiranana Province of Madagascar show internal features typical of _____ deposits.
   A. marble-hosted
   B. metamorphic
   C. basaltic-magmatic
   D. alluvial

Book REVIEWS

2001

EDITORS
Susan B. Johnson
Jana E. Miyahira-Smith

Jeweled Bugs and Butterflies

*By Marilyn Nissenson and Susan Jonas, 120 pp., illus., publ. by Harry N. Abrams, New York, 2000. US$29.95**

If you're a lover of jeweled bugs and butterflies, this is the book for you. It is highlighted by 127 magnificent full-color photographs of objects related to this theme. The fine quality of the photographs shows off the detail of the creatures. You will enjoy scarabs from ancient Egypt and objects from the Art Nouveau period (featuring the work of René Lalique), as well as pieces from many other artists and eras.

While at first glance you might purchase this book for your coffee table, it offers much more. You will gain a historical perspective on jeweled bugs through the ages, discover their lore, and even get a lesson in entomology. Did you know that insects first appeared on Earth some 350–400 million years ago? Or that at least 750,000 species of insects have been identified? Are you curious about the Art Nouveau period? Reading this text will give you some insight into these topics.

The book is divided into six chapters, by category of bugs. The first section is on "Creepy Crawlers;" spiders and beetles, among the most displeasing creatures to some, are featured in jeweled splendor. The next section is devoted to "Scarabs," or dung beetles. Perhaps the first insects to be used in jewelry, scarabs were worn for protection by early Egyptians. Flying insects—especially bees—are featured in "Buzzers and Stingers." Next, in "Dragonflies," you'll see pieces with delicate wings of plique-à-jour enamel. The juxtaposition of women and insects by Art Nouveau designers follows in "Winged Women." The last section features the bejeweled wings of "Butterflies and Moths."

The authors have compiled a wonderful tribute to *Jeweled Bugs and Butterflies*. I would highly recommend this book to anyone who has an affinity for these curious creatures and the period jewelry in which they were featured so prominently.

DIANE SAITO
Gemological Institute of America
Carlsbad, California

Paulding Farnham: Tiffany's Lost Genius

*By John Loring, 151 pp., illus., publ. by Harry N. Abrams, New York, 2000. US$49.50**

As the 19th century eased into the 20th, George Paulding Farnham of Tiffany and Co. was one of the world's most celebrated designers of jewelry and silver. His use of American gemstones is renowned (his beautiful iris brooch [illustrated on p. 31 of the Spring 1995 issue of *Gems & Gemology*] is the quintessential Montana sapphire jewel), and his enameled orchids are highly prized by collectors of fine jewelry. I personally had always wondered what the reasons were behind his apparently abrupt departure from Tiffany's, and John Loring not only answers this question, but he also gives insight into Farnham's personal history and inspirations.

The book's preface and introduction track Farnham's 22 years at Tiffany & Co. while giving glimpses into his personal life. They also explain that his departure came when Louis Comfort Tiffany inherited control of the company. Tiffany and Farnham had radically different views on design, and conflict was inevitable. The book is then divided into chapters that categorize Farnham's work. The first chapter, "Nature," highlights Farnham's beautiful floral brooches, many of which incorporated enamel along with gemstones. It also showcases a number of pieces that feature bees, beetles, lizards, snakes, and birds. The next chapter, "Orchids," features Farnham's famous enameled orchid brooches. Originally fabricated for the 1889 Paris Exposition Universelle, these brooches were realistically rendered in enamel, gold, and, often, gemstones. Highly collectible, they command high prices at auction today. "Native American Design" displays incredible bowls, vases, and vessels—in most cases, fashioned in silver—that were inspired by Native American pottery. There are also chapters on "The Louis' Revival," "Victorianism," and "The Renaissance Revival," which all do a wonderful job of discussing and illustrating these influences on Farnham's jewelry and silver.

Loring's book is lavishly illustrated, with photographs of many pieces as well as with actual renderings and sketches in Farnham's hand. They

**This book is available for purchase through the GIA Bookstore, 5345 Armada Drive, Carlsbad, CA 92008. Telephone: (800) 421-7250, ext. 4200; outside the U.S. (760) 603-4200. Fax: (760) 603-4266.*

reveal Paulding Farnham's brilliance and flair. In the preface, John Loring states that his book's mission is to "publish a substantial portion of Paulding Farnham's long-lost designs . . . . and to restore his reputation to its rightful position." He has succeeded with a visually attractive, easy-to-read, fascinating text.

JANA E. MIYAHIRA-SMITH
Gemological Institute of America
Carlsbad, California

The Crown Jewels: The History of the Coronation Regalia in the Jewel House of the Tower of London

By C. Blair, A. Grimwade, R. R. Harding, E. A. Jobbins, D. King, R. W. Lightbown, and K. Scarratt. Volume I: The History, 812 pp.; Volume II: The Catalogue, 630 pp. Illus., publ. by The Stationery Office, London, 1998. US$1,650

These two sumptuously produced volumes, with text and photographs printed on substantial, silk-surfaced paper, record the results of research into the history of the English Coronation and associated regalia in greater detail than has ever before been possible. Volume I is concerned entirely with the origins and history of the Coronation ceremony, but it is Volume II that documents a detailed examination of the Crown Jewels, revealing many discoveries and new insights about the gemstones. Each item has been newly photographed, and the team of three gemologists has taken the opportunity to examine the jewels with sophisticated gemological techniques.

The catalogue illustrates and describes the regalia, including not only the numerous crowns, orbs, and scepters, but also the various swords, plate, and textiles. Each chapter begins with a brief abstract giving the size and appearance of the item, followed by a history of the various formats and vicissitudes. The description of each major item concludes with a "gemmological commentary," and it is here that we get a listing of the sizes and weights of all the major gemstones, including details of their surface imperfections and any visible inclusions.

One of the many delights of this work lies in the numerous color photographs of the regalia. The price of these two magnificent volumes may prevent one from dashing out to buy a set, but this work records for posterity far more details of the gemstones in the regalia than have been available hitherto.

R. A. HOWIE
Royal Holloway,
University of London

OTHER BOOKS RECEIVED

Colored Stones of Yakutia and Places of Their Origin, *by V. G. Gadiatov and V. K. Marshinsev, 328 pp., illus., publ. by Yekaterinburg Bank of Cultural Information, Yekaterinburg, Russia, 2000, 150 rubles (about US$5.25) [in Russian].* For more than 300 years, the remote Siberian region of Yakutia has been a generous provider of gem materials for Russia and the entire world. Diamond, amethyst, garnet, topaz, and several other gem materials (as well as ornamental stones) are described, according to their location, characteristics, and geologic occurrence. The authors' analysis of Yakutia's geology suggests interesting directions for future development of the gem resources. Readers also will find useful information about the economics and resource management of the rough gem minerals, as well as facts about the global gem market.

Although the book contains a significant amount of scientific material and professional terminology, it is intended for a very broad audience—admirers of gemstones. Geologic charts, maps, and numerous colored illustrations of minerals provide a wealth of visual information that adds to the enjoyment of this book.

VLADISLAV DOMBROVSKIY
GIA Gem Trade Laboratory
Carlsbad, California

Gemmologia Europa VII—European Gemmologists on the Emerald, *edited by Margherita Superchi, 221 pp., illus., publ. by CISGEM, Milan, Italy, 2000, 35,000 lira (about US$16.00) [in Italian and English].* This volume on emerald is the proceedings of the seventh Gemmologia Europa (Milan, 1998), a biennial conference sponsored by the Centro Informazione e Servizi Gemmologici (CISGEM). Included are illustrated transcripts of presentations by Jan Kanis (African localities), Dietmar Schwarz (South American, Asian, and Australian localities), Henry Hänni (synthesis and enhancement), Elena Gambini (CISGEM Laboratory emerald grading procedures), and Giorgio Graziani (geographic provenance of archeological emeralds).

STUART D. OVERLIN
Gemological Institute of America
Carlsbad, California

Mughals, Maharajas and the Mahatma, *by K. R. N. Swamy, 265 pp., illus., publ. by Harper Collins Publishers India, New Delhi, 1997, US$18.95.* This is a collection of 39 fascinating episodes in Indian history, 12 of which concern famous gems and diamonds, royal treasuries, and gem-encrusted thrones. Many of the remaining episodes revolve around the British Raj, Mahatma Gandhi, politics, and wars. The contributions to the history of Indian treasures, diamonds, and jewels make this book easily worth its price for the gem and jewelry enthusiast.

JOHN SINKANKAS
Peri Lithon Books
San Diego, California

Gemological **ABSTRACTS**

2001

COLORED STONES AND ORGANIC MATERIALS

Acute toxicity of formaldehyde to the pearl oyster *Pinctada fucata martensii*. K. Takayanagi, T. Sakami, M. Shiraishi, and H. Yokoyama, *Water Research*, Vol. 34, No. 1, 2000, pp. 93–98.

Formaldehyde is often used in fish hatcheries to treat parasitic infections. It is then discharged into the hatchery effluent, where it enters the marine environment. Although formaldehyde is biodegradable, there are few reliable data on its effects on saltwater organisms over time, particularly on nonmigratory shellfish that are vulnerable to degradation of water quality. Accordingly, acute toxicities of formaldehyde to one- and two-year-old Akoya pearl oysters (*Pinctada fucata martensii*) were determined in a controlled laboratory environment. The oysters were not given any food during the experiments. Test solutions were made by adding various concentrations of formaldehyde to sand-filtered seawater. The oysters were observed at 24-hour intervals, and any dead oysters were removed.

During the first 24 hours, the oysters reduced their respiration by minimizing water intake to avoid exposure to the formaldehyde. However, within 96 hours all oysters had died. A sharp decrease in formaldehyde levels in the test solutions was observed during the experiment, especially in solutions with lower concentrations of the chemical. The results suggest that pearl oysters can detect the presence of formaldehyde in their surroundings and that they possess some form of defense mechanism from its toxic effects but, with time, they will succumb to its effects. No mortality was observed in a control group that was not exposed to formaldehyde. *MT*

This section is designed to provide as complete a record as practical of the recent literature on gems and gemology. Articles are selected for abstracting solely at the discretion of the section editor and his reviewers, and space limitations may require that we include only those articles that we feel will be of greatest interest to our readership.

Requests for reprints of articles abstracted must be addressed to the author or publisher of the original material.

The reviewer of each article is identified by his or her initials at the end of each abstract. Guest reviewers are identified by their full names. Opinions expressed in an abstract belong to the abstracter and in no way reflect the position of Gems & Gemology *or GIA.*

Comparative NIR and IR examination of natural, synthetic, and irradiated synthetic quartz. J. P. Bachheimer, *European Journal of Mineralogy*, Vol. 12, No. 5, 2000, pp. 975–986.

Since both natural and synthetic quartz crystals originate from hydrothermal solutions, hydrogen components (H_2O molecular water, OH point defects, and H situated near other impurities such as aluminum) form the dominant impurities in this material. There have been many studies on hydrogen impurities in natural and synthetic quartz of different origins by near infrared (NIR: 5500–3800 cm^{-1}) and infrared (IR: 3800–3125 cm^{-1}) absorption spectroscopy at room and low temperatures; however, there is a paucity of information on the quantitative relations between NIR and IR absorption bands for natural, synthetic, and X-ray irradiated quartz samples with a wide range of hydrogen concentrations.

Twenty-four natural and 14 synthetic quartz samples with various hydrogen concentrations were analyzed, and one synthetic sample was studied both before and after X-ray irradiation. The 4500 cm^{-1} band exists only above a certain hydrogen concentration (>8 ppm H/Si) in natural quartz, whereas the 4000 cm^{-1} absorption band exists in both natural and synthetic quartz, but the band shapes are different. Natural quartz shows two clear peaks at 3995 ± 5 and 3890 ± 2 cm^{-1}. The NIR and IR spectra of X-ray irradiated synthetic quartz are similar to those of natural quartz, with roughly the same relative intensities. *TL*

Diffraction colours of opal: First spectrometric data. M. Ostrooumov and H. A. Talay, *Australian Gemmologist*, Vol. 20, No. 11, 2000, pp. 467–472.

A spectrophotometric study of Mexican "fire" opals showed that the majority of these opals are characterized by diffraction colors with absorption bands in the red-orange and yellow-green regions. Two types of spectra were obtained: those due to a mixture of diffracted colors, and those due to pure diffracted colors. The wavelengths of the diffracted colors were studied as a function of the diameter of the silica spheres that constitute the opal. Opals composed of small spheres (diameters of 150–180 nm) generally will be purple, whereas those with large spheres (diameters of 240–316 nm) will be yellow, orange, and red. *RAH*

Hints for jadeite investors. S. Fengmin, *China Gems Magazine*, Vol. 10, No. 3, 2000, pp. 4–10.

Today's top-quality jadeite is produced in small quantities only from Myanmar, and has become an investment instrument in China and elsewhere. This article, addressed primarily to investors and collectors, is a primer on the classification and investment aspects of jadeite according to three classes (A, B, and C). Most emphasis is placed on polished jadeite (i.e., in the form of jewelry and carvings); dealing in rough jadeite is discouraged because it is extremely speculative. The value of jadeite in each class varies and is based on several factors, the main ones being shape, color, clarity, and the abundance and nature of imperfections (e.g., fractures). According to the classification proposed in this article:

- Class A jadeite has not been treated, altered, or enhanced in any way. There are four value categories in this class: low grade, medium grade, high grade, and "superfine." The latter two categories are the only ones that qualify as investment grade.
- Class B jadeite has been chemically (acid) treated and then impregnated with a polymer or colloidal silica. The durability of this type of jadeite has been compromised because of the acid treatment, and it will eventually become yellowish with the aging of the resin.
- Class C jadeite has undergone polymer or colloidal impregnation and the addition of new pigment; it has no investment value.

Small jadeite carvings with even, graceful lines, precise shapes, and a smooth polish are highly desired by collectors. Most valuable are the fine carvings that display well-conceived designs that use the rough to its full potential. *MT*

Identification of rumanite (Romanian amber) as thermally altered succinite (Baltic amber). E. C. Stout, C. W. Beck, and K. B. Anderson, *Physics and Chemistry of Minerals*, Vol. 27, No. 9, 2000, pp. 665–678.

Infrared spectroscopy and gas chromatography–mass spectrometry analyses of the ether-soluble fractions of 13 samples of Romanian amber show that this species of fossil resin is a class of 1a labdanoid resinite that has been produced by thermal alteration of Baltic amber or succinite, and therefore these ambers must have the same botanical source. This conclusion is contrary to recent opinion, but in agreement with earlier investigations based solely on mineralogy and geology. The close chemical relationship between Romanian and Baltic amber had not been recognized earlier because the Romanian material contains a number of compounds that can only be found in succinite after pyrolysis (chemical change caused by heating), and such analyses had not been performed. *RAH*

Luminescence studies in colour centres produced in natural topaz. C. Marques, L. Santos, A. N. Falcão, R. C. Silva, and E. Alves, *Journal of Luminescence*, Vol. 87-89, 2000, pp. 583–585.

From a natural Brazilian colorless topaz reference sample, two smaller pieces were cut and irradiated differently; both were subsequently annealed at 1,200°C. One sample was irradiated with fast neutrons and annealed; it turned green. The other sample became blue after irradiation with gamma rays (from a cobalt-60 source) and annealing. The luminescence of the irradiated samples was studied by steady-state and time-resolved spectroscopy, with the

objective of determining how the color centers—both of which are stable—were created.

The luminescence characteristics (including intensity) of the two samples were different. This suggests that different optical defects (color centers) are created by the different treatments. The color centers may be related impurities of "transition metal ions," analogous to color changes in other minerals. The intensity of the luminescence varied with changes in temperature, which is attributed to structural changes in the crystals. Thus, both impurities and structural changes may be involved in the luminescence characteristics of irradiated green and blue topaz. *KSM*

Mineral compositions and textures of jadeite jade and their relationships to quality types. F. Huang, Q. Gu, and Y. Zou, *Journal of Gems and Gemology*, Vol. 2, No. 1, 2000, pp. 7–14 [in Chinese with English abstract].

"Quality type" (*Zhong* and *Di* in Chinese) as it applies to jadeite is a relatively elusive concept, but it continues to be used in the trade. This article attempts to take some of the mystery out of jadeite grading by examining the relationship between quality type, mineral composition, and microtexture. It is based mainly on a study of 18 Burmese jadeite specimens (15 rough and three polished) of various qualities that were studied by polarized optical microscopy and electron microprobe analysis.

All the specimens were composed of jadeite (one with omphacite), together with minor feldspar and some opaque minerals. Pure jadeite shows a superior appearance, whereas specimens containing significant impurities such as feldspar and opaque minerals are often of poor quality. Nine textural types were observed (five of which are illustrated): crystalloblastic (including granular, equigranular, inequigranular, prismatic, and fibrous), mortar, mylonitic, fractured, and replacement. Fine jadeites with high diaphaneity show fibrous crystalloblastic or microgranular crystalloblastic textures, and were affected by post-crystallization geologic processes (recrystallization or replacement). Moderate-quality jadeites often show fine-granular crystalloblastic and/or mortar textures, which suggests that they have been influenced slightly by later geologic processes. Low-quality jadeites with low transparency usually show inequigranular crystalloblastic, prismatic crystalloblastic, and/or fractured textures; they did not undergo recrystallization or replacement. *TL*

Oxygen and carbon isotope study of natural and synthetic malachite. E. B. Melchiorre, R. E. Criss, and T. P. Rose, *Economic Geology*, Vol. 94, No. 2, 1999, pp. 245–260.

Malachite [$CuCO_3 \cdot Cu(OH)_2$] is a commonly exploited ore of copper, and its striking green color and interesting textures make it desirable to many jewelry artisans and mineral collectors. The mineral forms during the oxidation of primary copper sulfides at low temperatures, and is sometimes found as stalactites, crusts, and other speleothem-like forms.

One natural malachite sample each from 61 sites worldwide was obtained for analysis. Using oxygen- and carbon-isotopic ratios for both natural and synthetic specimens, the authors were able to determine the temperature range required for the formation of natural malachite. These data suggest that malachite generally forms between 5° and 35°C, and becomes unstable at temperatures greater than about 100°C. Oxygen-isotope data show that in the majority of samples, the water involved in the oxidation and precipitation processes has a local meteoric (atmospheric) source. *JL*

Plate tectonics and gemstone occurrences. C. C. Milisenda, *Applied Mineralogy*, Vol. 1., E. Rammlmair et al., Eds., 2000, Balkema, Rotterdam, pp. 53–55.

The worldwide distribution of major gemstone occurrences can best be explained in terms of plate tectonics. In this context, the genesis of a large variety of gems is closely associated with the development of the lower continental crust, where gem-bearing granulite terrains contain metasedimentary assemblages and often originated from continent–continent collision. The high-grade supracrustal rocks of Tanzania, Madagascar, Sri Lanka, and southern India contain similar gemstone deposits and, in the reconstructed Gondwana supercontinent, formed part of the Mozambique Belt. This elongate zone resulted from the collision of eastern and western Gondwana in Pan-African times, some 600 million years ago. *RAH*

Polymorph and morphology of calcium carbonate crystals induced by proteins extracted from mollusk shell. Q. L. Feng, G. Pu, Y. Pei, F. Z. Cui, H. D. Li, and T. N. Kim, *Journal of Crystal Growth*, Vol. 216, 2000, pp. 459–465.

The major calcium carbonate ($CaCO_3$) components of pearls and shells are calcite and aragonite. These polymorphs have similar crystal structures and thermodynamic stabilities, although in general aragonite is slightly less stable than calcite. This article investigates the role of soluble proteins extracted from different parts of mollusk shells in controlling the crystallization and morphology of the respective polymorphs.

Synthetic calcium carbonate crystals were grown by a slow diffusion process in a closed desiccator. EDTA-soluble and insoluble proteins extracted from the nacreous layer and the prismatic-crystallized layer of mollusk shell were added to the system. With X-ray diffraction, as well as scanning- and transmission-electron microscopy, it was found that the soluble proteins can induce the crystallization of specific crystal structures and characteristic morphologies of $CaCO_3$. The soluble proteins extracted from the nacreous layer induced aragonite formation, whereas those from the prismatic layer caused the growth of calcite with a preferred rhombohedral morphology. The insoluble proteins were shown to influence the den-

sity of nucleation sites as well as the sizes and quantities of the crystals.

Although these experimental conditions are significantly different from those encountered in pearl growth, this study demonstrates that the crystallization and morphological characteristics of $CaCO_3$ can be controlled by proteins present in mollusk shells. *TL*

A preliminary investigation of precious opal by laser Raman spectroscopy. A. Smallwood, *Australian Gemmologist*, Vol. 20, No. 9, 2000, pp. 363–366.

The author demonstrates that the laboratory gemologist can use Raman analysis to effectively discriminate natural from synthetic or imitation opal. Spectra are illustrated for natural sedimentary opal (White Cliffs, Coober Pedy, and Lightning Ridge in Australia) and volcanic opal (Mexico; Virgin Valley, Nevada; and New South Wales, Australia), as well as for various synthetics and imitations (Gilson synthetic black opal, Inamori synthetic white opal, Inamori polymer-impregnated imitation opal, and the laminate used in a plastic opal triplet). *RAH*

A study of photoluminescence spectrum of black pearl. B. Zhang, Y. Gao, and J. Yang, *China Gems*, Vol. 9, No. 4, 2000, pp. 111–113 [in Chinese].

The dark appearance of black pearls can be induced by enhancement processes, such as dyeing or irradiation. To help gemologists identify the color origin of such pearls, the authors obtained photoluminescence spectra of natural-color (Tahitian), dyed, and irradiated black cultured pearls using laser Raman microspectrometry. The dyed samples were obtained by placing three freshwater cultured pearls in a solution of silver nitrate. The irradiated cultured pearls were exposed to gamma rays (two specimens) or a combination of alpha + beta + gamma rays (four samples).

The cultured Tahitian cultured pearls showed strong photoluminescence features centered around 835 nm in the near-infrared region, and three bands at 630, 655 (dominant), and 680 nm in the visible range; the dyed cultured pearls exhibited the same features. However, the irradiated samples showed a distinctive, strong photoluminescence centered mainly around 610 nm. *TL*

The visible absorption spectroscopy of emeralds from different deposits. I. I. Moroz, M. L. Roth, and V. B. Deich, *Australian Gemmologist*, Vol. 20, No. 8, October-December 1999, pp. 315–320.

Visible absorption spectra of emeralds from 11 different regions (and one synthetic emerald) showed distinctive characteristics. The relative intensities of the Cr^{3+} (600 nm) and Fe^{2+}_6(810 nm) absorption bands reflect the Cr:Fe ratio in the emeralds. It is suggested that the presence of certain iron chromophores may be distinctive of emeralds from a specific deposit. Many emeralds exhibit a "mixed type" absorption pattern related to both an emerald component (Cr^{3+} and/or V^{3+}) and an aquamarine component (Fe^{2+} and Fe^{2+}/Fe^{3+}). The emeralds studied were classified into three groups based on the relative intensity or absence of the 810 nm band. Analyses for major and trace elements are tabulated. *RAH*

DIAMONDS

Carbon isotope ratios and nitrogen abundances in relation to cathodoluminescence characteristics for some diamonds from the Kaapvaal Province, S. Africa. B. Harte, I. C. W. Fitzsimons, J. W. Harris, and M. L. Otter, *Mineralogical Magazine*, Vol. 63, No. 6, 1999, pp. 829–856.

Secondary-ion mass spectrometry techniques were used to study variations in the carbon isotopic ratio ($\delta^{13}C$) and nitrogen (N) abundance within specific growth zones of diamond. The zones—both octahedral and cuboid, within diamonds showing a typical octahedral morphology—were observed using cathodoluminescence (CL). Different growth zones showed marked contrasts in N abundance, ranging from 0 to 1,400 parts per million within a single diamond; variations of several hundred parts per million are common across adjacent growth zones, and appear sharp at the boundaries of the zones. In general, for the common blue CL, luminescence increases with N abundance. The carbon isotope ratio, however, appears constant across many growth zone boundaries. Some original variations in $\delta^{13}C$ may have been eliminated by diffusion of C atoms subsequent to growth, while the diamonds resided in the Earth's mantle at 950–1,250°C for many millions of years. *RAH*

Extreme chemical variation in complex diamonds from George Creek, Colorado: A SIMS study of carbon isotope composition and nitrogen abundance. I. C. W. Fitzsimons, B. Harte, I. L. Chinn, J. J. Gurney, and W. R. Taylor, *Mineralogical Magazine*, Vol. 63, No. 6, 1999, pp. 857–878.

Diamonds from a George Creek (State Line district, Colorado) kimberlite dike preserve complex intergrowth textures between two major growth generations: (1) homogeneous diamond with yellowish cathodoluminescence (CL), and (2) diamond with blue-green CL and local growth zonation. Secondary-ion mass spectrometry has revealed large variations both in nitrogen (N) concentration and carbon isotope ($\delta^{13}C$) composition within these diamonds. Within a single diamond, N contents and $\delta^{13}C$ values can vary from 0 to 750 parts per million (ppm), and from 0 to –20 per mil (‰), respectively. The CL characteristics correlate with N concentration: Diamond with yellowish CL has a uniform N content, whereas zoned diamond has bright blue CL bands with high N (50–750 ppm) and dark blue or green CL bands with low N (0–20 ppm). The $\delta^{13}C$ values also vary between the two growth generations in any one diamond, but show no consistent correlation with either CL or N. *RAH*

Characteristics of the geotectonics in South China and their constraints on primary diamond. W. Tang and C. Bao, *Acta Geologica Sinica*, Vol. 74, No. 2, 2000, pp. 217–222.

A primary diamond deposit was discovered in 1998 in Longhou County, in the Chinese province of Zhejiang. This deposit consists of kimberlitic pipes in a Cretaceous basin near a deep-seated fault zone. Diamond typically forms here as octahedral crystals without visible impurities. The diamondiferous rock has a breccia structure and contains pyrope, chrome diopside, picotite (spinel), perovskite, magnetite, and numerous xenoliths of eclogite and pyrolite (basalt and dunite), as well as olivine and pyroxene aggregates. Chemical analyses of the kimberlitic rocks are provided. With more than 140 similar pipes in the area, this study could be helpful for future diamond prospecting. *RAH*

Colorado diamonds. J. A. Murphy, *Rocks & Minerals*, Vol. 75, No. 5, 2000, pp. 350–354.

The colorful history of diamond exploration and mining in Colorado began with the discovery of kimberlite there in 1964. It gained momentum in 1975 with the accidental discovery of the first Colorado diamond at the U.S. Geological Survey laboratory in Lakewood, Colorado, when a piece of kimberlite was being slabbed. Confirmation of a primary occurrence came later that year when diamonds were recovered from kimberlite pipes northwest of Fort Collins, near the Colorado-Wyoming state line. This discovery fueled exploration and the evaluation of numerous kimberlites in the district by several companies. To date, over 100 kimberlites have been discovered. The Sloan No. 1 and No. 2 and the Kelsey Lake pipes are the largest and best known, and the ones with the greatest economic potential.

The Sloan pipes have so far proved uneconomic. The Kelsey Lake pipe was mined for a short period in 1996–1997. The largest faceted diamond from North America, a 16.86 ct light yellow gemstone, was cut from a 28.18 ct crystal recovered from Kelsey Lake in 1997. Despite financial hardships and land disputes, limited mining resumed at Kelsey Lake in 2000. The article describes various individuals (e.g., C. S. Ferris, Prof. J. Chronic) and companies (e.g., Superior Oil Company, Union Pacific Resources) involved with Colorado diamonds over the years. *MT*

Diamant (Diamond). *extraLapis*, No. 18, 2000, 104 pp. [in German]

This issue, like its predecessors in the *extraLapis* series, is devoted to a specific mineral or region—in this case, diamond. Of the volume's 21 articles, 11 were contributed by H. Malzahn. The other contributors are M. Glas, J. Howard, E. Misiorowski, G. Neumeier, P. Rustemeyer, W. Schmidt, H. Vollstädt, and the consulting firm Terraconsult. This superbly illustrated volume covers a wide range of subjects. With informative tables and diagrams, it is a valuable blend of information on the ancient and the modern.

The first two articles function as an Introduction and describe the role of diamond as a symbol of wealth, power, and success throughout history (e.g., its role in the Buddhist and Hindu traditions in India). Other forms of carbon, such as graphite and fullerenes, are also discussed. The next four articles are concerned primarily with the external aspects of diamonds. They feature crystal drawings from such classics as Victor Goldschmidt's *Atlas der Kristallformen* (1911), as well as modern photographs of such important diamonds as the Incomparable and the Tereshkova in their rough state. From a practical standpoint, it is emphasized that rough diamonds come in a great variety of crystal forms, colors, sizes, and clarity grades, which makes their evaluation difficult. And although rough diamonds from some mines may have characteristic external surface or morphological features, it is not possible to determine the origin of a single stone (emphasizing the dilemma presented by "conflict" diamonds).

The next five articles cover the beauty of fancy-color diamonds, methods of color enhancement (ranging from the century-old radium irradiation to the modern GE POL process), and fluorescence and double refraction in diamond. Four articles on geology cover the formation of diamonds and their parent rocks (kimberlite, orangeite, lamproite), including mention of diamonds found in secondary deposits (alluvials) and diamonds of metamorphic origin. Interesting information is presented on microdiamonds from various impact craters (e.g., in Ries, Germany, and Popigai, Siberia). A survey of present and future sources of production is followed by the description of two diamond localities in North America: the Prairie Creek pipe in Murfreesboro, Arkansas, and the new Ekati mine in Canada's Northwest Territories.

Four articles on diamonds as gemstones and their industrial importance contain an eclectic mix that includes the hardness and technical uses of diamond, the history of—and recent developments in—diamond synthesis, and a discussion of synthetic moissanite and other diamond simulants. The issue concludes with two articles under the section heading "Value and Jewelry," which review quality criteria for cut diamonds (especially the "Ideal" cut controversy) and the role diamonds have played in jewelry from antiquity to the present. *RT*

Diamond brilliance: Theories, measurement, and judgment. M. Cowing, *Journal of Gemmology*, Vol. 27, No. 4, 2000, pp. 209–227.

This paper explores the question: Does the work presented by Hemphill et al. ("Modeling the appearance…," Fall 1998 *Gems & Gemology*, pp. 158–183) give the diamond trade cause to abandon the American "Ideal" (also referred to as the Tolkowsky) cut? After a brief review of GIA course material and the AGS cut-grading system, the

paper offers two premises: Any measure of brilliance must agree with human judgment, and lighting must imitate the conditions in which brilliance is "normally judged."

Although the computer modeling of light movement by Hemphill et al. is praised, two arguments are presented against the use of diffuse, even illumination: It yields smaller differences in brilliance than can be judged by eye, and it lacks a viewer to block light from one direction. The author advocates the use of a single view—from directly overhead—for judging brilliance, rather than using an average, such as the weighted light return (WLR) metric described by Hemphill et al. A single viewing point is proposed for more clearly observing other aspects of appearance, such as contrast. It is further suggested that those diamonds that perform well in this position should also be checked in other positions.

The author discusses in depth the possible effects of the shadow from the observer's head when observing diamond brilliance. In particular, he proposes that this shadow interacts with a deep pavilion to cause the black-appearing center portions of a "nail-head" round brilliant. A comparison of virtual diamond images from Hemphill et al., model diamond images generated by GemCad with a close observer, and photographs of real diamonds (in diffuse light and in partially blackened diffuse light) is presented to demonstrate that a dark-appearing center is generated by reflections of a dark area directly over the diamond. A simple observation experiment is used to reinforce the concept that a "nail-head" owes more of its appearance to such reflections than to light leakage through the diamond's pavilion.

The appearance effects produced by shallower crown angles also are considered. A general result from Hemphill et al.—that WLR generally increases as crown angle decreases, with an interesting array of high WLR values for crown angles of 23°—is contrasted by photographs of two diamonds with similar proportions except for their crown angles (35.3° and 32.6°, respectively). These photos show that the two diamonds look similar in diffuse light, and in diffuse light with additional "hot spots," but when the overhead area of the diffuse light source is darkened, the diamond with the shallower crown angle looks less brilliant.

The article concludes with a historical review of Tolkowsky's 1919 work ("Diamond design…," E. & F. N. Spon, London), noting substantive differences in table size and girdle thickness between Tolkowsky's proposed proportions and a modern "Ideal." Despite the various simplifying assumptions of Tolkowsky's model, Mr. Cowing observes that "his [Tolkowsky's] basic findings concerning the best pavilion and crown angles have held up for eighty years." *Ilene M. Reinitz*

Diamond in the rough. *GPS World*, Vol. 11, No. 1, 2000, pp. 20–24.

Ensuring the security, safety, and efficiency of a diamond-mining operation is always a major concern. It is even more so for South Africa's Alexkor Ltd., a state-owned company with marine diamond-mining concessions along 100 km of shoreline between Alexander Bay and Port Nolloth. Alexkor relies on a fleet of diver-based diamond recovery vessels. Because this part of the Atlantic Ocean is notoriously stormy, mining is possible for only about 60–90 days each year. It is therefore essential for mining vessels to accurately position themselves as rapidly as possible, often in a low-visibility environment.

Offshore of South Africa there are three diamond-mining concessions, designated by the letters *a*, *b*, and *c* with increasing distance from the shoreline. Vessels can easily wander, either accidentally or intentionally, into the wrong concession. Alexkor has implemented differential GPS (global positioning system) technology for accurate positioning, real-time location data, and mapping of the ocean floor. The company has not yet been able to assess whether adopting GPS has had a positive impact on its operations. The company is, however, better able to track the location from which diamonds are being extracted, analyze database information, and decide whether an area should be mined a second time. *MT*

Diamond types I/II$_{ab}$. J. E. Shigley, *The Guide*, Vol. 19, No. 4, 2000, pp. 8–9.

Mention of diamond types (I and II) and their varieties (a and b) is becoming increasingly prominent in the gemological and jewelry trade literature, as they are helpful in explaining the reasons for color variations in natural diamonds, in distinguishing between natural and synthetic diamonds, and in understanding the GE POL and other color-enhancement processes. This article, designed primarily for retailers and dealers, presents a succinct and simplified explanation of diamond types.

Type I diamonds, the most abundant in nature, have certain characteristic features in the visible and infrared spectra that can be attributed to small amounts of nitrogen (N) in the diamond structure. In type Ia diamonds, the N atoms are in aggregates; whereas in type Ib diamonds, the N atoms occur as isolated, individual atoms dispersed throughout the crystal. Many diamonds contain both type Ia and Ib areas in different parts of the same crystal.

Type II diamonds do not contain N (or have it only in extremely small amounts) and are much less common than type I diamonds. Type II diamonds that do not conduct electricity are called type IIa; some of the world's largest, historic colorless diamonds are of this type. Type IIb diamonds (which do conduct electricity) contain boron substituting for carbon in the crystal structure and are generally blue or grayish blue in color. *AMB*

Etching of diamond in the silicate melt at the atmospheric pressure [sic]. V. M. Sonin, A. V. Naberukhina, E. N. Fedorova, and A. I. Turkin, *Proceedings of the Russian Mineralogical Society*, Vol. 129, No. 5, 2000, pp. 76–81 [in Russian with English abstract].

New results are presented for the etching of diamond crystals in low-temperature alkaline silicate melts. The different types of etch figures (corrosion mat surfaces, disc figures, and negative/positive trigons) are initiated on octahedral faces of diamonds in different melts. The etching is attributed to oxygen dissolved in the silicate melts. The composition of the melts influences the diffusion of oxygen and, consequently, affects the rate of etching and the morphology of the diamonds. *RAH*

Hazards associated with the mining of diamondiferous pipes. R. J. Butcher, *CIM Bulletin*, Vol. 93, No. 1037, 2000, pp. 65–67.

Although the vast majority of diamonds are mined from large, open-pit operations worldwide, numerous small underground mines, primarily in South Africa, exploit diamondiferous fissures and pipes. These underground operations face three principal hazards and challenges: mud rushes, block crushing, and the use of inappropriate mining methods.

Mud rushes occur when water interacts with rocks high in clay, causing instability; these rocks are usually the tuffaceous breccia in a kimberlite pipe or the shale comprising the country rock. This problem can be controlled by effective draining of the mining area. Block crushing results when compacted areas of old block caves or remnant pillars left in upper workings cause the collapse of new, deeper workings. Block crushing can be alleviated by starting new workings at least 50 m below the tunnel immediately above. Inappropriate mining methods are sometimes used because of the high capital costs associated with diamond mining. Using the wrong methods can have disastrous results. History has shown that chambering and block caving have been the most successful methods for underground diamond mining, but with certain restrictions. For example, a pipe must have minimum dimensions of 70 × 70 m for block caving to be effective, and tunnels in kimberlite larger than 2 × 2 m are likely to encounter instability problems. Skilled workers are another essential ingredient for the successful operation of an underground mine. *MT*

The nitrogen aggregation sequence and the formation of voidites in diamond. I. Kiflawi and J. Bruley, *Diamond and Related Materials*, Vol. 9, 2000, pp. 87–93.

High-temperature annealing of type IaB diamonds containing platelets [i.e., planar defects in the (001) planes] results in the conversion of the platelets to dislocation loops and in the formation of octahedral "voidite"-like defects. Natural voidites are octahedral-shaped, molecular nitrogen defects in the diamond lattice. Further investigation was required to confirm that the octahedral defects formed in the laboratory are the same as voidites observed in untreated natural diamonds—and, by extension, that the last stage of the nitrogen-aggregation sequence can be reproduced in the laboratory.

Electron energy loss spectroscopy (EELS) confirmed the presence of molecular nitrogen in the artificial defects produced in the annealed specimens. Quantitative analysis of the EELS data indicated that the nitrogen content in the artificial voidites agreed with the nitrogen content of "natural" voidites. Thus, the authors conclude that the voidite-like defects formed in the laboratory are very similar to the voidites observed in natural diamonds.

Experimental evidence at high temperatures (2,650°C) and pressures (9 gigapascals) is presented in support of a hypothesis describing the formation of B centers from A centers. N3 centers also are formed during the annealing process. In one annealed sample, the concentration of single nitrogen atoms was 25 ppm (2.5% of the total nitrogen present), and the concentration of N3 centers (formed by the annealing process) was 1.7 ± 0.4 ppm.

The authors maintain that these experimental data provide evidence in support of an extant hypothesis: The formation of B centers from A centers is through the dissociation of A centers to single nitrogen atoms, which then migrate to form B centers; and the formation of N3 centers is most likely an intermediate defect in the aggregation process, rather than a by-product of this transformation. *SW*

GEM LOCALITIES

Australia's gemstone resources and their markets. G. Browne, *Australian Gemmologist*, Vol. 20, No. 12, 2000, pp. 534–539.

At present, Australia is the world's largest producer of diamonds, opal, cultured South Sea pearls, and chrysoprase. In recent years, it has produced about one-quarter of the world's diamond production by volume, but currently it ranks sixth in terms of value. Opal production has been declining since 1990, as no new major opal fields have been discovered in over a decade. Australia produces 60% of the world's South Sea pearls. Chrysoprase is mined from two localities, in Queensland and Western Australia.

Australia is also a major, though declining, producer of sapphire. It contains an estimated 90% of the world's reserves of nephrite, although exploitation of the deposits on the Eyre Peninsula, South Australia, is limited at present. In the realm of synthetics, only the Biron hydrothermal synthetic emeralds are significant. *AAL*

The cause of colour of the blue alexandrites from Malacacheta, Minas Gerais, Brazil. M. V. B. Pinheiro, M. S. Basílio, K. Krambrock, M. S. S. Dantas, R. Paniago, A. L. Assunção, and A. C. Pedrosa-Soares, *Journal of Gemmology*, Vol. 27, No. 3, 2000, pp. 161–170.

An optical and structural study was made on what is commercially referred to as "peacock blue" alexandrite from Malacacheta, Minas Gerais. This alexandrite is known for its strong pleochroism—which ranges from blue to green or greenish yellow—as well as its strong color-change from blue or greenish blue in daylight to reddish purple in incan-

descent light. Advanced analytical techniques such as electron paramagnetic resonance and X-ray photoelectron spectroscopy were used to determine how chemical impurity–related point defects correlate to the stone's bodycolor.

The rare blue color of this alexandrite is due to Fe^{3+} and Cr^{3+} substituting for Al^{3+}, within specific limits of the ratio Fe/Cr, in the mirror sites of the crystal. The concentration of Cr^{3+} in sites with inversion symmetry, meanwhile, is negligible. The blue color correlates to intermediate Fe/Cr ratios ($0.4 < X_{Cr}/X_{Fe} < 1.2$, where X is the molar fractional content). The same amount of Cr with more Fe shifts the blue to green. A significantly lower Cr concentration causes the stone to become yellow and lose its alexandrite effect entirely. *WMM*

Characteristic mineralizations of metamorphic-metasomatic gemstone deposits in northern Vietnam. D. P. Tien, W. Hofmeister, and V. X. Quang, *Applied Mineralogy*, Vol. 1, E. Rammlmair et al., Eds., 2000, Balkema, Rotterdam, pp. 281–283.

One of the economically important gemstone deposits of the Yen Bai district, near the city of Luc Yen, Vietnam, occurs in amphibolite-facies metamorphic rocks. Three types of primary gemstone occurrences are found: (1) ruby and spinel hosted in marble; (2) large hexagonal prisms of translucent ruby in gneiss; and (3) color-zoned tourmaline crystals in granitic pegmatite. At present, most of the gems produced in the area are recovered from alluvial deposits derived from these rocks. *RAH*

A new find of spessartine garnets in Nigeria. T. Lind and U. Henn, *Journal of Gemmology*, Vol. 27, No. 3, 2000, pp. 129–132.

A new source of gem-quality spessartine garnet was recently discovered in Nigeria (locality not specified). The material ranges from yellow to "golden" yellow to brown-orange, and is available in polished sizes of 2–3 ct and larger. Tables compare the new material to spessartine from other localities with regard to refractive indices, specific gravity, chemical composition, and spectra. Chemical analyses show a very high spessartine component (89–95 mol%) with minor amounts of pyrope and almandine. The 1–6 mol% variation in the almandine component is responsible for the differences in color. Brown-orange is associated with a higher almandine component. Liquid-filled "fingerprints" are the main inclusions. *WMM*

Origin of some gem minerals in Sri Lanka: Evidence from corundum-spinel-scheelite-taaffeite–bearing rocks. G. W. A. Rohan Fernando and W. Hofmeister, *Applied Mineralogy*, Vol. 1, E. Rammlmair et al., Eds., 2000, Balkema, Rotterdam, pp. 293–295.

The origin of some gem minerals at Bakumuna (near Elahera) and at Rupaha (a new gem locality) is discussed. The deposits appear to have formed in two stages: (1) formation of silica-undersaturated reaction zones from the interaction of chemically dissimilar rocks at high temperatures, and (2) late-stage fluid-rock interaction processes involving the infiltration of saline fluids that transported metals such as sodium, beryllium, and tungsten. Chemical analyses are given for spinel, taaffeite, scapolite, phlogopite, nepheline, corundum, and sapphirine. *RAH*

INSTRUMENTS AND TECHNIQUES

Application of MPV-3 microphotometer in gemology. S. Ye, L. Qi, Y. Luo, and T. Guo, *Geological Science and Technology Information*, Vol. 18, No. 4, 1999, pp. 107–110 [in Chinese with English abstract].

The MPV-3 microphotometer is capable of measuring the absorbance, transmittance, and fluorescence of very small areas of a gem material as seen in a microscope. It operates primarily in the visible light range (400–700 nm); measurements are rapid and results are quantitative.

Applications of the instrument are illustrated for colorless beryl from Pingwu, China; sapphire from Changle, China; as well as various natural and synthetic rubies from several sources. Changes in hue and saturation after several types of enhancements could be identified and measured in some (but not all) cases. The instrument is particularly useful for color evaluation and fluorescence measurements of colored stones. *TL*

Cathodoluminescence method and its application in gemology. T. Miyata, H. Kitawaki, and M. Kitamura, *Journal of the Gemmological Society of Japan*, Vol. 20, Nos. 1–4, 1999, pp. 63–76.

Natural and synthetic gemstones experience fluctuations in their growth conditions and growth rates that manifest themselves as differences in morphology and homogeneity within a single crystal. These differences are ideally suited to recognition by cathodoluminescence (CL), a nondestructive analytical technique that is available in two modes: with a scanning electron microscope or with an attachment on an optical microscope (a "Luminoscope"). This article demonstrates the application of CL to the distinction between natural and synthetic diamonds, and between two types of synthetic emeralds, as representative examples.

By CL methods, the growth zones in natural diamonds are shown to consist of flat {111} faces with or without curved {100} faces, whereas both of these faces are always flat in synthetic diamonds. Every diamond has its own characteristic pattern of growth banding, so a CL image of each diamond is unique and can be used as a fingerprint. Flux-grown synthetic emeralds show straight (parallel) growth bands or "aurora-like" bright spots, whereas hydrothermally grown synthetic emeralds show a unique rhombic pattern or "comet-like" spots arranged in specific directions. Although some of the above features may be discernable with other techniques, CL is particularly suited to imaging differences that are a result of chemical

inhomogeneities. *AAL*

Characterization of gem stones (rubies and sapphires) by energy-dispersive X-ray fluorescence spectrometry. D. Joseph, M. Lal, P. S. Shinde, and B. D. Padalia, *X-Ray Spectrometry*, Vol. 29, 2000, pp. 147–150.

Trace-element analyses of natural rubies (from India, Kenya, Tanzania, and Myanmar), sapphires (from India, Australia, Vietnam, and Sri Lanka), and synthetic rubies (from India) were carried out by energy-dispersive X-ray fluorescence (EDXRF). This rapid, sensitive, and effective method is effective for the nondestructive determination of chemical composition. The number of samples studied in each category is not stated, nor is the method of synthesis of the rubies.

The authors report that K, Ti, Cr, Fe, Cu, Zn, Sr, and Ba generally were present in all the natural rubies examined, while Cr, Ni, Cu, and Zr were present in the synthetic rubies. Fe was found in all the naturally occurring rubies studied, but it was absent (limit of detection <10 ppm) in the synthetic rubies. Notable amounts of Ca, Fe, Sr, and Mo were detected in the Indian sapphires; their average concentrations were 0.10%, 0.18%, 0.029%, and 0.006%, respectively. *KSM*

Laser tomography: A new powerful method to identify natural, synthetic and treated stones. Case study of corundum. J. Shida, *Journal of the Gemmological Society of Japan*, Vol. 20, No. 1–4, 1999, pp. 79–92.

Tomography is a method of producing a three-dimensional image of the internal structure of a transparent solid object. Laser tomography (LT) is an optical microscopic technique that uses a laser beam as a light source (rather than ordinary light) at low magnification. This nondestructive technique is suitable for routine gemological testing, and can be used to observe the distribution of minute inclusions, crystal defects, and growth zoning in gemstones.

This article describes the instrumentation required for LT and offers some practical operating procedures. To prevent light scattering from the surface of a faceted stone, for example, the sample should be immersed in a liquid of approximately the same refractive index. The author presents numerous applications of LT, for both natural and synthetic ruby and sapphire, to demonstrate the utility and power of this technique. For instance, he describes various features that are diagnostic of certain synthetics. Heat-treated stones also have characteristic LT features. Both natural and synthetic gems form in a variety of environmental and growth conditions, which result in characteristic features that can be imaged by this technique. *AAL*

Letting loose a laser: MRM (Mobile Raman Microscopy) for archaeometry and ethnomineralogy in the next millennium. D. C. Smith, *Mineralogical Society Bulletin (Great Britain)*, No. 125, December 1999, pp. 3–8.

The identification of gems and archeological materials that must be analyzed nondestructively has always been a problem. In recent years, laboratory-based laser Raman microspectrometry has become the technique of choice in such situations, because the analyses are quick and cause no damage to the item; nor do they require any special sample preparation. In many cases, however, important or delicate gem-set objects (e.g., statues and other large objects, or crown jewels) cannot be brought to a laboratory for analysis.

This article describes the successful use, in a museum setting, of a mobile Raman microscopy (MRM) instrument to overcome this problem. MRM is now possible because of the miniaturization of the computer components and technological advances in the laser source, spectrometer, and detector. The mobility is enhanced by optical fibers (5–500 m long) that allow a remote "head" to be brought to the sample instead of the opposite. The uses of MRM are limited only by the imagination of the gemologist. *AAL*

Nondestructive testing for identifying natural, synthetic, treated, and imitation gem materials. T. Lu and J. E. Shigley, *Materials Evaluation*, Vol. 58, No. 10, 2000, pp. 1204–1208.

Accurate gem identification is essential to support the commercial value of gemstones and the stability of the jewelry industry. However, with the proliferation of new synthetics, treatments, and simulants, such testing is becoming increasingly difficult. A greater array of sophisticated instruments and techniques are needed, all of which must be nondestructive. This article reviews currently available nondestructive gem identification and testing techniques for a technical audience of diverse backgrounds.

Traditional gem testing instruments and methods are discussed first, and situations requiring advanced nondestructive testing are identified. Eleven traditional and 12 advanced nondestructive techniques are tabulated, along with their applications to gem identification. Particular attention is given to the separation of diamond from its most common simulants. Identification of synthetics (i.e., synthetic diamond, emerald, amethyst, and ruby) on the basis of crystal morphology and trace-element chemistry is also explored. Finally, the authors review the detection of gem treatments (i.e., fracture filling of diamond and emerald, and irradiation of diamond). They discuss the various advantages and disadvantages of gem treatments, and raise concerns about the long-term stability of fracture fillers. *Lila Taylor*

Precious metals and provenance enquiries using LA-ICP-MS. M. F. Guerra, C.-O. Sarthre, A. Gondonneau, and J.-N. Barrandon, *Journal of Archaeological Science*, Vol. 26, No. 8, 1999, pp. 1101–1110.

The geographic origin of precious metals (mainly gold and

silver) found in archeological objects is an important field of research. The traditional method of investigation has involved the use of diagnostic trace elements and/or isotope ratios (e.g., lead) to "fingerprint" ores from known localities and compare these with the chemical constituents of the artifact. However, most of the analytical procedures used until very recently were based on instrumentation that had insufficient sensitivity and, in some cases, required destruction of a small part of the sample. This article emphasizes the advantages of the relatively new laser ablation–inductively coupled plasma–mass spectrometry (LA-ICP-MS) technique. It is now possible to obtain highly sensitive analyses of trace elements and isotopes without any special sample preparation, virtually nondestructively.

The utility of the technique is illustrated by two case histories. The first involves the determination of the gold ores used in European countries as far back as 356–336 BC. In this case, it was shown that the coins struck in Gaul and Greece came from different ores. The second case involves tracing the gold trade routes in the occidental Muslim Empire (8th–11th century AD) based on such elements as Ir, Pt, Pd, and Ga. Although not specifically mentioned, the potential application of LA-ICP-MS to gemology appears to be extensive—not only for determining the provenance of the precious metals used to mount gemstones, but also for "fingerprinting" gemstones from classic (and even modern) localities virtually nondestructively. *AAL*

JEWELRY MANUFACTURING

Getting started on finishing. S. M. Sanford, *Lapidary Journal*, Vol. 54, No. 4, 2000, pp. 20–25, 55.

A good and appropriate finish (i.e., polish) for the metal used in jewelry is extremely important and requires time and planning. This article contains a wealth of information on the practice and theory of finishing. For example, if a high polish is desired, two distinct processes are involved. The first is abrasive polishing, whereby deep scratches are replaced with smaller and shallower ones until the surface is uniform. The second is buffing, which is nonabrasive. As the metal is compressed, molecules are actually moved from high spots and deposited in low spots, creating a smooth surface.

Polishing is not a quick task. It takes time to achieve the desired results. Many useful products are available for improving the efficiency of the finishing process. For example, abrasive paper or cloth, which is used initially, comes in a range of coarse to fine grit sizes. The next step involves polishing compounds for use on a buffing wheel. Only one polishing compound should be used on each buff; contaminating a fine buff with a coarse compound will ruin it. Storing buffs with their specific compound in separate containers is recommended. Also, separate buffs should be used for each type of metal polished. Buffs used for steel can never be used for other metals. There are four types of buffs available—cloth, felt, bristle, and leather (or chamois)—and choosing the wrong buff can be damaging to your piece.

Small hand buffs can be created from cotton crochet thread for hard-to-reach places not accessible to a motorized wheel. Small wooden tools can be made from Popsicle sticks, toothpicks, and dowels. *PT*

SYNTHETICS AND SIMULANTS

Growth and characterization of high-purity SiC single crystals. G. Augustine, V. Balakrishna, and C. D. Brandt, *Journal of Crystal Growth*, Vol. 211, 2000, pp. 339–342.

Silicon carbide (SiC) has several polytypes, depending on the stacking sequence of hexagonal atomic structural units. Many of these polytypes have been developed in the laboratory by various growth techniques. The synthetic moissanite used as a gem material is the 6H polytype, and is grown by a seeded sublimation process. Recently another moissanite polytype—4H, with properties very close to those of 6H synthetic moissanite—has been grown in large single crystals (to 50 mm in diameter) for semiconductor uses . These high-purity crystals are transparent, and therefore could be used in the jewelry industry; their color was not stated. The material was grown by the physical vapor transport technique in graphite, with SiC sublimation sources. The growth technique uses an induction-heated, cold-wall system in which high-purity graphite constitutes the hot zone of the furnace. The SiC was intentionally doped with vanadium (V) to obtain semi-insulating properties. In addition to V, trace amounts of Ti, Al, and B were detected in some of the SiC crystals. Electrical resistivity varies depending on the doped impurities. *TL*

The growth rate effect on the nitrogen aggregation in HTHP grown synthetic diamonds. Y. V. Babich, B. N. Feigelson, D. Fisher, A. P. Yelisseyev, V. A. Nadolinny, and J. M. Baker, *Diamond and Related Materials*, Vol. 9, 2000, pp. 893–896.

The relationship between nitrogen aggregation and crystal growth rate was studied using high pressure-high temperature (HPHT) synthetic diamonds. Octahedral yellow crystals up to 5 mm were grown in a "split-sphere" type of apparatus using the temperature gradient method and an Fe-Ni solvent-catalyst. Growth periods of up to 100 hours were maintained with a pressure of 6.0 GPa and temperature of 1,500°–1,550°C. Some of the synthetic diamonds were cut parallel to a (110) plane through the seed and polished into plates in order to determine growth rates of each octahedral growth sector. The authors used FTIR microspectroscopy to determine the degree of nitrogen aggregation at several points from seed plate to crystal surface within various growth sectors. Concentrations of single substitutional (C), pairs (A), and vacancy (N^+) nitrogen centers were evaluated for each point. On the basis of data obtained from these experiments, the

authors propose the following:

1. Growth sectors of a single crystallographic form can grow at different rates in crystals produced by the temperature gradient method.
2. Distribution of C and A defects through the {111} growth sectors is consistent with the current model, which asserts that nitrogen enters the crystal lattice as isolated substitutional atoms; A-defects form in the crystal as a result of solid-state thermally activated nitrogen aggregation.
3. Growth sectors formed at higher average growth rates show elevated levels of nitrogen aggregation (A defects), probably due to greater nickel uptake.

SW

Growth of synthetic diamond monocrystals weighing up to six carats and perspectives of their application. Yu. M. Borzdov, A. G. Sokol, Yu. N. Pal'yanov, A. F. Khokhryakov, and N. V. Sobolev, *Doklady Earth Science*, Vol. 374, No. 7, 2000, pp. 1113–1115.

During the past two decades, researchers at the Institute of Mineralogy and Petrography in Novosibirsk have been among the leaders in the synthesis of diamond using the multianvil (split-sphere) apparatus (BARS), which was first developed in Russia in the mid-1970s. This short article summarizes recent efforts by this research group to improve the growth of large, high-quality synthetic diamonds.

Brownish yellow, cuboctahedral crystals weighing up to 6 ct have been produced. These crystals are relatively free of inclusions and other growth-related defects. Improvements in the controls of growth temperature, directional rates of formation of the various crystal faces, and the concentration of trace elements in the growth environment have all combined to optimize the crystallization of these experimental crystals. High-quality synthetic diamonds have a number of important uses, and the development of improved growth technology promises the availability of crystals for industrial uses (e.g., as surgical blades, optical and X-ray lenses, laser sources, heatsinks, and other components in electronic devices). Future work will be directed at growing synthetic diamonds with particular properties for specific high-technology applications. *JES*

Large diamonds grown at high pressure conditions. H. Kanda, *Brazilian Journal of Physics*, Vol. 30, No. 3, 2000, pp. 482–489.

Scientists at the National Institute for Research in Inorganic Materials (NIRIM) in Tsukuba, Japan, have extensively studied the growth of single-crystal synthetic diamonds. This article, by a NIRIM scientist, reviews current knowledge of the temperature gradient method used to grow large synthetic diamond crystals. Details are provided on crystal size and morphology, growth features such as inclusions and defects, and impurities related to color in synthetic diamonds. In addition to colorless crystals, synthetic diamonds with yellow, blue, green, and brown coloration can be produced, depending on the impurities present. Crystals up to 2 cm can be grown. Future improvements in the growth technique should allow for the production of synthetic diamonds in greater quantities and at lower costs. This article is a good technical summary of a topic that is of continued interest to gemologists. *JES*

Present Russian synthetic and enhanced gemstones. V. S. Balitsky, *Australian Gemmologist*, Vol. 20, No. 11, 2000, pp. 458–466.

Following a brief review of the production of synthetic crystals (including gemstones) in the former U.S.S.R., Dr. Balitsky summarizes the present production of 26 synthetic gemstones in Russia. Several varieties of quartz, corundum, and beryl are grown. Up to 100 kg/year of synthetic emeralds are produced, mainly by hydrothermal methods, although small quantities are also produced by more expensive flux growth techniques. The production of synthetic diamonds is listed as ≤1 kg/year. Several tens of kilograms per year of synthetic moissanite are being grown, with crystals weighing up to 300 ct. Enhancement of the color and appearance of 13 gem materials (including corundum, topaz, danburite, scapolite, beryl, and turquoise) is also reported. *RAH*

Russian colourless synthetic diamond—Now available in the market. J. C. C. Yuan, *Australian Gemmologist*, Vol. 20, No. 12, 2000, pp. 529–533.

Colorless to near-colorless synthetic diamonds, manufactured in Russia using the "split sphere" apparatus, have been available on the U.S. market since the late 1990s. These type IIa synthetic diamonds have a cubo-octahedral crystal habit. When faceted, they yield colors mostly in the G–K range. Forty crystals weighing 0.23–1.18 ct were faceted into synthetic diamonds weighing 0.07–0.45 ct. They could be identified by their metallic inclusions, magnetic properties, characteristic UV luminescence, and cross-shaped pattern of anomalous birefringence. The De Beers DiamondView instrument was also useful in differentiating these synthetics from natural diamond. *RAH*

TREATMENTS

Colouration in natural beryls: A spectroscopic investigation. G. Mathew, R. V. Karanth, T. K. Gundu Rao, and R. S. Deshpande, *Journal of the Geological Society of India*, Vol. 56, No. 3, 2000, pp. 285–303.

Irradiation of colorless beryl from the Badmal mines, Orissa, changed the material to yellow-green. Subsequent heating at 300°C turned the samples yellow, and further heating produced a more attractive and commercially desirable sky-blue color. Continued heating to above 500°C returned them to colorless. Similar studies were carried out on natural yellow, blue, and green beryls from Orissa. All acquired a greenish hue on irradiation, and

turned colorless on heating above 500°C.

Electron microprobe analysis of the beryls identified iron as the major transition-element impurity, with 0.5–0.7 wt.% FeO. Electron spin resonance, optical absorption, and Mössbauer spectroscopy showed that the colors were produced by Maxixe-type defect centers as well as by radiation-induced oxidation of Fe^{2+} to Fe^{3+} and its associated charge-transfer processes. The yellow and blue treated colors were similar to those of naturally colored samples, both of which result from similar charge-transfer processes. Thus, it is inferred that naturally yellow, blue, and green beryls with low Fe contents are produced by prolonged exposure to natural irradiation.

RAH

MISCELLANEOUS

De Beers formally drops market custodian role: Announces its "Supplier of Choice" program. *Mazal U'Bracha*, Vol. 15, No. 124, 2000, pp. 23–26, 29, 31, 33.

De Beers is initiating the "Supplier of Choice" program in an effort to tighten its relationship with its clients and encourage them to develop stronger downstream marketing. The key objective of this program is to create a steady and growing demand for De Beers diamonds among retailers and consumers, while becoming a more attractive supplier through better assortments and lower prices. The program is expected to expedite industry consolidation, causing some sightholders to merge with others.

Diamond Trading Company (DTC) clients will no longer be allowed to use the name *De Beers* in their promotions. Instead they may advertise that they "acquire their rough from the Diamond Trading Company." The DTC "Forevermark" brand and the famous slogan "A Diamond Is Forever" may be used in promotions only by qualified sightholders. Through these promotional changes, De Beers hopes to establish a new identity aimed at protecting its sightholders and, ultimately, retailers and consumers. De Beers has also announced its strict eligibility criteria for DTC sightholding privileges. The DTC reserves the right to determine whether a sightholder's business is consumer-demand growth-oriented, and whether their strategic investment and marketing plans are sound.

The new arrangement between the DTC and its sightholders goes into effect in July 2001, at which time the relationship will be covered by a 24-month initial contract. Three months before the end of the contract, either side can terminate the relationship. Otherwise, the contract is automatically renewed for another 12 months.

MT

Geological knowledge: A key to the future of the diamond industry. A. A. Levinson and F. A. Cook, *Geoscience Canada*, Vol. 27, No. 1, 2000, pp. 19–22.

During the first half of the 20th century, De Beers owned most of the world's important gem diamond deposits and controlled the geologic knowledge to find them, but this is no longer the case. This article examines the successes since 1950 in finding new deposits in countries outside of the De Beers sphere of influence, advances in exploration technology, dissemination of the geologic knowledge needed for diamond exploration, and how these combined factors have affected the diamond industry, especially since 1990.

Major discoveries in Russia, Australia, and Canada were made by governments and companies not affiliated with De Beers. This is the result of the development of a vast pool of exploration expertise, much of it in the public domain, that is currently being used to find additional deposits worldwide. As diamond exploration technology becomes more sophisticated, new economic diamond deposits are being found at an accelerated rate. For example, more than 300 kimberlite pipes have been identified in Canada's Slave Geological Province (Northwest Territories) since 1991. The authors caution that a rise in the supply of rough diamonds may affect the balance of supply and demand unless the industry can develop markets to consume them.

PGY

Lung function, biological monitoring, and biological effect monitoring of gemstone cutters exposed to beryls. R. Wegner, R. Heinrich-Ramm, D. Nowak, K. Ohma, B. Poschadel, and D. Szadkowski, *Occupational and Environmental Medicine*, Vol. 57, 2000, pp. 133–139.

Beryllium (Be) metal and some of its compounds are carcinogenic to humans, with the lungs particularly at risk. The lung disease *berylliosis* occurs in workers involved with ceramic manufacturing, space engineering, and other occupations in which such materials are used. This article reports on the results of detailed tests designed to determine the environmental hazards faced by gemstone cutters in Idar-Oberstein with occupational exposure to beryl ($Be_3Al_2Si_6O_{18}$), the most important Be-containing gemstone.

Fifty-seven out of 100 gemstone cutters in 12 factories that cut beryl underwent extensive medical examinations that included chest X-rays, lung-function testing, urine monitoring (for Be, Al, Cr, Ni), and blood analysis (for Pb). Special tests included BeLT (beryllium lymphocyte transformation), which examines the prevalence of lung disease induced by Be. Airborne concentrations of Be (in the form of dust) were measured in the factories.

No adverse clinical health effects were found in this group of gemstone workers. However, Be was measurable (but apparently not at dangerous levels) in the urine of all workers in one factory that had airborne Be concentrations well above the threshold limit permitted in Germany. Notwithstanding the generally favorable results of this study, the authors recommend improvement in workplace ventilation (to remove Be-containing dust) accompanied by routine urine Be analysis of workers in those factories that cut beryl.

AMB